Beyond Deep Learning: Scalable Methods and Models for Learning

Oriol Vinyals

Electrical Engineering and Computer Sciences
University of California at Berkeley

Technical Report No. UCB/EECS-2013-202
http://www.eecs.berkeley.edu/Pubs/TechRpts/2013/EECS-2013-202.html

December 12, 2013

Copyright © 2013, by the author(s).
All rights reserved.

Permission to make digital or hard copies of all or part of this work for personal or classroom use is granted without fee provided that copies are not made or distributed for profit or commercial advantage and that copies bear this notice and the full citation on the first page. To copy otherwise, to republish, to post on servers or to redistribute to lists, requires prior specific permission.

Beyond Deep Learning:
Scalable Methods and Models for Learning

by

Oriol Vinyals

A dissertation submitted in partial satisfaction
of the requirements for the degree of

Doctor of Philosophy

in

Engineering – Electrical Engineering and Computer Sciences

in the

GRADUATE DIVISION

of the

UNIVERSITY OF CALIFORNIA, BERKELEY

Committee in charge:

Professor Nelson Morgan, Chair
Professor Trevor Darrell
Professor Bruno Olshausen

Fall 2013

Beyond Deep Learning:
Scalable Methods and Models for Learning

Copyright © 2013

by

Oriol Vinyals

Abstract

Beyond Deep Learning:
Scalable Methods and Models for Learning

by

Oriol Vinyals

Doctor of Philosophy in Engineering – Electrical Engineering and Computer Sciences

University of California, Berkeley

Professor Nelson Morgan, Chair

In my thesis I explored several techniques to improve how to efficiently model signal representations and learn useful information from them. The building block of my dissertation is based on machine learning approaches to classification, where a (typically non-linear) function is learned from labeled examples to map from signals to some useful information (e.g. an object class present an image, or a word present in an acoustic signal). One of the motivating factors of my work has been advances in neural networks in deep architectures (which has led to the terminology "deep learning"), and that has shown state-of-the-art performance in acoustic modeling and object recognition – the main focus of this thesis. In my work, I have contributed to both the learning (or training) of such architectures through faster and robust optimization techniques, and also to the simplification of the deep architecture model to an approach that is simple to optimize. Furthermore, I derived a theoretical bound showing a fundamental limitation of shallow architectures based on sparse coding (which can be seen as a one hidden layer neural network), thus justifying the need for deeper architectures, while also empirically verifying these architectural choices on speech recognition. Many of my contributions have been used in a wide variety of applications, products and datasets as a result of many collaborations within ICSI and Berkeley, but also at Microsoft Research and Google Research.

To my girlfriend, family, and friends.

Contents

Acknowledgements

Getting a PhD was more fun and interactive than I thought it would be when I first started thinking about it during my undergrad at the Universitat Politecnica de Catalunya. Many people have helped me a lot in a day to day basis, and while pursuing my PhD I have been lucky enough to find my life partner, Meire Fortunato. My parents, Jordi and Rosa, have always been extremely helpful and supporting to everything I have done, and taught me from the principles of freedom that let me achieve such a big dream. My sister Georgina has always been there to give me a good laugh and her wonderful family sets a very high example for me to try to follow. Many friends and special people have always been there to share a drink and give me a laugh, and I want to specially thank Osito, Ruben, Carlos, Maria, Bea, Ivan, Marcos, Renato, Sebastian, Marcelo, Clarissa, Gabriel, Andrew, and many others that I am forgetting right now!

I now come to realize how many amazing people I have worked and been lucky enough to learn from during this years. A PhD is definitely not done in isolation! My advisor Nelson Morgan who, through his experience and points of view, has always given me good advice and put me right in track to research towards this dissertation. Trevor Darrell, whom I consider a co-advisor, has been an extremely motivating source of knowledge in vision and learning, and has helped me broadening my skills beyond speech recognition. Ruzena Bajcsy has also been an extremely kind and energetic person to work with, and Bruno Olshausen always had something more to say about current trends in machine learning, and his intuition and insights were extremely valuable and will help in the future.

At ICSI, I was able to collaborate with many postdocs, researchers, and students, so big thanks to them all, specially Yangqing, Suman, Adam, Mary, Gerald, Kofi, Dan, Steve, Arlo, Korbinian, Chuck, Howard and Vijay, as well as all the staff members. Special thanks as well to Fernando from CMU for introducing me to research in the US, and to MSR for supporting me through their Fellowship program that made my grad student life even easier.

Last but not least, through conferences and internships, I met a group of excellent researchers. Thanks to Li Deng, Dan Povey, Dan Bohus, Geoff, Patrick, Jasha, Mike, Alex, Rich, Eric whom I met at MSR, and Vincent, Patrick (again!), Mike, Eric, Carolina, Andrew from Google. Also, kudos to George, James, Ilya, Alex, and Hinton from Toronto for the many useful discussions about deep learning.

Chapter 1

Introduction and Summary

In this thesis I present results from work that I hope will provide contributions to the speech, vision, and machine learning communities. As a result of working in these different areas, my thesis is interdisciplinary. The main emphasis is, however, common to all three: to learn something from data (or signal representations) with the objective of extracting useful information. Learning is a very general word, so it is important to formalize exactly what it means in the context of machine learning and computer science. In Chapters 2, 3 and 4, several parts of the learning process are carefully defined, but for the purpose of this introductory chapter, it is enough to think of learning as something that aims to find a function that maps an input (e.g., a speech signal or an image) to an output (e.g., a word spoken in a speech utterance, or an object class present in an image).

Thanks to increased computational power and data availability, machine learning is continuously evolving, and many algorithms and models are continuously revisited. This trend has been very clear in the beginning of the era of "Big Data". As a result, some methods that rely on large amounts of data are making a comeback. In particular, neural networks, which are a powerful non-linear model to act as the function to map from inputs to outputs, have seen a renaissance. These models involve several layers of computation (typically with matrix-vector products and non-linearities). This is the main idea behind "Deep Learning", which has been very popular amongst researchers and industry due to achieving state-of-the-art in many tasks and domains.

My main interests with regards to deep learning have been both in the learning itself (i.e., optimization), and the modeling part where, by trying to explore simpler optimization problems, one can achieve the same power in the function learned. My other main focus has been to apply these techniques to a wide variety of problems to show that, indeed, these techniques can generalize, with little to no tuning, to many learning tasks. However, there is no magic, and every problem has singularities that require for us – the researchers – to find the appropriate representation, model, and learning techniques that achieve the best performance.

My main contributions that are covered in this thesis have been:

- To optimization research by providing a robust and efficient second order method to optimize functions (Chapter 3)

- To deep learning research, by proposing simple models that can be efficiently learned in parallel and have powerful representation power and regularization properties (Chapter 4)
- To deep learning research, by theoretically demonstrating why size matters and how depth is important in learning (Chapter 5)
- To speech research, for advances in acoustic modeling by proposing new recurrent neural nets as a way to perform acoustic modeling, and for the analysis of various acoustic models under different noise conditions (Chapter 6)
- Also to the speech research, for advances in keyword detection in both big data and scarcity of data (e.g., minority languages) conditions (Chapter 6), which resulted in a patent that is being used in millions of phones distributed in the latest Google Android Operating System

This thesis is organized in different chapters, which I summarize here. The reader is encouraged to read further in each chapter, which should be largely self contained (although some references will be provided in lieu of a more complete explanation in some cases).

Chapter 2 explains current state of the art and puts in perspective each of the elements of deep learning, emphasizing its success in applied fields such as speech recognition and computer vision. Although I leave some related work that is more specialized in its own chapter, the object of Chapter 2 is to give a general overview of the state of the art. Furthermore, this chapter will define some of the jargon that will be used later in the thesis, which should help the reader unfamiliar with machine learning. This is intended to put in perspective the technical contributions that are presented in the following chapters. Readers that have experience with deep learning should jump ahead to chapters that report these contributions, as they also describe previous work on the field (though in a less general way).

Chapter 3 proposes a new optimization algorithm specifically designed to train deep architectures, which are often challenging due to the non-convexity of the error surface and the requirement to train such models with large amounts of data. Having these algorithms not only simplifies and speeds up the learning, but sometimes enables learning of models that would be impossible with traditional methods. As such, this chapter also presents revisiting Recurrent Neural Networks (RNNs) for acoustic modeling as an application of the optimization algorithm.

In **Chapter 4**, even though optimizing challenging models is possible, I propose a deep learning architecture which would require the solution of several simpler (i.e., convex) problems instead of one big non-convex problem. Since there seems to be a trade off between model capacity and training difficulty, this chapter contrasts with Chapter 3 in that it is trying to simplify the optimization algorithm while sacrificing as little model capacity as possible. Empirical evidence shows that this is, in general, possible with such models, although I also point out some weaknesses and limitations of the simplified, easier to optimize model.

Given these observations, **Chapter 5** changes focus from the methods and the models, and tries to explain two fundamental characteristics that have made the current deep learning "comeback" possible: first, I propose a theoretic framework to explain how size in

a single layer model relates to accuracy, and why there may be a need for depth. Secondly, I do an empirical study on how depth matters – although no theory is developed, the case study of a single layer network may help developing theory that solidifies our knowledge on deep architectures versus shallow ones, which is currently an important open problem in the machine learning community.

Chapter 6 presents several applications which show that, even though learning methods try to be as general as possible, many tasks have singularities that need to be dealt with. There is no magic formula that solves every problem, thus implying that machine learning is an evolving research field, by no means solved, and that for some problems (including some presented in this chapter), deep learning is not well suited and other methodologies should be applied.

Chapter 7 concludes the thesis. This chapter aims to give a very personal and subjective vision on what the future of machine learning may be, giving advice to future generations working on deep learning and applied machine learning, and summarizing the contributions of this thesis, looking forward to the next decade doing applied machine learning research.

Chapter 2

Current Trends

2.1 Problem Statement and Definitions

The main focus of this thesis is the task of classification, which is a subfield of machine learning (and which, itself, is as a subfield of artificial intelligence). Throughout the thesis I will refer to the classification task with other names such as supervised learning, or learning, but it should be clear what I am referring to given the context.

A classification function f takes inputs (usually called features) $\mathbf{x}$, which typically live in the d-dimensional space $\mathbb{R}^d$, and maps them to an output space. This output space may range from a one dimensional binary space (in which we want to classify whether an image contains a face or not), to the space of all English sentences (in which we are decoding an acoustic utterance into its transcription), or even real valued spaces (e.g., when we are trying to predict the temperature given some observed variables from the weather). The latter is often called regression, but in this thesis I will make little distinction between the two.

Classification can can be thought of as a two stage process: the training (or learning) phase, and the testing (or inference). Almost all the efforts in this thesis concern the training phase, paying little to no attention to inference (other than computational considerations which will be clear in Chapters 4 and 6).

Although I go further in detail in Chapters 3 and 4, here I will briefly go over what machine learning entails. The goal is to "learn" a function f that maps an input $\mathbf{x}$ to an output $\mathbf{y}$ (both generally vectors, hence these symbols are bolded). This is a pretty vague statement, but the ingredients are all there already: f (the model), and pairs of $\mathbf{x}$ and $\mathbf{y}$ (the data). Fundamentally, we want to find a function that performs a classification task with human performance (sometimes, we can exceed human performance, but more often than not, this is not the case). To achieve this, most of the approaches aim to maximize a merit function (or minimize a cost) on how well f performs given some data, and in some cases one could give a probabilistic interpretation to what is being learned (e.g. the merit function could be the likelihood when f is a probabilistic model).

One of the contributions of my thesis is the optimization algorithm which is used to maximize the merit function, and is given in Chapter 3, while in Chapter 4 I focus on methods to simplify f whilst keeping the maximization problem fairly straightforward (i.e.,

convex). This thesis also proposes novel applications of models to several classification tasks, and the remainder of this chapter will focus on giving historical perspective to the proposed solutions to each of these tasks.

2.2 Optimization Techniques and Machine Learning

Many algorithms in machine learning and other scientific computing fields rely on optimizing a function with respect to a parameter space. In many cases, the objective function being optimized takes the form of a sum over a large number of terms that can be treated as identically distributed: for instance, labeled training samples. In deep learning, the problem often consists of minimizing the negated log-likelihood:

$$f(\boldsymbol{\theta}) = -\log(p(\mathbf{Y}|\mathbf{X};\boldsymbol{\theta})) = -\sum_{i=1}^{N} \log(p(\mathbf{y}_i|\mathbf{x}_i;\boldsymbol{\theta})) \tag{2.1}$$

where $(\mathbf{X}, \mathbf{Y})$ are the observations and labels respectively (which are assumed independent and identically distributed), and p is the posterior probability of the labels which is modeled by a deep neural network with parameters $\boldsymbol{\theta}$. In this case it is possible to use subsets of the training data to obtain noisy estimates of quantities such as gradients; the canonical example of this is Stochastic Gradient Descent (SGD) [13].

My main interest is on batch methods (i.e., methods that process the whole sum, or a large portion of the sum in equation 2.1), as they are easy to parallelize across several machines [34], which is often desirable in language and speech as we typically have millions of training examples. However, some methods have been studied where a powerful single computational device (such as a Graphical Processing Unit (GPU)) is used to quickly compute a small subset of the sum, and updates the model very frequently (but not as accurately as one would with batch methods), leading to stochastic or mini-batch methods [13], which can outperform batch method in terms of compute time to convergence. These methods are hard to parallelize because their main characteristic is very frequent updates of the parameters, which requires low latency and large memory bandwidth. Besides the discussion of batch versus mini-batch (or stochastic) methods in terms of accuracy of gradients versus more frequent model updates, a chief advantage of batch methods is that we can add second order information. In practice, some mini-batch methods have shown improvements when using curvature [42], but in general best results are obtained when considering batch methods due to having no noise in the estimation of our objective function.

The simplest reference point to start from when explaining second order methods is Newton's method with line search, where on iteration m we do an update of the form:

$$\boldsymbol{\theta}_{m+1} = \boldsymbol{\theta}_m - \alpha \mathbf{H}_m^{-1} \mathbf{g}_m, \tag{2.2}$$

where $\mathbf{H}_m$ and $\mathbf{g}_m$ are, respectively, the Hessian and the gradient on iteration m of the objective function (2.1); here, α would be chosen to minimize (2.1) at $\boldsymbol{\theta}_{m+1}$. For high dimensional problems it is not practical to invert the Hessian; however, we can efficiently approximate (2.2) using only multiplication by $\mathbf{H}_m$, by using the Conjugate Gradients (CG) method with a truncated number of iterations. In addition, it is possible to multiply by $\mathbf{H}_m$ without explicitly forming it, using what is known as the "Pearlmutter trick" [103] for

multiplying an arbitrary vector by the Hessian (the algorithm is described in Chapter 3); this is described for neural networks but is applicable to quite general types of functions[1]. This type of optimization method is known as "truncated Newton" or "Hessian-free inexact Newton" [89]. In [20], this method is applied but using only a subset of data to approximate the Hessian $\mathbf{H}_m$. A more sophisticated version of the same idea was described in the earlier paper [82], in which preconditioning is applied, the Hessian is damped with the unit matrix in a Levenberg-Marquardt fashion, and the method is extended to non-convex problems by using the Gauss-Newton matrix (described in Chapter 3) as a substitute the Hessian. These changes made it possible to use HF to effectively train deep networks from random initializations, which would not have been possible with any previously described versions of HF.

2.3 Neural Networks and Deep Learning

A Neural Network (NN) in the context of machine learning and computer science refers to an artificial neural network, but it was back in 1943 when McCulloch and Pitts – a neurophysiologist and a mathematician – presented results on how neurons may work and modeled a neural network using circuits. In the late 50s and early 60s, Widrow at Stanford successfully applied neural networks to solve a real problem (related to speech processing in phone lines). Neural Networks are sometimes referred as Multi Layer Perceptrons (MLP), which are related to the perceptron algorithm introduced in 1957 [113], and which can be seen as a neural network without hidden units. It is out of the scope of this their to review the history of neural networks, but the enthusiast reader is encouraged to read [111]. A lot of work has been done in neural networks for acoustic modeling, and further details are given in the following section.

Leaping forward in time, neural networks are back in fashion with the somewhat hyped term "Deep Learning", which rose from the 2006 work of Hinton [58]. One of the main properties of deep learning (or deep architectures) is to compose (or stack) several layers of computation (deep typically refers to having many "hidden" layers). In [137], the concept of stacking was proposed where simple modules of functions or classifiers are "stacked" on top of each other in order to learn complex functions or classifiers. Since then, various ways of implementing stacking operations have been developed, which can be categorized as unsupervised and supervised approaches.

Unsupervised approaches perform stacking in a layer-by-layer fashion that typically involves no label information. This gives rise to multiple layers in unsupervised feature learning, as exemplified in Deep Belief Networks [59, 57], layered Convolutional Neural Networks [63], Deep Auto-encoder [59, 37], etc. Applications of such stacking methods includes object recognition [63, 27], speech recognition [88], etc.

Supervised approaches, which are closer to the focus of this thesis, carry out stacking with the help of labels in the learning of each layer, which is typically a simple classifier. The new features for the stacked classifier at a higher level of the hierarchy come from combination of the classifier output of lower modules and the raw input features. Cohen and de Carvalho [28] developed a stacking architecture where the simple module is a Conditional Random Field. Another successful stacking architecture reported in [38] uses supervised

[1]This was actually known to the optimization community prior to [103]; see [97, Chapter 8] and [53].

information for stacking where the basic module is a simplified form of multilayer perceptron where the output units are linear and the hidden units are sigmoidal nonlinear. The linearity in the output units permits highly efficient, closed-form estimation (results of convex optimization) of the output network weights given the hidden units' outputs. Stacked context has also been used in [14], where a set of classifier scores are stacked to produce a more reliable detection. The proposed method in Chapter 4 will build a stacked architecture where each layer is a linear SVM, which has proven to be a successful classifier for many applications.

One of the challenges with the MLP and the DNN is that the objective function is non-convex, and as more hidden layers are added, finding a good local minima becomes more challenging. Motivated by this problem, DNNs with pretraining based on Restricted Boltzman Machines, denoted as Deep Belief Networks (DBNs), were introduced in [58] and have been applied to several fields such as computer vision (see [59]), phone classification (see [86]), speech recognition [133, 88, 119, 31], and speech coding (see [37]). The new idea is to train each layer independently in a greedy fashion, by sequentially using the hidden variables as observed variables to train each layer of the deep structure. Recently, the use of DNNs with no pretraining has also been studied [31, 119].

2.4 Speech Recognition, Acoustic Modeling, and Keyword Detection

Speech Recognition and Acoustic Modeling

The main focus of this thesis with regards to speech processing is acoustic modeling and keyword spotting. Acoustic modeling aims to predict a phonetic unit (a monophone, triphone state, or similar) from a segment of audio. This (generally probabilistic) model is then used in many current systems in a Hidden Markov Model (HMM) as the emission probability model, in which the hidden state (typically a triphone state) emits the observation (speech signal). HMM is a powerful statistical sequence model that was proposed in [7] and first introduced in speech recognition independently by [5] and [4]. Adding a Language Model (LM) one can decode a speech signal to its most likely sentence. A non-expert reader that has interest in the whole speech recognition pipeline is encouraged to read further details in one of the many references that exist in this topic (e.g. [50]).

Acoustic modeling is one of the key components in the performance of a speech recognition system. The most common trend up to the explosion of deep learning research focused on using Mel Frequency Cepstral Coefficients (MFCC) as features to train a Gaussian Mixture Model (GMM). Using features other than MFCCs has long been a focus of research in the speech recognition community, and the combination of various feature streams has proven useful in a variety of speech recognition systems. A common technique to merge streams is to use a Tandem method [54], in which processed phone posterior probabilities are appended to standard MFCCs.

As noted above, neural networks have been used for speech recognition for some time; in fact, there were early experiments at Stanford by B. Widrow and his students in the 1960s [124]. In the 1980s, a number of laboratories in Europe, the U.S, and Japan revived work on using neural networks to classify speech categories, and ultimately to generate speech

category probabilities for use with hidden Markov models, which by then were the dominant method for dealing with the sequence of sounds in speech. In general these networks used a single hidden layer and a modest number of categories, although as noted above there were notable exceptions. For example, the HNN/ACID approach of J. Fritsch [47] used a tree of networks in order to estimate a large number of context-dependent classes, using the simple factoring trick expounded in [90]. Input to the Fritsch system was processed by a number of networks in order to derive probability estimates at the leaves, and thus was an example of an extremely deep network that was also context-dependent. It performed quite well on a number of large vocabulary tasks at the time. This network and many others were examples of the hybrid HMM/MLP approach [91]. However, by 2000 it had become quite difficult for such systems to keep up competitively with the plethora of engineering advances that were developed for HMM/GMM systems, given the huge number of excellent laboratories that focused on improving the latter. The turning point for some of us was the Aurora task, in which we were required to use an HMM/GMM system with fixed characteristics and only could modify the front end. And so the Tandem approach [54] was adopted by many of us, in which the same networks we had developed were now used to generate features for an HMM/GMM system. This permitted researchers to continue to develop neural network approaches while taking advantage of advances in HMM/GMM systems.

Using these approaches, other systems were developed in which networks trained for an intermediate goal were then incorporated in larger networks, resulting in a deep structure; for example, a hierarchical system focused on temporal modulations of the spectrum [55] and systems that trained networks to focus on temporal characteristics within each critical band and then combined these networks with another network, e.g., [24]. Thus, many experiments were done in which some input variables (e.g., MFCC or mel spectra) were processed by multiple layers of artificial neurons prior to use by an HMM of some form. However, all of these techniques were largely relegated to providing an assist to a larger HMM/GMM system prior to the recent revival of hybrid HMM/MLP systems that has gone under the name of "deep neural networks" of various kinds.

One of the problems with MLPs is that the objective function is non-convex, and as more hidden layers are added, finding a good local minimum becomes more challenging. Motivated by this problem, Deep Belief Networks were introduced in [59] and have been applied in several fields such as computer vision (see [59]), phone classification (see [86, 88]), and speech coding (see [37]). The new idea is to train each layer independently in a greedy fashion, by sequentially using the hidden variables as observed variables to train each layer of the deep structure.

Initial success using DBNs on fairly small datasets and using small models quickly evolved, and the positive results of having deep models that yielded state-of-the-art acoustic modeling was adopted and generalized in many tasks and with much larger models [31, 119, 62, 57]. In the following paragraphs, I discuss previous work that focuses on the analysis and understanding of why neural networks have seen such a renaissance for acoustic modeling.

Since in this thesis I attempt to explain, in a limited context, the main contributing factors that make deep learning successful are, I next review some of the previous work that discussed such key points in chronological order.

In [31], many interesting points were raised. First, in a large system such as the one that was used there (with 2000 hours), having triphone units as targets instead of monophones

(which were more commonly use in previous work, with exceptions, as noted above) may have been the main contributing factor to the results obtained (4% absolute gains). Adding layers generally resulted in better accuracy, but the number of parameters was increased with every layer added, so that it was not entirely clear what was the main contributing factor to the good results - the depth, or the larger number of parameters. However, a flat (or shallow) model having the same parameters as the deepest model was also trained, which was 2% worse than the deep model. Additionally, pretraining added 2% in accuracy.

In [119], another method for pretraining was used, and again the depth of the model was demonstrated to be one of the key contributions to the 30% relative improvement. An important contribution in that work was the effect of pretraining. For smaller tasks such as TIMIT or MNIST, pretraining was found important as, besides helping the optimization of a deep architecture, provided a form of regularization to the network by using unsupervised learning. In the work by Seide et al, the architecture rather than pretraining seemed to be more important, and other forms of pretraining such as discriminative pretraining was able to perform as well as RBM pretraining.

Recent work in [35, 87] analyzed the input to the networks, and showed that log filter banks may be a better input instead of other transformations (e.g., MFCC), which have been the mainstream feature in classical GMMs due to some assumptions such as diagonal covariance.

Keyword Detection

Although heavily related to speech recognition, keyword spotting (or detection) is similar to the object recognition task in computer vision, where given a signal (image or speech utterance), the goal is to predict if a given object is present in it (this could be a chair in a image, or the word "capital" in an utterance). Besides detecting if a word is present, we can also predict the location of that word (similarly for an object in an image). The research on keyword spotting has paralleled the development of the Automatic Speech Recognition (ASR) domain in the last years. Like ASR, keyword spotting has first been addressed with models based on Dynamic Time Warping (DTW) [19, 56]. Then, approaches based on discrete HMMs were introduced [67]. Finally, discrete HMMs have been replaced by continuous HMMs [108]. There have been many attempts to do discriminative training, but the most relevant one is [51], which targets a figure of merit instead of the error rate, and which is the baseline that I used in Section 6.2.

2.5 Computer Vision and Object Classification

There has been a trend in object, acoustic and image classification to move the complexity from the classifier to the feature extraction step. The main focus of many state of the art systems has been to build rich feature descriptors (e.g., SIFT [79], HOG [32] or MFCC [33]), and use sophisticated non-linear classifiers, usually based on kernel functions and SVM or mixture models. Thus, the complexity of the overall system (feature extractor followed by the non-linear classifier) is shared in the two blocks. Vector Quantization [44], and Sparse Coding [100, 139, 142] have theoretically and empirically been shown to work well with linear classifiers. In [27], the authors note that the choice of codebook does not seem to impact performance significantly, and encoding via an inner product plus a

non-linearity can effectively replace sparse coding, making testing significantly simpler and faster.

A disturbing issue with sparse coding + linear classification is that with a limited codebook size, linear separability might be an overly strong statement, undermining the use of a single linear classifier. This has been empirically verified: as we increase the codebook size, the performance keeps improving [27], indicating that such representations may not be able to fully exploit the complexity of the data [12]. In fact, recent success on PASCAL VOC could partially be attributed to a huge codebook [140]. While this is theoretically valid, the practical advantage of linear models diminishes quickly, as the computation cost of feature generation, as well as training a high-dimensional classifier (despite linear), can make it as expensive as classical non-linear classifiers.

Despite this trend to rely on linear classifiers and overcomplete feature representations, sparse coding is still a flat model, and efforts have been made to add flexibility to the features. In particular, Deep Coding Networks [78] proposed an extension where a higher order Taylor approximation of the non-linear classification function is used, which shows improvements over coding that uses one layer. My approach can be seen as an extension to sparse coding used in a stacked architecture.

I illustrate the feature extraction pipeline that is composed of encoding dense local patches and pooling encoded features later in this thesis in Figure 5.1, and provide a brief review here. This pipeline is architecturally very similar to Convolutional Neural Networks (see [76, 73]), but instead relies on unsupervised learning (rather than fine tuning) of the network parameters. Specifically, starting with an input image $\mathbf{I}$, I formally define the encoding and pooling stages as follows.

(1) Coding. In the coding step, one extracts local image patches[2], and encode each patch to c activation values based on a dictionary of size c (learned via a separate dictionary learning step). These activations are typically binary (in the case of vector quantization) or continuous (in the case of e.g., sparse coding), and it is generally believed that having an over-complete ($c >$ the dimension of patches) dictionary while keeping the activations sparse helps classification, especially when linear classifiers are used in the later steps.

I will mainly focus on the decoupled encoding methods, in which the activation of one code does not rely on other codes, such as threshold encoding [27], which computes the inner product between a local patch $\mathbf{x}$ and each code, with a fixed threshold parameter α: $\mathbf{c}(\mathbf{x}) = \max\{0, \mathbf{x}^\top \mathbf{D} - \alpha\}$ where $\mathbf{D} \in \mathbb{R}^{d \times c}$ is the dictionary. Such methods have been increasingly popular mainly for their efficiency over coupled encoding methods such as sparse coding, for which a joint optimization needs to be carried out. Their employment in several deep models (e.g., [73]) also suggests that such a simple non-linearity may suffice to learn a good classifier in the later stages.

(2) Learning the dictionary: Recently, it has been found that relatively simple dictionary learning and encoding approaches lead to surprisingly good performances [26, 117]. For example, to learn a dictionary $\mathbf{D} = [\mathbf{d}_1, \mathbf{d}_2, \cdots, \mathbf{d}_c]$ of size K from a set of local patches

[2] Although I use the term "patches" throughout the thesis, the pipeline works with local image descriptors, such as SIFT, as well.

$\mathcal{X} = \{\mathbf{x}_1, \mathbf{x}_2, \cdots, \mathbf{x}_N\}$ each reshaped as a vector of pixel values, one could simply adopt the K-means algorithm, which aims to minimize the squared distance between each patch and its nearest code: $\min_{\mathbf{D}} \sum_{i=1}^{N} \min_j \|\mathbf{x}_i - \mathbf{d}_j\|_2^2$. I refer to [26] for a detailed comparison about different dictionary learning and encoding algorithms.

(3) Pooling. Since the coding result are highly over-complete and highly redundant, the pooling layer aggregates the activations over a spatial region of the image to obtain a c dimensional vector, where each dimension of the pooled feature is obtained by taking the output of the corresponding code in the given spatial region (also called receptive field in the literature) and performing a predefined operator (usually average or max). Figure 5.1 shows an example when average pooling is carried out over the whole image. In practice one may define multiple spatial regions per image (such as a regular grid or a spatial pyramid), and the global representation for the image will then be a vector of size c times the number of spatial regions.

Chapter 3

Optimization Challenges in Learning

Part of the work that appears on this chapter has been published in peer reviewed conferences. The optimization algorithm was presented at NIPS 2011 an AISTATS 2012 [132], and the Recurrent Neural Network work was presented at ICASSP 2012 [134].

The main challenges in optimizing

$$f(\boldsymbol{\theta}) = -\log(p(\mathbf{Y}|\mathbf{X};\boldsymbol{\theta})) = -\sum_{i=1}^{N} \log(p(\mathbf{y}_i|\mathbf{x}_i;\boldsymbol{\theta})) \tag{3.1}$$

are as follows:

- $\boldsymbol{\theta}$ can be very high dimensional
- $\mathbf{Y}$ and $\mathbf{X}$ could be very large (both in dimensionality and in number of training samples)
- The function to optimize f (or, equivalently, the model p) can be expensive to compute
- The objective function to optimize can be non-convex and ill-conditioned

As a result, I propose a new algorithm which I call Krylov Subspace Descent (KSD) which partially copes with the above issues by:

- Never storing more than a few copies of the parameter $\boldsymbol{\theta}$, whilst achieving second order convergence rates
- Using large batches and accurate updates of parameters, thus being able to efficiently use compute clusters
- Using curvature information, which tremendously helps some problems which are ill-conditioned (near zero curvature)
- Being mostly hyperparameter free, thus being applicable to a large number of models, merit functions, and problem scales (the same parameter settings have been used for many different models, datasets, and scales)

My method is quite similar to the one described in [82], which I will refer to as Hessian Free (HF). I also multiply by the Hessian (that is, the matrix of second derivatives w.r.t. the parameters) using the Pearlmutter trick on a subset of data. The Pearlmutter trick computes the product of $\mathbf{H}$ times a vector without explicitly storing the matrix, at the cost of a forward and backward pass through the neural network, hence the name "Hessian Free" (see Algorithm 1 for more details). The chief difference between KSD and HF is that, in each iteration, instead of approximately computing $(\mathbf{H}_m + \lambda\mathbf{I})^{-1}\mathbf{g}_m$ using truncated Conjugate Gradient (CG), I compute a basis for the Krylov subspace of dimension K which is defined by the span of $\mathbf{g}_m, \mathbf{H}_m\mathbf{g}_m, \ldots \mathbf{H}_m^{K-1}\mathbf{g}_m$ for some K fixed in advance (e.g., $K = 20$), and numerically optimize the parameter change within this subspace, using BFGS[1] [96] to minimize the original nonlinear objective function measured on a subset of the training data. It is easy to show that, for any λ, the approximate solution to $\mathbf{H}_m + \lambda\mathbf{I}$ found by K iterations of CG will lie in this subspace, so I am in effect automatically choosing the optimal λ in the Levenburg-Marquardt smoothing method of HF – although the algorithm is free to choose a solution more general than this. This is clear from the CG algorithm itself, and from the fact that the order-K Krylov subspaces generated by $\mathbf{g}$ and $\mathbf{H} + \lambda\mathbf{I}$ are all the same irrespective of λ. Note that both my method and HF use preconditioning, which I have glossed over in the discussion above. Compared with HF, the advantages of my method are:

- Greater simplicity and robustness: there is no need for heuristics to initialize and update the smoothing value λ.
- Generality: unlike HF, my method can be applied even if $\mathbf{H}$ (or whatever approximation or substitute used) is not positive semidefinite.
- Empirical advantages: my method generally seems to work better than HF in both optimization speed and classification performance.

The chief disadvantages versus HF are:

- Memory requirement: it requires storage of K times the parameter dimension to store the subspace (HF does not require memory proportional to the number of CG iterations).
- Convergence properties: the use of a subset of data to optimize over the subspace will prevent convergence to an optimum.

Regarding the convergence properties: for deep neural networks, this is more of a theoretical than a practical problem, since for typical setups in training deep networks the residual parameter noise due to the use of data subsets would be far less than that due to overtraining. One would hope that not-too-restrictive conditions could be found under which the algorithm (or a modified version of it, with increasing subset sizes) could be shown to converge; however, I do not have either the time or the skills needed to perform this type of analysis by myself. I also believe that application of the normal types of convergence proof would fail to capture the reasons why the algorithm is better than gradient

[1] BFGS (named after its inventors) is a second order method that uses a low rank approximation of the Hessian matrix so that it can be efficiently inverted thanks to the Matrix Inversion Lemma.

descent, and it would be very hard to obtain convergence results that were strong enough to be interesting. However, empirical evidence suggests that convergence to a local minima is faster using methods such as KSD or HF than with vanilla SGD.

My motivation for the work presented here is twofold: firstly, I am interested in large-scale non-convex optimization problems where the parameter dimension and the number of training samples is large and the Hessian has a large condition number. I have previously investigated quite different approaches based on preconditioned Stochastic Gradient Descent (SGD) to solve an instance of this type of optimization problem (my method could be viewed as an extension to [114]), but after reading [82] my interest switched to methods of the HF type. Secondly, I have an interest in deep neural nets, particularly to solve problems in speech recognition, and I was intrigued by the suggestion in [82] that the use of optimization methods of this type might remove the necessity for pretraining, which would result in a welcome simplification. Other recent work on the utility of second order methods for deep neural networks includes [9] and [75].

3.1 The Hessian matrix and the Gauss-Newton matrix

The Hessian matrix $\mathbf{H}$ can be used implicitly in HF optimization whenever it is guaranteed positive semidefinite, i.e., when minimizing functions that are convex in the parameters. For non-convex problems, it is possible to substitute a positive definite approximation to the Hessian. One option is the Fisher information matrix,

$$\mathbf{F} = \sum_i \mathbf{g}_i \mathbf{g}_i^T, \tag{3.2}$$

where indices i correspond to samples and the $\mathbf{g}_i$ quantities are the gradients for each sample. This is a suitable stand-in for the Hessian because it is in a certain sense dimensionally the same, i.e. it changes the same way under transformations of the parameter space. If the model can be interpreted as producing a probability or likelihood, it is possible under certain assumptions (including model correctness) to show that close to convergence, the Fisher and Hessian matrices have the same expected value. The use of the Fisher matrix in this way is known as Natural Gradient Descent [3]; in [114], a low-rank approximation of the Fisher matrix was used instead. Another alternative that has less theoretical justification but which seems to work better in practice in the case of neural networks is the Gauss-Newton matrix, or rather a slight generalization of the Gauss-Newton matrix that we will now describe.

3.1.1 The Gauss-Newton matrix

The Gauss-Newton matrix is defined when we have a function (typically nonlinear) from a vector to a vector, $f : \mathbb{R}^n \to \mathbb{R}^m$. Let the Jacobian of this function be $\mathbf{J} \in \mathbb{R}^{m \times n}$, then the Gauss-Newton matrix is $\mathbf{G} = \mathbf{J}^T \mathbf{J}$, with $\mathbf{G} \in \mathbb{R}^{n \times n}$. If the problem is least-squares on the output of f, then $\mathbf{G}$ can be thought of as one term in the Hessian on the input to f. In its application to neural-network training, for each training example I consider the network as a nonlinear function from the neural-network parameters $\boldsymbol{\theta}$ to the output of the network, with the neural-network input treated as a constant. As in [118], I generalize

this from least squares to general convex error functions by using the expression $\mathbf{J}^T\mathbf{H}\mathbf{J}$, where $\mathbf{H}$ is the (positive semidefinite) second derivative of the error function w.r.t. the neural network output. This can be thought of as the part of the Hessian that remains after ignoring the nonlinearity of the neural-network in the parameters. In the rest of this document, following [82] I will refer to this matrix $\mathbf{J}^T\mathbf{H}\mathbf{J}$ simply as the Gauss-Newton matrix, or $\mathbf{G}$, and depending on the context, I may actually be referring to the summation of this expression over a number of neural-network training samples.

3.1.2 Efficiently multiplying by the Gauss-Newton matrix

As described in [118], it is possible to efficiently multiply a vector by $\mathbf{G}$ using a version of the "Pearlmutter trick"; the algorithm is similar in spirit to backprop and for completeness I give it here as Algorithm 1; however, the reader should feel free to skip over this section if this level of detail is not required.

My notation and my derivation for this algorithm differ from [103, 118], and I will explain this briefly with the hope that my explanation is easier to follow. The basic idea is to write down an algorithm that efficiently computes the inner product of the Gauss-Newton matrix with two given vectors (i.e. $s = \boldsymbol{\theta}_2^T\mathbf{G}\boldsymbol{\theta}_1$), and then use reverse-mode automatic differentiation (similar to neural-net backprop) to compute the derivative of this scalar w.r.t. $\boldsymbol{\theta}_2$, which will equal the desired product $\mathbf{G}\boldsymbol{\theta}_1$.

First I will explain how I compute the inner product. Imagine that we are given a parameter vector $\boldsymbol{\theta}$, and two vectors $\boldsymbol{\theta}_1$ and $\boldsymbol{\theta}_2$ which we interpret as directions in parameter space; we want to write down an algorithm that computes the scalar $s = \boldsymbol{\theta}_2^T\mathbf{G}\boldsymbol{\theta}_1$. Assume the neural-network input is given and fixed; let $\mathbf{v}$ be the network output, and write it as $\mathbf{v}(\boldsymbol{\theta})$ to emphasize the dependence on the parameters, and then let $\mathbf{v}_1$ be defined as

$$\mathbf{v}_1 = \lim_{\alpha \to 0} \frac{1}{\alpha} \left(\mathbf{v}(\boldsymbol{\theta} + \alpha\boldsymbol{\theta}_1) - \mathbf{v}(\boldsymbol{\theta}) \right), \tag{3.3}$$

so that $\mathbf{v}_1 = \mathbf{J}\boldsymbol{\theta}_1$. I define $\mathbf{v}_2$ similarly. These can both be computed in a modified forward pass through the network, using forward-mode automatic differentiation. Then, if $\mathbf{H}_\mathcal{E}$ is the Hessian of the error function in the output of the network (taken at parameter value $\boldsymbol{\theta}$), s is given by

$$s = \mathbf{v}_2^T\mathbf{H}_\mathcal{E}\mathbf{v}_1, \tag{3.4}$$

since $\mathbf{v}_2^T\mathbf{H}_\mathcal{E}\mathbf{v}_1 = \boldsymbol{\theta}_2^T\mathbf{J}^T\mathbf{H}_\mathcal{E}\mathbf{J}\boldsymbol{\theta}_1 = \boldsymbol{\theta}_2^T\mathbf{G}\boldsymbol{\theta}_1$. The Hessian $\mathbf{H}_\mathcal{E}$ of the error function would typically not be constructed as a matrix, but we would compute (3.4) given some analytic expression for $\mathbf{H}$. This Hessian $\mathbf{H}_\mathcal{E}$ w.r.t. the output activations for a particular sample should not be confused with the Hessian w.r.t. the parameter vector. Suppose we have written down the algorithm for computing s (I have not done so here because of space constraints). Then we treat $\boldsymbol{\theta}_1$ as a fixed quantity, but compute the derivative of s w.r.t. $\boldsymbol{\theta}_2$, taking $\boldsymbol{\theta}_2$ around zero for convenience. This derivative equals the desired product $\mathbf{G}\boldsymbol{\theta}_1$. This is how I obtained Algorithm 1. In the algorithm I denote the derivative of s w.r.t. a quantity x by $\hat{x}$, i.e. by adding a hat. Note that in this algorithm, I have a "backward pass" for quantities with subscript 2, which did not appear in the forward pass, because they were zero (since we take $\boldsymbol{\theta}_2 = 0$) and I optimized them out.

Something to note here is that when the linearity of the last layer is softmax and the error is negated cross-entropy (equivalently negated log-likelihood, if the label is known),

I actually view the softmax nonlinearity as part of the error function. This is a closer approximation to the Hessian, and the error function remains positive semidefinite.

To explain the notation of Algorithm 1: $\mathbf{h}^{(i)}$ is the input to the nonlinearity of the i'th layer and $\mathbf{v}^{(i)}$ is the output; $\odot$ means elementwise multiplication; $\phi^{(i)}$ is the nonlinear function of the i'th layer, and when we apply it to vectors it acts elementwise; $\mathbf{W}^{(1)}$ is the matrix of neural-network weights for the first layer (so $\mathbf{h}^{(1)} = \mathbf{W}^{(1)}\mathbf{v}^{(0)}$, and so on); I use the subscript 1 for quantities that represent how quantities change when we move the parameters in direction $\boldsymbol{\theta}_1$ (as in Eq. (3.3)). The error function is written as $\mathcal{E}(\mathbf{v}^{(L)}, y)$ (where L is the last layer), and y, which may be a discrete value, a scalar or a vector, represents the supervision information which the network is trained with. Typically $\mathcal{E}$ would represent a squared loss or negated cross-entropy. In the squared-loss case, the quantity $\frac{\partial^2}{\partial \mathbf{v}^2}\mathcal{E}(\mathbf{v}^{(L)}, y)$ in Line 10 of Algorithm 1 is just the unit matrix. The other case I deal with here is negated cross entropy. I include the soft-max nonlinearity in the error function, treating the elements of the output layer $\mathbf{v}^{(L)}$ as unnormalized log probabilities. If the elements of $\mathbf{v}^{(L)}$ are written as v_j and we let $\mathbf{p}$ be the vector of probabilities, with $p_j = \exp(v_j)/\sum_i \exp(v_i)$, then the matrix $\mathbf{H}_{\mathcal{E}}$ of second derivatives is given by

$$\frac{\partial^2}{\partial \mathbf{v}^2}\mathcal{E}(\mathbf{v}^{(L)}, y) = \mathrm{diag}(\mathbf{p}) - \mathbf{p}\mathbf{p}^T. \tag{3.5}$$

Algorithm 1 Compute product $\hat{\boldsymbol{\theta}}_2 = \mathbf{G}\boldsymbol{\theta}_1$: MultiplyG$(\boldsymbol{\theta}, \boldsymbol{\theta}_1, \mathbf{x}, y)$

1: // Note, $\boldsymbol{\theta} = (\mathbf{W}^{(1)}, \mathbf{W}^{(2)}, \ldots)$ and $\boldsymbol{\theta}_1 = (\mathbf{W}_1^{(1)}, \mathbf{W}_2^{(2)}, \ldots)$.
2: $\mathbf{v}^{(0)} \leftarrow \mathbf{x}$
3: $\mathbf{v}_1^{(0)} \leftarrow \mathbf{0}$
4: **for** $l = 1 \ldots L$ **do**
5: $\quad \mathbf{h}^{(l)} \leftarrow \mathbf{W}^{(l)}\mathbf{v}^{(l-1)}$
6: $\quad \mathbf{h}_1^{(l)} \leftarrow \mathbf{W}^{(l)}\mathbf{v}_1^{(l-1)} + \mathbf{W}_1^{(l)}\mathbf{v}^{(l-1)}$
7: $\quad \mathbf{v}^{(l)} \leftarrow \phi^{(l)}(\mathbf{h}^{(l)})$
8: $\quad \mathbf{v}_1^{(l)} \leftarrow \phi'^{(l)}(\mathbf{h}^{(l)}) \odot \mathbf{h}_1^{(l)}$
9: **end for**
10: $\hat{\mathbf{v}}_2^{(L)} \leftarrow \frac{\partial^2}{\partial \mathbf{v}^2}\mathcal{E}(\mathbf{v}^{(L)}, y)\mathbf{v}_1^{(L)}$
11: **for** $l = L \ldots 1$ **do**
12: $\quad \hat{\mathbf{h}}_2^{(l)} \leftarrow \hat{\mathbf{v}}_2^{(l)} \odot \phi'^{(l)}(\mathbf{h}^{(l)})$
13: $\quad \hat{\mathbf{v}}_2^{(l-1)} \leftarrow \mathbf{W}^{(l)\,T}\,\hat{\mathbf{h}}_2^{(l)}$
14: $\quad \hat{\mathbf{W}}_2^{(l)} \leftarrow \hat{\mathbf{h}}_2^{(l)}\,\mathbf{v}^{(l-1)\,T}$
15: **end for**
16: **return** $\hat{\boldsymbol{\theta}}_2 \equiv \left(\hat{\mathbf{W}}_2^{(1)}, \ldots, \hat{\mathbf{W}}_2^{(L)}\right)$

3.2 Krylov Subspace Descent: overview

Now I describe the method, and how it relates to Hessian Free (HF) optimization. The discussion in the previous section (on the Hessian versus Gauss-Newton matrix) is orthogonal to the distinction between KSD and HF, because either method can use any Hessian substitute, with the proviso that my method can use the Hessian even when it is not positive definite.

In the rest of this section I will use $\mathbf{H}$ to refer to either the Hessian or a substitute such as $\mathbf{G}$ or $\mathbf{F}$. In [82] and in the work I describe here, these matrices are approximated using a subset of data samples. In both HF and KSD, the whole computation is preconditioned using the diagonal of the Fisher matrix $\mathbf{F}$ (since this is easy to compute, although other approaches have been recently proposed [23]); however, in this overview I will gloss over this preconditioning. In HF, on each iteration the CG algorithm is used to approximately compute

$$\mathbf{d} = -(\mathbf{H} + \lambda \mathbf{I})^{-1}\mathbf{g}, \tag{3.6}$$

where $\mathbf{d}$ is the step direction, and $\mathbf{g}$ is the gradient. As described in [82], CG aims to minimize the function $\frac{1}{2}\mathbf{x}^T(\mathbf{H} + \lambda \mathbf{I})\mathbf{x} - \mathbf{x}^T\mathbf{g}$ which is a quadratic approximation of the objective function. The approximate solution $\mathbf{d}_{CG}$ reached after K iterations of CG will lie in the Krylov subspace of dimension K which is, by definition, the subspace spanned by $\{\mathbf{g}, (\mathbf{H} + \lambda \mathbf{I})\mathbf{g}, \ldots, (\mathbf{H} + \lambda \mathbf{I})^{K-1}\mathbf{g}\}$. This is easy to see by looking at the CG algorithm.

In HF, the step size to take in the direction $\mathbf{d}_{CG}$ is determined by a backtracking line search. The value of λ is kept updated by Levenburg-Marquardt style heuristics. Other heuristics are used to control the stopping of the CG iterations. In addition, the CG iterations for optimizing $\mathbf{d}$ are not initialized from zero (which would be the natural choice) but from the previous value of $\mathbf{d}$; this loses some convergence guarantees but seems to improve performance, perhaps by adding a kind of momentum to the updates.

In my method, I compute an orthogonal basis $\mathbf{P}$ for the subspace spanned by $\{\mathbf{g}, \mathbf{H}\mathbf{g}, \ldots, \mathbf{H}^{K-1}\mathbf{g}, \mathbf{d}_{\text{prev}}\}$, which is the Krylov subspace of dimension K generated by $\mathbf{g}$ and $\mathbf{H}$, augmented with the previous search direction. Note that the Krylov subspace of dimension $\mathbf{K}$ generated by $\mathbf{g}$ and $\mathbf{H} + \lambda \mathbf{I}$ is the same as that generated by $\mathbf{g}$ and $\mathbf{H}$, which is easy to verify. The method optimizes the objective function f over this subspace using BFGS, approximating the objective function using a subset of samples. The BFGS phase may be viewed as a modification of the line search phase of HF, but done in a higher dimension and using a subset of the data. The BFGS phase uses a different subset of data from that used to compute the Hessian; if I used the same subset I would get a very biased estimate of the optimal step to take within the subspace.

The complete algorithm is given as Algorithm 2. The most important parameter is K, the dimension of the Krylov subspace (e.g. 20). The flooring constant ϵ is an unimportant parameter; I used 10^{-4}. The subset sizes may be important; I recommend that $\mathcal{A}_n$ should be all of the training data, and $\mathcal{B}_n$ and $\mathcal{C}_n$ should each be about $1/K$ of the training data, and disjoint from each other but not from $\mathcal{A}_n$. This is the subset size that keeps the computation approximately balanced between the gradient computation, subspace construction and subspace optimization. Implementations of the BFGS algorithm would typically also have parameters: for instance, parameters of the line-search algorithm and stopping criteria; however, I expect that in practice these would not have too much effect on performance because the algorithm is likely to converge almost exactly (since the subspace dimension and the number of iterations are about the same).

Each iteration of Algorithm 2 computes a Krylov subspace of dimension K from the gradient and the Hessian or Hessian substitute, and optimizes over this subspace using BFGS with the objective function approximated using a data subset $\mathcal{C}_n$. Lines 7 to 9 are an additional preconditioning step to help the BFGS to converge faster, in which I try to find new co-ordinates in which $\bar{\mathbf{H}}$ is the unit matrix. Line 7 is needed to handle cases where $\bar{\mathbf{H}}$

Algorithm 2 Krylov Subspace Descent

1: $\mathbf{d}_{\text{prev}} \leftarrow \mathbf{e}_1$ // or any arbitrary nonzero vector
2: **for** $n = 1, 2 \ldots$ **do**
3: // Sample three sets from training data, $\mathcal{A}_n$, $\mathcal{B}_n$ and $\mathcal{C}_n$.
4: $\mathbf{g} \leftarrow \frac{1}{|\mathcal{A}_n|} \sum_{i \in \mathcal{A}_n} \mathbf{g}_i(\boldsymbol{\theta})$ // Get average function gradient over this batch.
5: Set $\mathbf{D}$ to diagonal of Fisher matrix on $\mathcal{A}_n$, floored to ϵ times its maximum.
6: Find $\mathbf{P}$ and $\bar{\mathbf{H}}$ on subset $\mathcal{B}_n$ (algorithm omitted)
7: Let $\hat{\mathbf{H}}$ be the result of flooring the eigenvalues of $\bar{\mathbf{H}}$ to ϵ times the maximum.
8: Do the Cholesky decomposition $\hat{\mathbf{H}} = \mathbf{C}\mathbf{C}^T$
9: Let $\bar{\mathbf{P}} = \mathbf{P}\mathbf{C}^{-T}$ (do this in-place; $\mathbf{C}^{-T}$ is upper triangular)
10: $\mathbf{a} \leftarrow 0 \in \mathbb{R}^{K+1}$
11: Find the value $\mathbf{a}^*$ that minimizes the objective function measured on $\mathcal{C}_n$, using about K iterations of BFGS, with objective function measured at $\boldsymbol{\theta} + \bar{\mathbf{P}}\mathbf{a}$ and gradient $\bar{\mathbf{P}}^T\mathbf{g}$ (where $\mathbf{g}$ is the gradient w.r.t. the parameters, measured at parameter-value $\boldsymbol{\theta} + \bar{\mathbf{P}}\mathbf{a}$).
12: $\mathbf{d}_{\text{prev}} \leftarrow \bar{\mathbf{P}}\mathbf{a}^*$
13: $\boldsymbol{\theta} \leftarrow \boldsymbol{\theta} + \mathbf{d}_{\text{prev}}$
14: **end for**

Dataset	#Train	#Test	Input	Output	Model	Task
CURVES	20K	10K	784 (bin.)	784 (bin.)	400-200-100-50-25-5	AE
MNIST_{AE}	60K	10K	784 (bin.)	784 (bin.)	1000-500-250-30	AE
MNIST_{CL}	60K	10K	784 (bin.)	10 (class)	500-500-2000	Class
$\text{MNIST}_{CL,PT}$[1]	60K	10K	784 (bin.)	10 (class)	500-500-2000	Class
Aurora	1.2M	100K[2]	352 (real)	56 (class)	512-1024-1536	Class
Starcraft	900	100	5077 (mix)	8 (class)	10	Class

Table 3.1. Datasets and models used in my setup.

has zero or negative eigenvalues. The flooring described in Line 7 may be done as follows: do the Singular Value Decomposition $\bar{\mathbf{H}} = \mathbf{U}\mathbf{D}\mathbf{V}^T$, then let $\hat{\mathbf{D}}$ be a floored version of $\mathbf{D}$, with diagonal elements $\hat{d}_i = \max(d_i, \epsilon \max_i d_i)$; then let $\hat{\mathbf{H}} = \mathbf{U}\hat{\mathbf{D}}\mathbf{U}^T$ (note: the use of $\mathbf{U}$ on both sides is not a typo). This has the effect of flipping the sign of negative eigenvalues, and then imposing a floor of ϵ times the largest eigenvalue.

3.3 Experiments

To evaluate KSD, I performed several experiments to compare it with SGD and with other second order optimization methods[2], namely L-BFGS and HF. I report both training and cross validation errors, and running time (I terminated the algorithms with an early stopping rule using held-out validation data). My implementations of both KSD and HF are based on Matlab using Jacket[3] to perform the expensive matrix operations on a Geforce GTX580 GPU with 1.5GB of memory.

[2]Note: I may properly speak of HF and KGD as second-order methods only when $\mathbf{H}$ is the actual Hessian matrix

[3]www.accelereyes.com

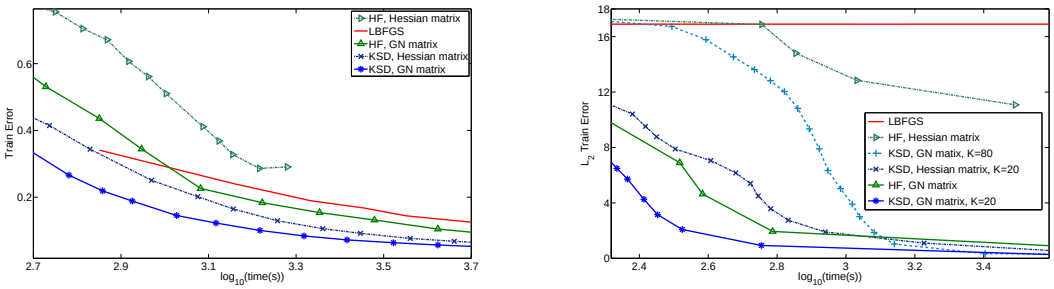

Figure 3.1. Aurora and CURVES convergence curves for various algorithms.

3.3.1 Datasets and models

Here I describe the datasets that I used to compare KSD to other methods.

- CURVES: Artificial dataset consisting of curves at 28×28 resolution. The dataset consists of 20K training samples, and 10K testing samples. I considered an autoencoder network, as in [59].
- MNIST: Single digit vision classification task. The digits are 28×28 pixels, with a 60K training, and 10K testing samples. I considered both an autoencoder network, and classification [59].
- Aurora: Spoken digits dataset, with different levels of real noise (airport, train station, ...). I used Perceptual Linear Prediction features and performed classification of 56 English phones. These frame level phone error rates are the ones reported in Table 3.2. Also reported in the text are Word Error Rates, which were produced by using the phone posteriors in a Tandem system, concatenated with standard MFCC to train a Hidden Markov Model with Gaussian Mixture Model emissions. Further details on the setup can be found in [133].
- Starcraft: The dataset consists of a real time strategy video game sequences from 1000 games. The goal is to predict the strategy the opponent chose based on a fully observed game sequence after five minutes, and features contain orderings between buildings, presence/absence features, or times that certain buildings were built.

The models (i.e. network architectures) for each dataset are summarized in Table 3.1. I tried to explore a wide variety of models covering different sizes, input and output characteristics, and tasks. Note that the error reported for the autoencoder (AE) task is the L2 norm squared between input and output, and for the classification (Class) task is the classification error (i.e. 100 - accuracy). The non linearities considered were logistic functions for all the hidden layers except for the "coding" layer (i.e. middle layer) in the autencoders, which was linear, and the visible layer for classification, which was softmax.

[1]For $\text{MNIST}_{CL,PT}$ I initialize the weights using pretraining RBMs as in [59]. In the other experiments, I did not find a significant difference between pretraining and random initialization as in [82].

[2]I report both classification error rate on a 100K CV set, and word error rate on a 5M testing set with different levels of noise

	HF			KSD		
Dataset	Tr. err.	CV err.	Time	Tr. err.	CV err.	Time
CURVES	0.13	**0.19**	1	0.17	0.25	0.2
MNIST_{AE}	1.7	2.7	1	1.8	**2.5**	0.2
MNIST_{CL}	0%	2.01%	1	0%	**1.70%**	0.6
$\text{MNIST}_{CL,PT}$	0%	1.40%	1	0%	**1.29%**	0.6
Aurora	5.1%	8.7%	1	4.5%	**8.1%**	0.3
Starcraft	0%	11%	1	0%	**5%**	0.7

Table 3.2. Results comparing two second order methods: Hessian Free and Krylov Subspace Descent. Time reported is relative to the running time of HF (lower than 1 means faster).

3.4 Results and discussion

Table 3.2 summarizes my results. Observe that KSD converges faster than HF, and tends to lead to lower generalization error. My implementation for the two methods is almost identical; the steps that dominate the computation (computing objective functions, gradients and Hessian or Gauss-Newton products) are shared between both and are computed on a GPU.

For all the experiments I used the Gauss-Newton matrix unless otherwise specified. The dimensionality of the Krylov subspace was set to 20, the number of BFGS iterations was set to 30 (although in many cases the optimization on the projected gradients converged before reaching 30), and an L2 regularization term was added to the objective function. However, motivated by the observation that on CURVES, HF tends to use a large number of iterations, I experimented with a larger subspace dimension of $K = 80$ and these are the numbers I report in Table 3.2.

For comparability in memory usage with KSD, I used a moving window of size 10 for the L-BFGS methods. I do not show SGD performance in Figures 3.1 and 3.1 as it was worse than L-BFGS.

When using HF or KSD, pre-training helped significantly in the MNIST classification task, but not for the other tasks (I do not show the results with pre-training in the other cases; there was no substantial difference in training or testing errors). However, when using SGD or CG for optimization (results not shown), pre-training helped on all tasks except Starcraft (which is not a deep network). This is consistent with the notion put forward in [82] that it might be possible to do away with the need for pre-training if one uses powerful second-order optimization methods. The one case in which pre-training helped even when using HF or KSD, is MNIST; this dataset had zero training errors, which in consistent with the regularization interpretation of pre-training which is put forward in [43]. The experiments support the notion that when using advanced second-order optimization methods and when overfitting is not a major issue, pre-training is not necessary.

In Figures 3.1 and 3.1, I show the convergence of KSD and HF with both the Hessian and Gauss-Newton matrices. HF eventually "gets stuck" when using the Hessian; the algorithm was not designed to be used for non-positive definite matrices, and the CG routine terminates when it detects a non-descent direction. Even before getting stuck, it is clear that it does not work well with the actual Hessian. My method also works better with

the Gauss-Newton matrix than with the Hessian, although the difference is smaller. My method is always faster than HF and L-BFGS.

Lastly, I performed a new set of experiments while working at Google using much larger datasets and models. In particular, I took at convergence (using Google's approach to train their acoustic modeling [62]) the deep neural network that performs acoustic modeling and computed several epochs on a very large compute cluster. Unfortunately, I was not able to use KSD but, instead, used L-BFGS as a second order method (in contrast to Adagrad [42], the first order method that Google used). With this, I obtained about 0.5% absolute improvement on frame accuracy (Google system had around 30% error on a system trained on thousands of hours), making a stronger point for second order methods finding better solutions than first order methods (not related to local optima, but rather to low curvature spaces in which stochastic gradient descent gets stuck).

3.5 An Application: Revisiting RNNs for Acoustic Modeling

3.5.1 Motivation

In this section, I show how the new training principles and optimization techniques for neural networks that I described in this chapter can be used for different network structures. In particular, besides training regular deep neural networks (DNN), I revisit the Recurrent Neural Network (RNN), which explicitly models the Markovian dynamics of a set of observations through a non-linear function with a much larger hidden state space than traditional sequence models such as an HMM. I apply pretraining principles used for DNNs and second-order optimization techniques to train an RNN. Moreover, I explore its application in the Aurora2 speech recognition task under mismatched noise conditions using a Tandem approach. I observe top performance on clean speech, and under high noise conditions, compared to multi-layer perceptrons (MLPs) and DNNs, with the added benefit of being a "deeper" model than an MLP but more compact than a DNN.

In this work, I propose a new point of view to the deep learning paradigm:

- Given advances in understanding deep architectures, I pose RNNs as an instantiation of these models, and re-explore previous work on the subject [112], comparing traditional MLPs, DNNs[4], and RNNs under noise environments.

The RNN (see Figure 3.2) is a natural extension to DNNs for temporal sequence data such as speech. In RNN, the depth comes from layers through time. Furthermore, due to the large hidden space that RNNs can represent (exponential in the number of hidden units), plus the non-linear dynamics that they can model, they can learn to memorize events with longer context, and may be a better fit for speech data.

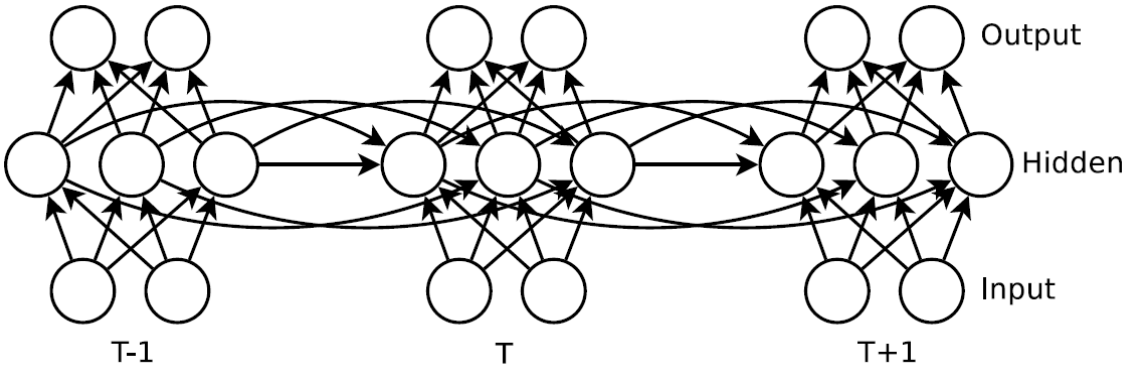

Figure 3.2. *Structure of a Recurrent Neural Network.*

3.5.2 Using RNNs

Recurrent Neural Networks

Recurrent Neural Networks were first applied to large vocabulary speech recognition in [112]. RNNs are powerful models that can model non-linear dynamics through connections between hidden layers, as can be seen in Figure 3.2. One of the key challenges for training RNNs is that long term dependencies are difficult to capture since vanishing gradients over time preclude the update of weights from the far past. Back Propagation Through Time and approximations to it have been used before. More recently, applications in Language Modeling [84] and advances in optimization [123] have seen state of the art performance by the usage of RNNs for sequence modeling.

Pretraining and optimization

In this work, I further explore the interaction between pretraining and the optimization method to learn the model parameters for both DNN and RNN models for robust speech recognition. Analysis on why pretraining is useful has been discussed in both the machine learning [8] and speech recognition [31, 119] communities. Given that the training and stability of RNNs is more problematic than of DNNs due to the vanishing gradient problem [10], I developed a new second order optimization algorithm derived from Hessian Free optimization, which is presented in this chapter and in [132].

My RNN approach follows the same formulation as in [123]. Unlike in the DNN case, only the current frame without context is used at the observation at time t, $\mathbf{x}_t$. The RNN is able to "remember" context naturally due to its large hidden state representation and its recurrent nature. The architecture is as follows:

$$\mathbf{h}_t = \tanh(\mathbf{W}_{hx}\mathbf{x}_t + \mathbf{W}_{hh}\mathbf{h}_{t-1})$$

[4]In this section, I use MLP to denote a single hidden layer Neural Network architecture, whereas DNN implies a deeper architecture with two or more hidden layers. Deep Belief Network (DBN) is used when I use pretraining to train a DNN.

$$\mathbf{o}_t = \text{softmax}(\mathbf{W}_{oh}\mathbf{h}_t)$$

where the bias terms are omitted for simplicity, $\mathbf{h}_t$ represents the hidden state of the network at time t, and $\mathbf{W}_{hx}$, $\mathbf{W}_{hh}$ and $\mathbf{W}_{oh}$ are parameters to be learned. Note that, due to the recursion over time on $\mathbf{h}_t$, the RNNs can be seen as a very deep network with T layers, where T is the number of time steps. I define the initial seed of the network $\mathbf{h}_0$ to be another parameter of the model, and I optimize the cross entropy between the predicted phone posterior output $\mathbf{o}_t$, and the true target (given by forced alignment), similar to how DNNs and MLPs are trained.

As I report in Section 3.5.3, there are some considerations in the training of the RNN that are important. First, I pretrain the RNN by "disconnecting" the hidden layers temporally, that is, I first optimize forcing $\mathbf{W}_{hh}$ to be zero (in which case, the training reduces to simple MLP training), and then switch to jointly optimize all parameters. Secondly, the MLPs and DNNs have access to future context of four frames (when using a nine frame context, i.e. $t \pm 4$ frames). I enforce this in the RNNs by delaying the output by four frames. Finally, I constrain the length of the utterances T to be at most 60 (which is equivalent to reset the hidden state $\mathbf{h}$ to $\mathbf{h}_0$ every 60 frames), as this results in more efficient learning in my GPU implementation. However, I have also experimented with not truncating utterances at test time. All these factors are empirically evaluated in Section 3.5.3.

The outputs of the MLP, DNN, and RNN provide an estimate of the posterior probability distribution for phones. I apply Karhunen-Loève Transform to the log-probabilities of the merged posteriors to reduce the dimensionality to 32 dimensions and orthogonalize those dimensions. I then mean and variance normalize the features by utterance. Finally, I append the resulting feature vector to the MFCC feature. The augmented feature vector then becomes the observation stream for the decoder, which is described in the next section.

3.5.3 Experimental Setup and Results

For this work, I use the Aurora2 data set described in [60], a connected digit corpus which contains 8,440 sentences of clean training data and 56,056 sentences of clean and noisy test data. The test set comprises 8 different noises (subway, babble, car, exhibition, restaurant, street, airport, and train-station) at 7 different noise levels (clean, 20dB, 15dB, 10dB, 5dB, 0dB, -5dB), totaling 56 different test scenarios, each containing 1,001 sentences. Since I am interested in the performance of MLP, DNN and RNN features in mismatched conditions, all systems were trained only on the clean training set but tested on the entire test set. In this study, I compare 13-dimensional perceptual linear prediction (PLP) features with first and second derivatives used as input features for either an MLP, DNN, or RNN. This Tandem feature is also appended to a 13-dimensional MFCC with first and second derivatives in all the experiments.

The parameters for the HTK decoder used for this experiment are the same as that for the standard Aurora2 setup described in [60]. The setup uses whole word HMMs with 16 states with a 3-Gaussian mixture with diagonal covariances per state; skips over states are not permitted in this model. This is the setup used in the ETSI standards competition. More details on this setup are available in [60].

The architecture considered for the DNNs and MLPs was inspired by the MNIST hand written digit recognition task [59] and is the same that I used in recent work [133]. Further

details on the training procedure can be found in [133], but it is worth noting that, in order for the deep network to use temporal information, a context window totaling nine frames is used. This was found helpful in related work as well [119]. For fairness of comparing DNNs with RNNs, I also include a partial study of how pretraining and differing optimization procedures affect the results (I do so by comparing DNNs with and without pretraining).

The details of every system, with hyperparameters (such as model size) tuned using cross validation, are as follows:

- MLP: As described in [133], I train a 720 hidden unit neural network with stochastic gradient descent (using ICSI's Quicknet[5]), with 9 frames of context using 39 dimensional PLP as input.
- DBN: As described in [133], I train a deep belief network with generative pretraining, and conjugate gradient descent. The structure of the network is of 500-1000-1500 hidden units, with 9 frames of context using 39 dimensional PLP as input.
- DNN: With the same structure of the DBN, but instead of using pretraining and conjugate gradient descent, I use a modified version of the second order optimizer HF [132].
- RNN: Using an RNN with 1000 hidden units, training segments of 60 frames, with a delayed output of 4 frames, and initialized as a regular MLP (i.e., disconnected). At test time, the network is run on the whole sequence (i.e. the limit of 60 frames is not used).

Phone Recognition

When training the networks, I leave the first 800 utterances for cross validation (as my training algorithms look at CV error for early stopping). Thus, I get error rates for a phone classification task (without an HMM, i.e. frame wise) from the held out data. In Table 3.3, I observe how the phone error rate in this frame-by-frame classification of the RNN is comparable to a DNN (with less than half number of parameters), and better than the DBN proposed in previous work. There is, however, a fundamental difference between the DBN and both DNN/RNN: due to the pretraining, I am starting the optimization in a more promising region, which may help finding a more desirable local optima. For small recognition tasks such as Aurora2, this has been shown to generalize better. Thus, under mismatched/noisy conditions, the DBN may still outperform the DNN or RNN.

Recurrent Neural Network system In this section, I explore how the RNNs perform when training and testing conditions are changed. As seen in Table 3.4, adding in the non-linear dynamic term $\mathbf{W}_{hh}$ yields the biggest improvement to the system, showing the usefulness of temporal context. Also, as one can expect, adding future context (which, in the context of DNN/MLP training is done by adding 4 frames of future context to the input), helped. One of the most surprising facts is that long term context seems to help more than I expected: if I restart the RNN state every 60 frames, I achieve 10.2% PER,

[5] `http://www.icsi.berkeley.edu/Speech/qn.html`

System	MLP	DBN	DNN[2]	RNN[2]
HU	720	500-1K-1.5K	500-1K-1.5K	1K
#parameters	350K	2.3M	2.3M	1M
PER (%)	15.4%	10.1%	8.3%	8.5%

Table 3.3. *Phone Error Rate on Cross-Validation Set. The first two columns correspond to the reported PER in [133]. The third column is the same as the second but with no pretraining, and using a better optimization technique. The last column corresponds to an RNN with 1K hidden units.*

whereas if I let the RNN run on the whole utterance without restarts, the performance is almost 2% absolute better. This indicates that the RNN is capturing long term effects that yield significantly better PER.

It is worth noting that if I do not use the discriminatively trained disconnected network to initialize the RNN (which is similar to layerwise backpropagation [119]), convergence is rather slow and, even with the second order optimization method, the solution is far from optimal (worse than 40% PER).

System	PER
Disconnected RNN ($\mathbf{W}_{hh} = 0$)	18.8%
RNN	11.8%
+ future context (4 frames)	10.2%
+ non truncated testing	8.5%

Table 3.4. *Phone Error Rate on Cross-Validation Set with different training/testing schemes for RNNs. Error rates are reported for 1000 hidden units.*

Speech Recognition

Typical results on the Aurora2 test set using the ETSI setup report accuracies (or mean accuracy) across the 8 noises at 7 noise conditions. I do not report accuracies here for two reasons. The first and rather mundane reason is that reporting hundreds of numbers will result in a table too large for the length constraints of this paper. Second, and perhaps more importantly, I do not think that reporting accuracies in general (even with a reduced table) is properly illustrative of the performance of the system. Consider, for instance, a table consisting of results for two systems in two noise conditions, one clean and one extremely noisy. If the baseline achieved a 98% accuracy rate on the clean test and 3% accuracy on the noisy one, and the proposed system achieved a 99% and 1.9% accuracy on the clean and noisy conditions, respectively, one would clearly choose the latter system as that system reduced over half the errors on the clean test while performing roughly similarly on the noisy one (that is, neither really worked in noise). If I simply look at mean accuracy, however, I see that the baseline actually outperforms the compared system. The reduction in errors corresponds fairly well to the common costs of using a system (for instance, how often a

[2]Trained using a Hessian Free derived second order method [132].

system must retreat to a human operator). For this reason, I report WER results, which for many years have been the standard for most speech recognition tasks.

For this work, I average WER across noises and report scores for each noisy condition. Finally, all results are significant with a p-value of 0.002 using the differences of proportions significance test.

Tandem systems For this set of experiments, I concatenate the processed posterior probabilities with MFCC features (i.e. Tandem system). As noted in [133], it is generally better to append MFCC features to the discriminatively trained networks (except for very noisy conditions, in which case MFCCs degrades performance of MLP/DNN/RNN).

In Table 3.5 the results for the MFCC baseline are shown, and several Tandem systems. As can be seen, adding a deep network in Tandem with MFCCs clearly outperforms the MFCC baseline. It is interesting that the DBN is generally more competitive under mild noise conditions than DNN and RNN, presumably due to the generative initialization, which is known to yield better generalization (specially in small datasets). The RNN outperforms every model under clean speech, which is interesting and should be further explored with a larger speech database. The fact that the RNN is also better under very noisy conditions may indicate that, in those cases, longer term dependencies that the MLP/DBN/DNN models cannot capture may be necessary. Lastly, the number of hidden units for the RNN did not seem to have a big effect: 200 units seemed to underfit the data, and 1500 units were a bit better under high noise condition, but worse on clean (presumably due to overfitting). I expect this parameter to be more relevant when the training set exhibits more variance and is larger, but I leave this for future work.

SNR	MFCC	MLP	DBN	DNN	RNN
Clean	1.60%	1.56%	0.88%	0.78%	**0.70%**
20dB	5.33%	3.68%	**2.69%**	3.05%	3.59%
15dB	14.77%	7.47%	**6.35%**	**6.38%**	6.89%
10dB	36.59%	16.63%	15.26%	**14.61%**	**14.77%**
5dB	66.65%	36.82%	34.34%	32.09%	**30.94%**
0dB	86.98%	63.80%	61.43%	58.98%	**57.19%**
-5dB	94.01%	87.09%	85.71%	84.42%	**81.51%**

Table 3.5. *Average WER for several systems under different noise conditions. The first three columns correspond to the reported results in [133]. Bold numbers indicate best performance. Note that, as before, DNN and RNN use the second order optimization method.*

3.5.4 Final Remarks

In this line of work with RNNs, I extend my work on deep learning, in which I already studied how the deep models integrate with MFCC using the Tandem approach, and the deep model is robust to different noise conditions present in the Aurora2 dataset.

My first extension is to study the effect of pretraining of the previously proposed model. I found that the standard approach to deep learning, that is, DBNs trained using pretraining and standard conjugate gradient descent, and the DNNs with no pretraining but trained

with a second order optimization method performed similarly under clean condition. DBNs were, however, able to perform better under mild noise conditions, which can be explained by the nature of pretraining to better generalize to unseen conditions during training.

I also revisit RNN, a model that seems natural for sequential data such as speech, but poses a difficult optimization problem. Using the proposed pretraining and the second order method, I was able to successfully train the RNN and use its outputs in a Tandem approach, which yields the best clean condition score for HMM Tandem system in the Aurora2 set, and better performance on the noisier conditions (although the WER in those scenarios is still too high for most practical applications).

Given the performance seen on clean speech, one of the lines of research is to apply this approach to a larger dataset. When orders of magnitude more data is available, the relative differences of each model may change (e.g. pretraining is not as valuable once the amount of training data is large enough).

Since both the RNN and DNN improve performance, one could combine the model to create a deep recurrent neural network, in which multiple hidden layers are used. Also, instead of using Tandem, I will try using a hybrid system, which will replace the GMM emission model by the RNN. Lastly, predicting subphone states of the HMM instead of phone posteriors is beneficial [31, 123] and, with more data available, could yield further improvements.

Chapter 4

Convex Deep Learning

Part of the work that appears on this chapter has been published in peer reviewed conferences. The shallow model based on Sparse Coding was presented in Interspeech 2012 [129], and the Deep Architecture version of it, that uses only convex optimization sub problems was presented at NIPS 2012 [130].

4.1 Shallow Models

4.1.1 Motivation on Sparse Models

Sparse coding has achieved state-of-the-art performance on many applications in computer vision and has attracted much research in recent years. The main idea behind sparse coding is to map the original feature space (e.g. pixels, spectrograms, etc.) to a (typically larger) sparse representation. Some evidence has been shown that this strategy may be utilized by the first stages of vision [100]. In particular, it seems that we have specialized neurons firing only when particular patterns are present (e.g. an edge in an image at a certain orientation).

Recently, the machine learning community has been exploring why sparse representations followed by a linear classifier performs as well as carefully designed features (such as SIFT or MFCC) followed by non-linear classifiers (e.g. kernel SVMs and Deep Neural Networks). In [143] a theoretical formulation shows that, if we want to learn a general non-linear mapping function (with some constrains such as Lipschitz smoothness) from the original features to a label, one can approximate such a function with a local, sparse coding step followed by a linear classifier. This is because one can approximate any smooth, non-linear function locally by a piecewise linear function to an arbitrarily accurate degree.

The paradigm of sparse coding followed by a linear classifier is appealing as learning linear classifiers is a well understood problem, both in terms of optimization (as it usually involves solving a convex objective function), and of overfitting (linear models, due to their simplicity, tend to exhibit less overfitting). In addition, the learning is very simple and time efficient, and the models can be interpreted thanks to the simple classification function.

Nonetheless, sparse coding has not been popular in speech recognition research until recently. The work in [121] is the closest to mine, and uses sparse coding as an input of a

neural network (NN) for phone recognition. The work in [120] explores inducing sparsity in hidden layers of a NN. Another approach is to do exemplar based speech recognition based on sparse representations, which was recently proposed in [115] with promising results. Also, the well established deep learning approach to acoustic modeling can be seen as sparse coding (as the unsupervised pre-training is akin to dictionary learning), and the sigmoid non-linearity can be interpreted as a sparsifying factor. Another important reason why sparse coding has had little attention is the fact that, even though specialized software and optimization techniques exist for efficient coding, to convert the original feature vector into a sparse code, one has to solve an optimization problem for each sample during train and test time. This makes the approach not as computationally attractive as a neural network or a GMM, which typically can be computed with a few matrix/vector multiplications.

However, recent advances in understanding sparse coding observed that the set of basis (or dictionary) was not crucial, and that the encoding could be carried out with a simple matrix vector multiplication [27]. Empirical results suggest that data preprocessing step is more important than learning the dictionary in achieving good performance when using fast approximations to sparse coding. In particular, zero-phase whitening filters (ZCA) and contrast normalization are typically applied as a preprocessing step to the data.

The main contributions of this line of work is to apply sparse representations based on a very simple and fast approximation to sparse coding on a widely studied acoustic modeling benchmark; giving an interpretation of the unsupervised learned basis that are most relevant for certain classes (phones); and providing an alternative to deep learning that can be implemented in a few lines of code.

4.1.2 Related Work in Sparse Coding

In this section I give an overview of sparse coding. It is out of the scope of this section to describe all previous work on other techniques based on sparsity, such as compressed sensing, and the authors encourage interested readers to refer to [41] for further information.

Sparse Coding

Sparse representations were initially motivated by neuroscience in [100], where it was shown that the receptive fields in the early stages of the virtual cortex could be learned by applying sparse coding to a set of natural images. In sparse coding, we are given a set of d dimensional observations $\mathbf{x}_i$ (e.g. images), and the objective is to jointly learn a code $\mathbf{c}_i$ (of dimension k) and a dictionary $\mathbf{D}$ such that the reconstruction of the original signal is as close as possible in L2 norm, and the codes are sparse through the following objective function:

$$\min_{\mathbf{c}_i, \mathbf{D}} \sum_i ||\mathbf{x}_i - \mathbf{D}\mathbf{c}_i||_2^2 + \alpha ||\mathbf{c}_i||_1 \tag{4.1}$$

Note that $\mathbf{D}$ is a $d \times k$ matrix whose columns are the basis (or dictionary elements or codebooks), and α a parameter to control the sparsity of the solution (note that if $\alpha = 0$, then a solution with 0 error exists if we choose $k \geq d$). Typical approaches to solve Eq. 4.1

involve coordinate descent on two convex sub-problems, alternating between minimizing $\mathbf{D}$ (simple least squares), and $\mathbf{c}_i$ (well studied problem in the compressed sensing community).

Understanding sparse coding has been of interest for the machine learning community, as excellent results were obtained in computer vision by adopting a sparse coding step followed by a linear classifier (typically a linear Support Vector Machine (SVM)), in contrast to learning complicated kernel functions and features to solve object recognition [94]. In recent work, the authors of [143] gave the explanation that an overcomplete sparse coding scheme (one where the codebook size, k, is larger than the dimensionality of the input feature space d) would serve as a way to locally encode a smooth non-linear function, which can then be approximated as a globally linear function, and thus learned through, for example, linear SVM. Several state-of-the-art results have been published on computer vision benchmarks such as object recognition, face detection, or action recognition [94, 22].

Application to Acoustic Modeling One of the main drawbacks for applying sparse coding in speech recognition is that, for a fix $\mathbf{D}$, for each sample $\mathbf{x}_i$ one has to find $\mathbf{c}_i$ through minimizing Eq. 4.1. This problem has been extensively studied in the optimization community, and efficient solutions exist that are only a few times slower than a straightforward matrix-vector multiplication (the typical cost of other approaches such as Deep Neural Networks (DNN) or Gaussian Mixture Models (GMM)). In fact, vector quantization, a technique that has been used to model emission probabilities for Hidden Markov Models (HMM), can be seen as a crude approximation to sparse coding, where a signal $\mathbf{x}_i$ is coded with just the closest element in the dictionary in the following way:

$$\begin{aligned} \mathbf{c}_i &= \arg\min_{\mathbf{c}_i} ||\mathbf{x}_i - \mathbf{D}\mathbf{c}_i||_2^2 \\ & \quad s.t. ||\mathbf{c}_i||_0 = 1 \end{aligned}$$

where $||.||_0$ counts the number of non-zero elements.

Another possible alternative to this is to impose a sparse penalty to either the weights learned, or the activations of the hidden neurons in a DNN setting [120, 141]. At decoding time, the cost does not change (and in fact one can obtain speed ups if the weights become sparse), but the model still poses a non-convex objective function to find the parameters of a DNN.

In [121], the authors proposed to use sparse coding on the spectrotemporal representation of the acoustic signal, but their codebook size was fairly small, and the dictionary learned did not seem to capture the basics of human speech generation. Furthermore, a more complicated non-linear classifier was used to map the code to phone posterior estimates.

In light of recent developments and simplifications found in [27], I developed a very simple and efficient scheme to perform phone recognition based on an overcomplete sparse representation of the signal followed by a simple linear SVM classifier.

4.1.3 Proposed Method

In [27], two key observations motivated the simplified sparse coding scheme for acoustic modeling. First, the fact that the dictionary (or set of basis) learned is not as important

as the coding step, and that even random samples can help expressing a sample locally. This is in accordance to the result found in [121], where the difference between randomly initialized basis and the one found by sparse coding yielded similar results. Secondly, one can replace solving the optimization problem in Eq. 4.1, by an inner product followed by a sparsity inducing non-linearity, which was found to give similar results in various vision benchmarks.

Furthermore, two data normalization steps help in terms of capturing invariances and aiding the (simplified) dictionary learning step:

- The first is to normalize each $\mathbf{x}_i$ by subtracting its mean and dividing by the standard deviation, commonly known as contrast normalization (see the end of this section). Thus, for example, having a shift in all the value for a given sample gives the same feature, which helps making the feature invariant to different illumination conditions. In the spectrotemporal domain, this could, in principle, remove some valuable information, and I empirically verify this in Section 4.1.4.

- The second is to perform ZCA whitening of the data (Line 3 in Algorithm 3), as means to "spread" the data $\mathbf{X}$ uniformly around the sphere in order to help the simplified dictionary learning step (which is a modification of standard k-means). Even though the effect for this in images is quite important, the benefit of performing this step for speech data seems less obvious.

After normalizing the data, I form a dictionary by performing Orthogonal Matching Pursuit 1 (OMP1) [27] (Line 4 in Algorithm 3), which can be seen as a modification to the k-means algorithm. Thus, this algorithm can be applied to large amounts of data and is easy to parallelize (I ran it on the 1.1 million samples in TIMIT on a single machine in less than 20 minutes). Examples of dictionary elements learned are shown in Figure 4.1. The basis seem to capture relevant information about formants and energy distribution that will be used to code a given spectrogram.

The encoding step is trivial, involving just a matrix multiplication to code the data, followed by a element-wise max operation to induce sparsity (Line 5 in Algorithm 3):

$$\mathbf{c}_i = \max(0, \mathbf{D}^T\mathbf{x}_i - \alpha)^1$$

where α is a parameter that controls the amount of sparsity introduced, and was set to 0.25, the same value that was found via cross validation on vision benchmarks. The last step involves the discriminative training of a linear function on the code space, and I use a linear SVM where the data is $\mathbf{C}$ and the corresponding labels are phone states (Line 6 in Algorithm 3).

Note that a single machine implementation will require to store the matrix $\mathbf{C}$, which can be larger than the data itself as typically $k > d$. For large datasets as in speech, where N is also large, both k-means and SVM are trivial to parallelize via map-reduce, which is a big advantage when comparing to training a DNN, which is typically done with stochastic gradient descent, much harder to parallelize (other than the matrix operations).

[1] After this work was published, the usage of this non-linearity in neural networks (which is called rectified linear unit) has shown improvements in training speed. Considering this, modern neural networks and this kind of sparse coding become even more related.

The complete process for performing acoustic modeling from the spectrotemporal features is described in Algorithm 3.

Algorithm 3 Acoustic Modeling with Sparse Representations

1: // $\mathbf{x}_i$ is the i-th spectrotemporal frame, $\mathbf{X}$ is the $d \times N$ matrix whose columns are $\mathbf{x}_i$, and $\mathbf{Y}$ is the N dimensional vector with phone labels for each sample
2: Normalize each spectrotemporal frame $\mathbf{x}_i$
3: Apply ZCA whitening on the whole dataset $\mathbf{X}$
4: Run OMP1 on $\mathbf{X}$ to construct a $d \times k$ dictionary matrix $\mathbf{D}$
5: Form $\mathbf{C}$, a $k \times N$ matrix of codes by computing $\mathbf{C} = \max(0, \mathbf{D}^T\mathbf{X} - \alpha)$
6: Train a linear SVM on the pair $(\mathbf{C}, \mathbf{Y})$ (in one-vs-all fashion)

4.1.4 Experimental Results

In this experiment, I carry out a TIMIT phone classification task using the proposed paradigm. I use all 462 speakers data in the training set, which amounts to approximately 3 hours and about 1.12 million samples at 100 frames/second. I extract log-mel-spectrogram features with 24 filter banks and a window size of 25ms. I use a context of 5 frames on each side, with a total of 11 frames of context with 24 real numbers each. I also add delta and delta-delta as with many other standard pipelines, and I found that this did not significantly change the reported results.

I report the results on the standard TIMIT Core Test Set consisting of 192 utterances, using the standard development set to tune the only parameter in my Algorithm — the regularization coefficient in the SVM.

In my setup, I use a single machine. Given the size of the training samples, and that I did not do any splitting of the training set for simplicity, when using large values of k, I downsampled the training set by 3. This is obviously not optimal, and better results could probably be obtained by using multiple machines or sequentially loading the data instead of processing it all at once. However, since I released my code, I wanted to keep it as simple and conceptual as possible. As a consequence, when reporting numbers with 1600 or 2000 codes, all the training set was used, but when using 6000, only 1/3 was used in the SVM training phase. The whole training process took a little more than an hour to complete, with 95% of time spent in the SVM training. Since this step is trivial to parallelize, I expect my method to be very attractive when scaling up the training size by orders of magnitude.

The SVM is trained to predict one of the 61 phone states (making the number of total classes equal to 183). Besides reporting per frame accuracies, I take the naive approach of converting each frame to its predicted value from the multi-class SVM, and then using dynamic programming to take into account the dynamics at the utterance level. An even better approach would be to convert the SVM decisions to probabilities (typically done through logistic regression), and then use an HMM with a phonetic language model to decode.

Note that the approach falls in the category of "shallow" learning, and the most time consuming step involves solving convex, parallelizable problem. At test time, two simple matrix-vector multiplications need to be carried in order to convert from the spectrogram to the likelihoods that would be used for HMM decoding.

Code. size	Tr. Size	Tr. Frame Acc.	Tst. Frame Acc.
1600	Full	56.1%	50.1%
2000	Full	61.3%	50.6%
6000	1/3	68.2%	51.1%
SVM	Full	40.4%	39.7%
1-DCN[38]	Full	72.8%	50.2%
7-DCN[38]	Full	98%	55.3%

Table 4.1. Results on the TIMIT dataset comparing different dictionary sizes of sparse coding and a few baseline methods.

Method	Tr. Frame Acc.	Tst. Frame Acc.
OMP1	58.7%	50.1%
+ ZCA	71.3%	49.6%
+ contrast	59.5%	50.2%
+ ZCA + contrast	68.2%	51.1%
Random	69.4%	49.1%

Table 4.2. Results on the TIMIT dataset with codebook size of 6000, comparing different normalizations and coding strategies.

Table 4.1 shows the effect of the codebook size (value of k) on the per frame phone state accuracy, and compares the results with applying SVM directly to the raw features (SVM), and the Deep Convex Network (DCN) proposed in [27] in its shallow (1-DCN) and deep versions (7-DCN).

Learning discussion

As described in Algorithm 3, there are certain normalizations that can be done (Lines 2and 3), and the dictionary learning step which can be switched by a more trivial approach (Line 4). In Table 4.2 one can see this effect. Indeed, having ZCA whitening plus contrast normalization helps in terms of classification performance by 1% absolute, but it is surprising that ZCA alone seems to not help. Also, using a dictionary based on randomly selected spectrograms performs a little worse than the dictionary found by OMP1 (but not by a large amount).

Lastly, if I perform phone recognition with 39 categories using dynamic programming (but without phonetic language model), I obtain a phone recognition of 75.1%.

Dictionary Analysis

I have examined the learned dictionary elements associated with some typical phonetic categories. Since the training samples can be expressed as a linear sum of the basis functions in the dictionary, I expect the important dictionary elements contain useful acoustic patterns that code important phonetic distinctions consistent with phonetic literature.

In Figure 4.1 I show 16 examples of dictionary elements corresponding to each of three states of /aa/ (top), /t/ (middle), and /b/ (bottom). These are rows of the matrix **D**

in Eq. 4.1, as elements of the dictionary. Each row of $\mathbf{D}$ has the dimensionality of 11*24 (the number of frames by the number of filterbanks). To aid visual inspection, each row is re-arranged to form an 11 by 24 two-dimensional image as shown in Figure 4.1. The 16 selected dictionary elements associated with each of state correspond to 16 largest weights determined by the SVM.

From the top panel of Figure 4.1, one sees clear formant patterns in each of the three states. Both up and down formant transitions are seen in State 2, while in States 1 and 3, mainly one directional formant movements are represented. This is consistent with the intuition and acoustic-phonetic knowledge about formant movements [36].

In contrast, for the unvoiced stop consonant /t/, there are much noisier basis functions, corresponding to burst and aspiration portions of that sound. The amount of noise in voiced stop consonant /b/ appears to be smaller, reflecting the absence of large aspiration noise. Interestingly, in State 3 of /b/, I observe clear formant transitions, which is consistent with the following property of /b/: it is relatively short; And hence in its final state and with 5 frames appended to its right the /b/ segment tends to cover the transitional sounds into its right context vowel. Such transitions in the vowel are clearly visible in the basis functions associated with the final state of /b/.

4.2 Deep Models

4.2.1 Depth and Convexity in one Model

In this half of the chapter, I focus on the learning of a general-purpose non-linear classifier applied to perceptual signals such as vision and speech. The Support Vector Machine (SVM) has been a popular method for multimodal classification tasks since its introduction, and one of its main advantages is the simplicity of training a linear model. Linear SVMs often fail to solve complex problems however, and with non-linear kernels, SVMs usually suffer from speed and memory issues when faced with very large-scale data, although techniques such as non-convex optimization [29] or spline approximations [81] exist for speed-ups. In addition, finding the "oracle" kernel for a specific task remains an open problem, especially in applications such as vision and speech.

My aim is to design a classifier that combines the simplicity of the linear Support Vector Machine (SVM) with the power derived from deep architectures. The new technique I propose follows the philosophy of "stacked generalization" [137], i.e. the framework of building layer-by-layer architectures, and is motivated by the recent success of a convex stacking architecture which uses a simplified form of neural network with closed-form, convex learning [38]. Specifically, I propose a new stacking technique for building a deep architecture, using a linear SVM as the base building block, and a random projection as its core stacking element.

The proposed model, which I call the Random Recursive SVM (R^2SVM), involves an efficient, feed-forward convex learning procedure. The key element in the convex learning of each layer is to randomly project the predictions of the previous layer SVM back to the original feature space. As I will show in the paper, this could be seen as recursively transforming the original data manifold so that data from different classes are moved apart, leading to better linear separability in the subsequent layers. In particular, I show that

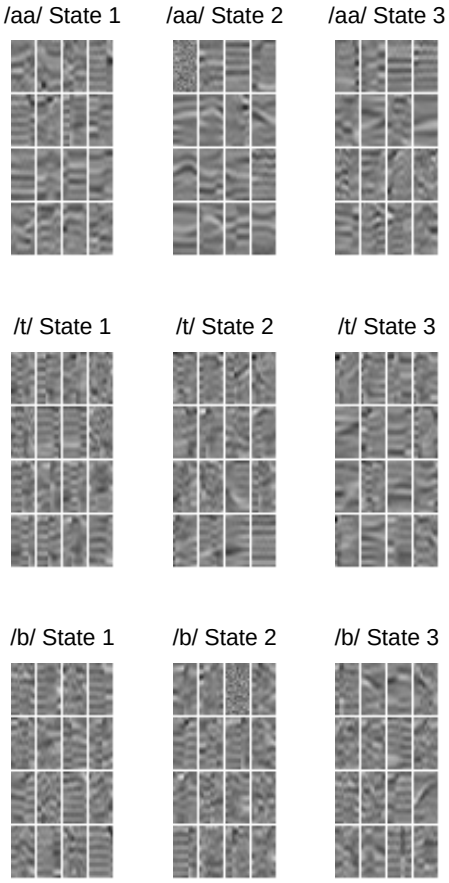

Figure 4.1. Most discriminant basis for some sub-phone states in TIMIT.

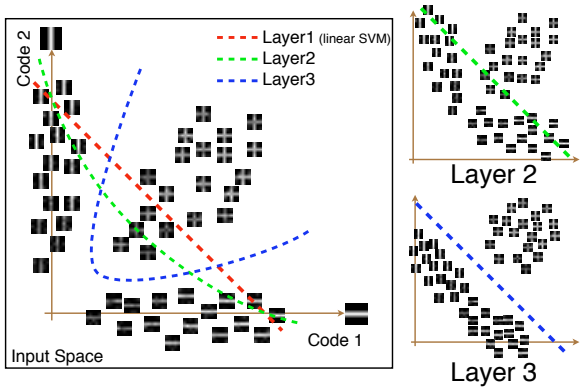

Figure 4.2. A conceptual example of Random Recursive SVM separating edges from crossbars. Starting from data manifolds that are not linearly separable, the method transforms the data manifolds in a stacked way to find a linear separating hyperplane in the high layers, which corresponds to non-linear separating hyperplanes in the lower layers. Non-linear classification is achieved without kernelization, using a recursive architecture.

randomly generating projection parameters, instead of fine-tuning them using backpropagation, suffices to achieve a significant performance gain. As a result, my model does not require any complex learning techniques other than training linear SVMs, while canonical deep architectures usually require carefully designed pre-training and fine-tuning steps, which often depend on specific applications.

Using linear SVMs as building blocks the model scales in the same way as the linear SVM does, enabling fast computation during both training and testing time. While linear SVM fails to solve non-linearly separable problems, the simple non-linearity in my algorithm, introduced with sigmoid functions, is shown to adapt to a wide range of real-world data with the same learning structure. From a kernel based perspective, my method could be viewed as a special non-linear SVM, with the benefit that the non-linear kernel naturally emerges from the stacked structure instead of being defined as in conventional algorithms. This brings additional flexibility to the applications, as task-dependent kernel designs usually require detailed domain-specific knowledge, and may not generalize well due to suboptimal choices of non-linearity. Additionally, kernel SVMs usually suffer from speed and memory issues when faced with large-scale data, although techniques such as non-convex optimization [29] exist for speed-ups.

My findings suggest that the proposed model, while keeping the simplicity and efficiency of training a linear SVM, can exploit non-linear dependencies with the proposed deep architecture, as suggested by the results on two well known vision and speech datasets. In addition, the model performs better than other non-linear models under small training set sizes (i.e. it exhibits better generalization gap), which is a desirable property inherited from the linear model used in the architecture presented in the paper.

There have been several ways to combine output of different classifiers to improve classification accuracy. Ensemble methods are commonly used to combine classifiers, and Random forests [18] an instance of such methods. The approach consists of a set of decision trees trained with randomness (e.g. bagging), which then are combined at the output level by means of a voting scheme. Another family of methods focus on feeding the output of

a classifier into another classifier. In [2], a two level architecture using kernel based SVMs is proposed, where the kernel activations from the first layer are used as features for the second layer. My method differs from these in two ways: I use the output of the classifier to transform the original features, and I add a non-linearity to make the whole architecture more flexible in learning non-linear functions.

4.2.2 The Random Recursive SVM

In this section I formally introduce the Random Recursive SVM model, and discuss the motivation and justification behind it. Specifically, I consider a training set that contains N pairs of tuples $(\mathbf{d}^{(i)}, y^{(i)})$, where $\mathbf{d}^{(i)} \in \mathbb{R}^D$ is the feature vector, and $y^{(i)} \in \{1, \ldots, C\}$ is the class label corresponding to the i-th sample.

As depicted in Figure 4.3(b), the model is built by multiple layers of blocks, which I call Random SVMs, that each learns a linear SVM classifier and transforms the data based on a random projection of previous layers SVM outputs. The linear SVM classifiers are learned in a one-vs-all fashion. For convenience, let $\boldsymbol{\theta} \in \mathbb{R}^{D \times C}$ be the classification matrix by stacking each parameter vector column-wise, so that $\mathbf{o}^{(i)} = \boldsymbol{\theta}^T \mathbf{d}^{(i)}$ is the vector of scores for each class corresponding to the sample $\mathbf{d}^{(i)}$, and $\hat{y}^{(i)} = \arg\max_c {\boldsymbol{\theta}_c}^T \mathbf{d}^{(i)}$ is the prediction for the i-th sample for the final predictions. From this point onward, I drop the index $\cdot^{(i)}$ for the i-th sample for notational convenience.

Recursive Transform of Input Features

Figure 4.3(b) visualizes one typical layer in the pipeline of the algorithm. Each layer takes the output of the previous layer, (starting from $\mathbf{x}_1 = \mathbf{d}$ for the first layer as the initial input), and feeds it to a standard linear SVM that gives the output $\mathbf{o}_1$. In general, $\mathbf{o}_1$ would not be a perfect prediction, but would be better than a random guess. I then use a random projection matrix $\mathbf{W}_{2,1} \in \mathbb{R}^{D \times C}$ whose elements are sampled from $N(0, 1)$ to project the output $\mathbf{o}_1$ into the original feature space, in order to use this noisy prediction to modify the original features. Mathematically, the additively modified feature space after applying the linear SVM to obtain $\mathbf{o}_1$ is:

$$\mathbf{x}_2 = \sigma(\mathbf{d} + \beta \mathbf{W}_{2,1} \mathbf{o}_1),$$

where β is a weight parameter that controls the degree with which I move the original data sample $\mathbf{x}_1$, and $\sigma(\cdot)$ is the sigmoid function, which introduces non-linearity in a similar way as in the multilayer perceptron models, and prevents the recursive structure to degenerate to a trivial linear model. In addition, such non-linearity, akin to neural networks, has desirable properties in terms of Gaussian complexity and generalization bounds [6].

Intuitively, the random projection (modulated by class label estimates) aims to push data from different classes towards different directions, so that the resulting features are more likely to be linearly separable. The sigmoid function controls the scale of the resulting features, and at the same time prevents the random projection to be "too confident" on some data points, as the prediction of the lower-layer is still imperfect. An important note is that, when the dimension of the feature space D is relatively large, then the column vectors of W_l are much likely to be approximately orthogonal, known as the quasi-orthogonality property of high-dimensional spaces [71]. At the same time, the column vectors correspond

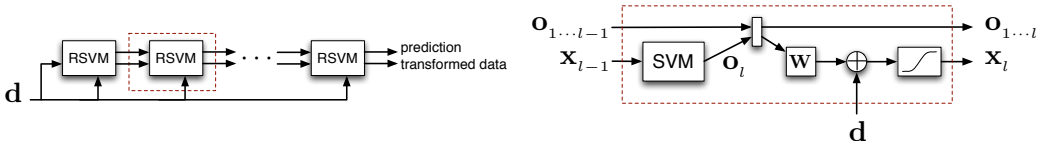

(a) Layered structure of R^{2}SVM (b) Details of an RSVM layer.

Figure 4.3. The pipeline of the proposed Random Recursive SVM model. (a) The model is built with layers of Random SVM blocks, which are based on simple linear SVMs. Speech and image signals are provided as input to the first level. (b) For each random SVM layer, I train a linear SVM using the transformed data manifold by combining the original features and random projections of previous layers' predictions.

to the per class bias applied to the original sample $\mathbf{d}$ if the output was close to ideal (i.e. $\mathbf{o}_l = \mathbf{e}_c$, where $\mathbf{e}_c$ is the one-hot encoding representing class c), so the fact that they are approximately orthogonal means that (with high probability) they are pushing the per-class manifolds apart.

The training of the R^{2}SVM is then carried out in a purely feed-forward way. Specifically, I train a linear SVM for the l-th layer, and then compute the input of the next layer as the addition of the original feature space and the random projection of previous layers' outputs, which is then passed through a simple sigmoid function:

$$\mathbf{o}_l = \boldsymbol{\theta}_l^T \mathbf{x}_l$$

$$\mathbf{x}_{l+1} = \sigma(\mathbf{d} + \beta \mathbf{W}_{l+1}[\mathbf{o}_1^T, \mathbf{o}_2^T, \cdots, \mathbf{o}_l^T]^T)$$

where $\boldsymbol{\theta}_l$ are the linear SVM parameters trained with $\mathbf{x}_l$, and $\mathbf{W}_{l+1}$ is the concatenation of l random projection matrices $[\mathbf{W}_{l+1,1}, \mathbf{W}_{l+1,2}, \cdots, \mathbf{W}_{l+1,l}]$, one for each previous layer, each being a random matrix sampled from $N(0, 1)$.

Following [38], for each layer I use the outputs from *all* lower modules, instead of only the immediately lower module. A chief difference of the proposed method from previous approaches is that, instead of concatenating predictions with the raw input data to form the new expanded input data, I use the predictions to modify the features in the original space with a non-linear transformation. As will be shown in the next section, experimental results demonstrate that this approach is superior than simple concatenation in terms of classification performance.

On the Randomness in R^{2}SVM

The motivation behind the method is that projections of previous predictions help to move apart the manifolds that belong to each class in a recursive fashion, in order to achieve better linear separability (Figure 4.2 shows a vision example separating different image patches).

Specifically, consider a two class problem which is non-linearly separable. The following Lemma illustrates the fact that, if given an oracle prediction of the labels, it is possible to add an offset to each class to "pull" the manifolds apart with this new architecture, and to guarantee an improvement on the training set if I assume perfect labels.

Lemma 4.2.1 *Let $\mathcal{T}$ be a set of N tuples $(\mathbf{d}^{(i)}, y^{(i)})$, where $\mathbf{d}^{(i)} \in \mathbb{R}^D$ is the feature vector, and $y^{(i)} \in \{1, \ldots, C\}$ is the class label corresponding to the i-th sample. Let $\boldsymbol{\theta} \in \mathbb{R}^{D \times C}$ be the corresponding linear SVM solution with objective function value $f_{\mathcal{T},\boldsymbol{\theta}}$. Then, there exist $\mathbf{w}_i \in \mathbb{R}^D$ for $i = \{1, \ldots, C\}$ such that the translated set $\mathcal{T}'$ defined as $(\mathbf{d}^{(i)} + \mathbf{w}_{y^{(i)}}, y^{(i)})$ has a linear SVM solution $\boldsymbol{\theta}'$ which achieves a better optimum $f_{\mathcal{T}',\boldsymbol{\theta}'} < f_{\mathcal{T},\boldsymbol{\theta}}$.*

Proof Let $\boldsymbol{\theta}_i$ be the i-th column of $\boldsymbol{\theta}$ (which corresponds to the one vs all classifier for class i). Define $\mathbf{w}_i = \frac{\boldsymbol{\theta}_i}{||\boldsymbol{\theta}_i||_2^2}$. Then I have

$$\max(0, 1 - \boldsymbol{\theta}_{y^{(i)}}^T(\mathbf{d}^{(i)} + \mathbf{w}_{y^{(i)}})) = \max(0, 1 - (\boldsymbol{\theta}_{y^{(i)}}^T \mathbf{d}^{(i)} + 1)) \leq \max(0, 1 - (\boldsymbol{\theta}_{y^{(i)}}^T \mathbf{d}^{(i)})),$$

which leads to $f_{\mathcal{T}',\boldsymbol{\theta}} \leq f_{\mathcal{T},\boldsymbol{\theta}}$. Since $\boldsymbol{\theta}'$ is defined to be the optimum for the set $\mathcal{T}'$, $f_{\mathcal{T}',\boldsymbol{\theta}'} \leq f_{\mathcal{T}',\boldsymbol{\theta}}$, which concludes the proof. ■

Lemma 4.2.1 would work for any monotonically decreasing loss function (in particular, for the hinge loss of SVM), and motivates the search for a transform of the original features to achieve linear separability, under the guidance of SVM predictions. Note that I would achieve perfect classification under the assumption that I have oracle labels, while I only have noisy predictions for each class $\hat{y}^{(i)}$ during testing time. Under such noisy predictions, a deterministic choice of $\mathbf{w}_i$, especially linear combinations of the data as in the proof for Lemma 4.2.1, suffers from over-confidence in the labels and may add little benefit to the learned linear SVMs.

A first choice to avoid degenerated results is to take random weights. This enables us to use label-relevant information in the predictions, while at the same time de-correlate it with the original input $\mathbf{d}$. Surprisingly, as shown in Figure 4.5(a), randomness achieves a significant performance gain in contrast to the "optimal" direction given by Lemma 4.2.1 (which degenerates due to imperfect predictions), or alternative stacking strategies such as concatenation as in [38]. I also note that beyond sampling projection matrices from a zero-mean Gaussian distribution, a biased sampling that favors directions near the "optimal" direction may also work, but the degree of bias would be empirically difficult to determine and may be data-dependent. In general, one aims to avoid supervision in the projection parameters, as trying to optimize the weights jointly would defeat the purpose of having a computationally efficient method, and would, perhaps, increase training accuracy at the expense of over-fitting. The risk of over-fitting is also lower in this way, as I do not increase the dimensionality of the input space, and I do not learn the matrices $\mathbf{W}_l$, which means the model passes a weak signal from layer to layer. Also, training Random Recursive SVM is carried out in a feed-forward way, where each step involves a convex optimization problem that can be efficiently solved.

While not a layered model, sparse coding [100, 139, 142] have theoretically and empirically been shown to work well with linear classifiers, especially in vision tasks. Furthermore, an extended analysis justifying the use of sparse coding, together with simplifications to reduce its complexity, is shown in [27].

Synthetic examples

To visually show the effectiveness of the approach in learning non-linear SVM classifiers without kernels, I apply the algorithm to two synthetic examples, neither of which can be

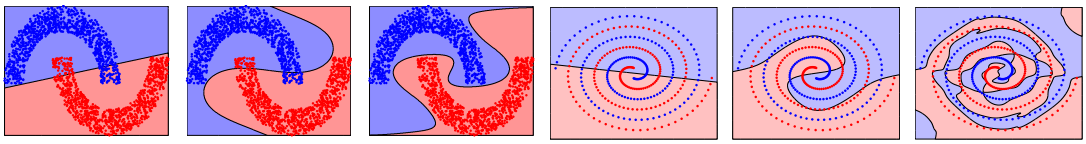

(a) (b) (c) (d) (e) (f)

Figure 4.4. Classification hyperplane from different stages of my algorithm: first layer, second layer, and final layer outputs. (a)-(c) show the two-moon data and (d)-(f) show the spiral data.

linearly separated. The first example contains two classes distributed in a two-moon shaped way, and the second example contains data distributed as two more complex spirals. Figure 4.4 visualizes the classification hyperplane at different stages of the algorithm. The first layer of the approach is identical to the linear SVM, which is not able to separate the data well. However, when classifiers are recursively stacked in my approach, the classification hyperplane is able to adapt to the nonlinear characteristics of the two classes.

4.2.3 Experimental Results

In this section I empirically evaluate my method, and support my claims: (1) for low-dimensional features, linear SVMs suffer from their limited representation power, while R^2SVMs significantly improve performance; (2) for high-dimensional features, and especially when faced with limited amount of training data, R^2SVMs exhibit better generalization power than conventional kernelized non-linear SVMs; and (3) the random, feed-forward learning scheme is able to achieve state-of-the-art performance, without complex fine-tuning.

I describe the experimental results on four well known classification benchmarks: CIFAR-10, Caltech101, MNIST and TIMIT. The CIFAR-10 dataset and the MNIST dataset both contain large amount of training/testing data, with the former focusing on object classification and the latter focusing on conventional OCR task. Caltech101, on the other hand, has a much smaller amount of training data with large feature dimensions, enabling us to test the stability of the algorithms against over-fitting. TIMIT is a speech database that contains two orders of magnitude more training samples than the other datasets, and the largest output label space.

Recall that the method relies on two parameters: β, which is the factor that controls how much to shift the original feature space, and C, the regularization parameter of the linear SVM trained at each layer. β is set to $\frac{1}{10}$ for all the experiments, which was experimentally found to work well for one of the CIFAR-10 configurations. C controls the regularization of each layer, and is an important parameter – setting it too high will yield overfitting as the number of layers is increased. As a result, I learned this parameter via cross validation for each configuration, which is the usual practice of other approaches. Lastly, for each layer, I sample a new random matrix $\mathbf{W}_l$. As a result, even if the training and testing sets are fixed, randomness still exists in my algorithm. Although one may expect the performance to fluctuate from run to run, in practice I never observe a standard deviation larger than 0.25 (and typically less than 0.1) for the classification accuracy, over multiple runs of each experiment.

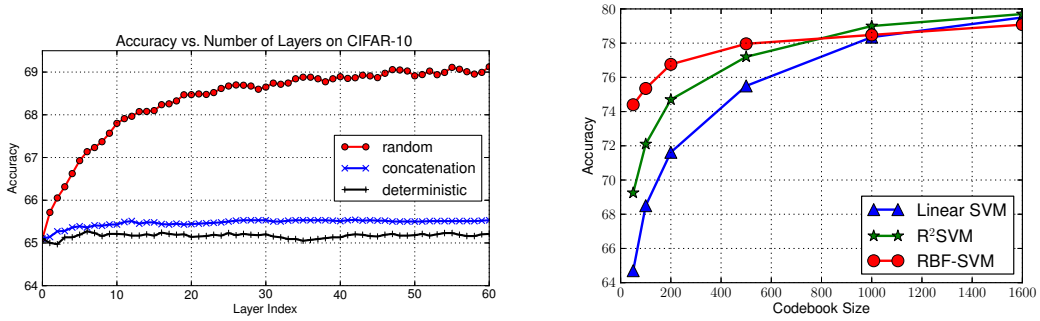

(a) (b)

Figure 4.5. Results on CIFAR-10. (a) Accuracy versus number of layers on CIFAR-10 for Random Recursive SVM with all the training data and 50 codebook size, for a baseline where the output of a classifier is concatenated with the input feature space, and for a deterministic version of recursive SVM where the projections are as in the proof of Lemma 4.2.1. (b) Accuracy versus codebook size on CIFAR-10 for linear SVM, RBF SVM, and my proposed method.

CIFAR-10

The CIFAR-10 dataset contains 10 object classes with a fair amount of training examples per class (5000), with images of small size (32x32 pixels). For this dataset, I follow the standard pipeline defined in [27]: dense 6x6 local patches with ZCA whitening are extracted with stride 1, and thresholding coding with $\alpha = 0.25$ is adopted for encoding. The codebook is trained with OMP-1. The features are then average-pooled on a 2×2 grid to form the global image representation. I tested three classifiers: linear SVM, RBF kernel based SVM, and the Random Recursive SVM model as introduced in Section 4.2.2.

As have been shown in Figure 4.5(b), the performance is almost monotonically increasing as I stack more layers in R^2SVM. Also, stacks of SVMs by concatenation of output and input feature space does not yield much gain above 1 layer (which is a linear SVM), and neither does a deterministic version of recursive SVM where a projection matrix as in the proof for Lemma 4.2.1 is used. For the R^2SVM, in most cases the performance asymptotically converges within 30 layers. Note that training each layer involves training a linear SVM, so the computational complexity is simply linear to the depth of my model. In contrast to this, the difficulty of training deep learning models based on many hidden layers may be significantly harder, partially due to the lack of supervised information for its hidden layers.

Figure 4.5(b) shows the effect that the feature dimensionality (controlled by the codebook size of OMP-1) has on the performance of the linear and non-linear classifiers, and Table 4.3 provides representative numerical results. In particular, when the codebook size is low, the assumption that I can approximate the non-linear function f as a globally linear classifier fails, and in those cases the R^2SVM and RBF SVM clearly outperform the linear SVM. Moreover, as the codebook size grows, non-linear classifiers, represented by RBF SVM in the experiments, suffer from the curse of dimensionality partially due to the large dimensionality of the over-complete feature representation. In fact, as the dimensionality of the over-complete representation becomes too large, RBF SVM starts performing worse than linear SVM. For linear SVM, increasing the codebook size makes it perform better with

Method	Tr. Size	Code. Size	Acc.	Method	Tr. Size	Code. Size	Acc.
Linear SVM	All	50	64.7%	Linear SVM	25/class	50	41.3%
RBF SVM	All	50	74.4%	RBF SVM	25/class	50	42.2%
R^2SVM	All	50	69.3%	R^2SVM	25/class	50	42.8%
DCN	All	50	67.2%	DCN	25/class	50	40.7%
Linear SVM	All	1600	79.5%	Linear SVM	25/class	1600	44.1%
RBF SVM	All	1600	79.0%	RBF SVM	25/class	1600	41.6%
R^2SVM	All	1600	79.7%	R^2SVM	25/class	1600	45.1%
DCN	All	1600	78.1%	DCN	25/class	1600	42.7%

Table 4.3. Results on CIFAR-10, with different codebook sizes (hence feature dimensions). The table on the right uses only 25 training examples per class.

respect to non-linear classifiers, but additional gains can still be consistently obtained by the Random Recursive SVM method. Also note how my model outperforms DCN, another stacking architecture proposed in [38].

Similar to the change of codebook sizes, it is interesting to experiment with the number of training examples per class. In the case where I use fewer training examples per class, little gain is obtained by classical RBF SVMs, and performance even drops when the feature dimension is too high (Table 4.3), while Random Recursive SVM remains competitive and does not overfit more than any baseline. This again suggests that the proposed method may generalize better than RBF, which is a desirable property when the number of training examples is small with respect to the dimensionality of the feature space, which are cases of interest to many computer vision applications.

In general, my method is able to combine the advantages of both linear and nonlinear SVM: it has higher representation power than linear SVM, providing consistent performance gains, and at the same time has a better robustness against overfitting. It is also worth pointing out again that R^2SVM is highly efficient, since each layer is a simple linear SVM that can be carried out by simple matrix multiplication. On the other hand, non-linear SVMs like RBF SVM may take much longer to run especially for large-scale data, when special care has to be taken [29].

Caltech101 The Caltech-101 dataset is known to have few training examples while the features used are usually high-dimensional [139, 140]. This makes robustness a particularly important issue, as non-linear methods such as kernel SVMs may easily overfit to the training data. I adopted the ScSPM pipeline to extract features that are then fed into Random Recursive SVM, as evidence shows that sparse coding on SIFT features perform better than simple encoding methods in this case [27].

The results reported in Table 4.4 indicate a similar behavior of the algorithm to that on CIFAR-10, with consistent improvements of Random Recursive SVM over the linear baseline, but diminishing returns as I increase the codebook size. I also note that the Caltech 101 setup exhibits the "curse of dimensionality" trait, as only few examples per class are available at training time on a relatively large dimensional feature space. Typical kernel based SVMs were found harmful in the original ScSPM work in [139] (a 7% performance drop, as discussed in Section 5.5.5 of their paper). However, Random Recursive SVM

Table 4.4. Results on Caltech101 with different codebook sizes. Over multiple runs, an average improvement of 0.6% with 0.35 standard deviation for the 128 codebook size, and an average improvement of 0.3% with 0.25 standard deviation for the 1024 codebook size.

Method	Tr. Size	Code. Size	Acc.
Linear SVM	30/class	128	66.4%
R^2SVM	30/class	128	67.0%
Linear SVM	30/class	1024	72.9%
R^2SVM	30/class	1024	73.2%

Table 4.5. Performance comparison on MNIST. Note that error percentages are reported following the conventional protocol. Remarks: DCN used a codebook of 3000; NCA with Deep Auto Encoder used nearest neighbor for final classification; the last three methods all adopted pretraining and fine-tuning for the parameters.

Method	Err.
Linear SVM	1.02%
RBF SVM	0.86%
R^2SVM	0.71%
DCN [38]	0.83%
NCA w/ DAE [116]	1.0%
Conv NN [63]	0.53%

is more resilient to this (which is consistent with the observations in Section 5.1.5), and achieves improvements on the tested conditions.

MNIST I also applied my method to handwritten digit recognition on the MNIST dataset, where convolutional deep learning models are particularly effective. I adopted the same pipeline as CIFAR-10: local patches of size 6×6 are extracted with a stride of 1, a codebook of size 800 is trained via OMP-1, and threshold coding with $\alpha = 0.25$ is used to encode the local patches (increasing the codebook size above 800 was not helpful on MNIST). The features are then average-pooled over a 2×2 grid to produce the global representation of the images.

Table 4.5 summarizes the results from my setup. The R^2SVM is able to add flexibility to the linear model and achieves the best performance among the three. Importantly, although MNIST has a relatively large training data (60K training images), I still find the RBF SVM to generalize worse than the R^2SVM. In practice, the improvement of RBF over linear SVM would be severely compromised by the fact that it is almost V times slower than linear SVM, where V is the number of support vectors (usually large). On contrary, the method shows a better generalization ability with relatively low computation overhead.

Note that, even though a pipeline that is not tailored to generate feature for digit recognition is used, I achieved similar performance to several deep convolutional neural networks where all the parameters are discriminatively trained.

TIMIT

Finally, I report my experiments using the popular speech database TIMIT. The speech data is analyzed using a 25-ms Hamming window with a 10-ms fixed frame rate. I represent the speech using first- to 12th-order Mel frequency cepstral coefficients (MFCCs) and

Table 4.6. Performance comparison on TIMIT.

Method	Phone state accuracy
Linear SVM	50.1% (2000 codes) 53.5% (8000 codes)
R^2SVM	53.5% (2000 codes) 55.1% (8000 codes)
DCN, learned per-layer	48.5%
DCN, jointly fine-tuned	54.3%

energy, along with their first and second temporal derivatives. The training set consists of 462 speakers, with a total number of frames in the training data of size 1.1 million, making classical kernel SVMs virtually impossible to train. The development set contains 50 speakers, with a total of 120K frames, and is used for cross validation. Results are reported using the standard 24-speaker core test set consisting of 192 sentences with 7333 phone tokens and 57920 frames.

The data is normalized to have zero mean and unit variance. All experiments used a context window of 11 frames. This gives a total of $39 \times 11 = 429$ elements in each feature vector. I used 183 target class labels (i.e., three states for each of the 61 phones), which are typically called "phone states", with a one-hot encoding.

The pipeline adopted is otherwise unchanged from the previous dataset. However, I did not apply pooling, and instead coded the whole 429 dimensional vector with a dictionary with 2000 and 8000 elements found with OMP-1, with the same parameter α as in the vision tasks. The competitive results with a framework known in vision adapted to speech [129], as shown in Table 4.6, are interesting on their own right, as the optimization framework for linear SVM is well understood, and the dictionary learning and encoding step are almost trivial and scale well with the amounts of data available in typical speech tasks. On the other hand, R^2SVM boosts performance quite significantly, similar to what I observed on other datasets.

In Table 4.6 I also report recent work on this dataset [38], which uses multi-layer perceptron with a hidden layer and linear output, and stacks each block on top of each other. In their experiments, the representation used from the speech signal is not sparse, and uses instead Restricted Boltzman Machine, which is more time consuming to learn. In addition, only when jointly optimizing the network weights (fine tuning), which requires solving a non-convex problem, the accuracy achieves state-of-the-art performance of 54.3%. The method does not include this step, which could be added as future work; I thus think the fairest comparison of my result is to the per-layer DCN performance.

In all the experiments above I have observed two advantages of R^2SVM. First, it provides a consistent improvement over linear SVM. Second, it can offer a better generalization ability over non-linear SVMs, especially when the ratio of dimensionality to the number of training data is large. These advantages, combined with the fact that R^2SVM is efficient in both training and testing, suggests that it could be adopted as an improvement over the existing classification pipeline in general.

Also note that in the current work I have not employed techniques of fine tuning similar to the one employed in the architecture of [38]. Fine tuning of the latter architecture has accounted for between 10% to 20% error reduction, and reduces the need for having large depth in order to achieve a fixed level of recognition accuracy. Development of fine-tuning is

expected to improve recognition accuracy further, and is in the interest of future research. However, even without fine tuning, the recognition accuracy is still shown to consistently improve until convergence, showing the robustness of the proposed method.

In this chapter, I investigated low level vision and audio representations. By combining the simplicity of linear SVMs with the power derived from deep architectures, I proposed a new stacking technique for building a better classifier, using linear SVM as the base building blocks and employing a random non-linear projection to add flexibility to the model. My work is partially motivated by the recent trend of using coding techniques as feature representation with relatively large dictionaries. The chief advantage of this method lies in the fact that it learns non-linear classifiers without the need of kernel design, while keeping the efficiency of linear SVMs. Experimental results on vision and speech datasets showed that the method provides consistent improvement over linear baselines, even with no learning of the model parameters. The convexity of the model could lead to better theoretical analysis of such deep structures in terms of generalization gap, adds interesting opportunities for learning using large computer clusters, and would potentially help understanding the nature of other deep learning approaches, which is the main interest of future research.

Chapter 5

Analysis – Why and how does depth matter?

Part of the work that appears in this chapter has been published in peer reviewed conferences. The analysis regarding layer size has been published in ICML 2013 [65], together with an algorithm to exploit redundancy in computer vision (which was mostly developed by Yangqing Jia, but that I add as an example on how theory can help develop more efficient algorithms). I also propose one of the first studies regarding depth with a budget (i.e., whilst keeping the number of parameters fixed) on a challenging noisy speech recognition task. This work has been recently presented at Interspeech 2013 [131]. Lastly, I present some visualizations of the activations at certain depths in a complex vision task, showing how each layer extracts different kinds of information.

5.1 Analysis – Regarding Layer Size

5.1.1 The Importance of Size

In the recent decade, overcompletely encoded features have been shown to provide state-of-the-art performance on various applications. In computer vision, locally encoded and spatially pooled feature extraction pipelines work particularly well for image classification. Such pipelines usually start from densely extracted local image patches (either normalized raw pixel values or hand-crafted descriptors such as SIFT or HOG), and perform dictionary learning to obtain a dictionary of codes (filters). The patches are then encoded into an over-complete representation using various algorithms such as sparse coding [100, 135] or simple inner product with a non-linear post-processing [27, 73]. After encoding, spatial pooling with average or max operations are carried out to form a global image representation [139, 15]. The encoding and pooling pipeline may be stacked in a deep structure to produce a final feature vector, which is then used to predict the labels for the images usually via a linear classifier.

There is an abundance of literature on single-layered networks for unsupervised feature encoding. Various dictionary learning methods have been proposed to find a set of basis that reconstructs local image patches or descriptors well [80, 27], and encoding methods have

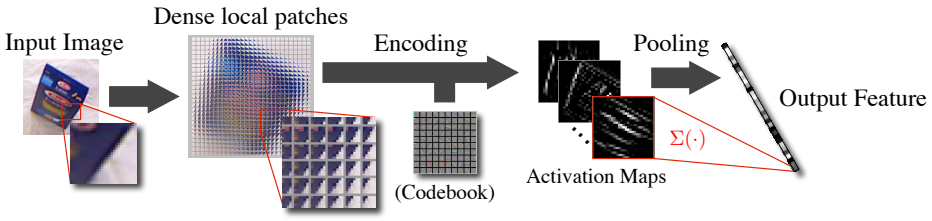

Figure 5.1. The feature extraction pipeline, composed of dense local patch extraction, encoding, and pooling. Illustrated is the average pooling over the whole image for simplicity, and in practice the pooling can be carried out over finer grids of the image as well as with different operations (such as max).

been proposed to map the original data to a high-dimensional space that emphasizes certain properties, such as sparsity [100, 139, 140] or locality [135]. Among these, a particularly interesting finding in the literature [26, 110, 27, 117] is that very simple patch-based algorithms like K-means or even random selection, combined with feed-forward encoding methods with a naive nonlinearity, produces state-of-the-art performance on various datasets. Explanation of such phenomena often focuses on the local image patch statistics, such as the frequency selectivity of random samples [117].

A potential problem with local patch-based dictionary learning methods for vision is that they may learn redundant features when we consider the pooling stage, as two codes that are uncorrelated may become highly correlated after pooling due to the introduction of spatial invariance. While using a larger dictionary almost always alleviates this problem, in practice we often want the dictionary to have a limited number of codes, as feature computation has become the dominant factor in the state-of-the-art image classification pipelines, even with purely feed-forward methods [27] or speedup algorithms [135]. A reasonably sized dictionary also helps to more easily learn further tasks that depends on the encoded features; this is especially true when we have more than one coding-pooling stage such as stacked deep networks, or when one applies more complex pooling stages such as second-order pooling [21], as a large encoding output would immediately drive up the number of parameters in the next layer. Thus, it would be beneficial to design a dictionary learning algorithm that takes pooling into consideration and learns a compact dictionary.

In this chapter I address the above questions by providing a novel view of the single-layer feature encoding based on kernel methods and Nyström sampling. In particular, I view the coding of a data point with a local representation based on a dictionary with fewer elements than the number of total data points as an approximation to the actual function that would compute pair-wise similarity to all data points (often too many to compute in practice), where the approximation is done by a random or K-means based selection of data points.

Furthermore, since bounds are known for the approximation power of Nyström sampling as a function of how many samples we consider (i.e., the dictionary size), I derive bounds on the approximation of the exact (but expensive to compute) kernel matrix. I then use it as a proxy to predict accuracy as a function of the dictionary size, which has been observed to increase but also to saturate as one increases its size. The Nyström view helps explaining the behavior of feature learning with increasing dictionary sizes, and justifies the use of simple algorithms such as K-means in dictionary learning [74]. It may also help justifying the need

to stack more layers (often referred to as deep learning), as flat models are guaranteed to saturate as we add more complexity.

I then show that the empirical findings in Nyström sampling view lead to a particularly simple yet effective algorithm that is analogous to the patch-based K-means method for dictionary learning, but that takes into account the additional redundancy introduced in the pooling stage. Specifically, I present a two-stage clustering method to learn a dictionary that identifies post-pooling invariant features. The resulting dictionary yields a higher classification accuracy while introducing no additional computational overhead during classifier training and testing time.

The Nyström sampling based explanation provides a new view of the unsupervised visual feature extraction pipeline, and may inspire new algorithms to perform efficient unsupervised feature learning in a deeper structure, such as the one presented in this thesis, mainly developed in conjunction with Yangqing Jia.

5.1.2 Relationship Between Random Dictionaries and Nyström Sampling

An important empirical observation was made in [27] with regards to the importance of the dictionary learned from the data and the encoding technique. The authors implied that, with a rather simple coding scheme and dictionary learning, the results were in most cases comparable to the widely used but more computationally expensive sparse coding technique. It was particularly noteworthy that selecting random dictionaries yielded close to state-of-the-art results. Further work on this domain [39] suggests that the encoding technique used is a proxy to solving sparse coding (but in a simple and faster fashion).

Still, the fact that random dictionaries perform well especially when operating with large codebook sizes poses interesting questions such as how the dictionary size affects performance, and why sufficiently large random dictionaries match learned dictionaries. In addition, even though the size of the dictionary (or codebook) is important, the accuracy seems to saturate, which is a phenomenon that was empirically verified in many tasks, and for which I now give a theoretical interpretation by linking random dictionaries with Nyström sampling.

The Nyström Sampling View

Nyström sampling (or method) [98] in the context of low rank matrix approximation is a technique that, given an $n \times n$ positive semi-definite (PSD) matrix $\mathbf{C}$, defines a good approximation to $\mathbf{C}$, $\mathbf{C}'$, as:

$$\mathbf{C}' = \mathbf{E}\mathbf{W}^{+}\mathbf{E}^{T}$$

with

$$\mathbf{E} = \begin{pmatrix} | & | & & | \\ \mathbf{c}_{\pi(1)} & \mathbf{c}_{\pi(2)} & \cdots & \mathbf{c}_{\pi(k)} \\ | & | & & | \end{pmatrix}$$

where $\mathbf{E}$ is formed by taking random columns of the original matrix $\mathbf{C}$. This technique is very cheap (it just requires sampling of $\mathbf{C}$) and provides reasonable low rank approximations that do not require to solve an eigenvalue problem or singular value decomposition (SVD).

In my case, I consider forming a dictionary by sampling our training set (although, as discussed below, better techniques exist that lead to further gains in performance). To encode a new data point $\mathbf{x} \in \mathbb{R}^d$, I apply a (generally non-linear) coding function $\mathbf{c}$ so that $\mathbf{c}(\mathbf{x}) \in \mathbb{R}^c$. The standard classification pipeline considers $\mathbf{c}(\mathbf{x})$ as the new feature space, and typically uses a linear classifier on this space. In this section, I consider the threshold encoding function as in [27], $\mathbf{c}(\mathbf{x}) = \max(0, \mathbf{x}^\top \mathbf{D} - \alpha)$, but the derivations are valid for other different coding schemes.

In the ideal case (infinite computation and memory), one can encode each sample $\mathbf{x}$ using the whole training set $\mathbf{X} \in \mathbb{R}^{d \times N}$, which can be seen as the best local coding of the training set $\mathbf{X}$, to the extent that overfitting is handled by the classification algorithm. In fact, larger dictionary sizes yield better performance assuming the linear classifier is well regularized, as it can be seen as a way to do manifold learning [135]. I define the new features in this high-dimensional coded space as $\mathbf{C} = \max(0, \mathbf{X}^\top \mathbf{X} - \alpha)$, where the i-th row of $\mathbf{C}$ corresponds to coding the i-th sample $\mathbf{c}(\mathbf{x}_i)$. The linear kernel function between samples i and j is $K(\mathbf{x}_i, \mathbf{x}_j) = \mathbf{c}(\mathbf{x}_i)^\top \mathbf{c}(\mathbf{x}_j)$. Thus, performing linear classification on the coded features effectively uses the kernel matrix $\mathbf{K} = \mathbf{C}\mathbf{C}^\top$.

In the context of Nyström sampling, one randomly samples a subset of the columns of $\mathbf{K}$ and then replaces the original matrix $\mathbf{K}$ with a low-rank approximation $\hat{\mathbf{K}}$. However, in this problem, naively applying Nyström sampling to the matrix $\mathbf{K}$ does not save any computation, as every column of $\mathbf{K}$ requires to encode the corresponding feature with the large dictionary of all N samples. However, if I approximate the matrix $\mathbf{C}$ with Nyström sampling to obtain $\mathbf{C}' \approx \mathbf{C}$, I would get an efficient approximation of the kernel matrix as $\mathbf{K}' \approx \mathbf{K}$:

$$\mathbf{C}' = \mathbf{E}\mathbf{W}^{-1}\mathbf{E}^\top, \text{ and} \tag{5.1}$$

$$\mathbf{K}' = \mathbf{C}'\mathbf{C}'^\top = \mathbf{E}\mathbf{W}^{-1}\mathbf{E}^\top\mathbf{E}\mathbf{W}^{-1}\mathbf{E}^\top = \mathbf{E}\mathbf{\Lambda}\mathbf{E}^\top, \tag{5.2}$$

where the first equation comes from applying Nyström sampling to $\mathbf{C}$, $\mathbf{E}$ is a random subsample of the columns of $\mathbf{C}$, and $\mathbf{W}$ the corresponding square matrix with the same random subsample of both columns and rows of $\mathbf{C}$.

Note that in the traditional coding scheme proposed in [27], $\mathbf{K}_{coding} = \mathbf{E}\mathbf{E}^\top$ if the dictionary is taken randomly, so by applying Nyström sampling to $\mathbf{C}$ I obtain almost the same kernel, where the matrix $\mathbf{\Lambda}$ acts as an additional Mahalanobis metric on the coded space. Adding the term $\mathbf{\Lambda}$ seemed to help in some cases, when the dictionary size is small (for example, in the CIFAR10 dataset, classification performance was improved by about 0.5% when $c < 500$.). I refer the interested reader to Section 5.1.4 to discuss the effect of $\mathbf{\Lambda}$ and how to efficiently find it without explicitly computing the original $N \times N$ matrix.

Error Bounds on the Approximation

Many existing analysis have computed bounds on the error made in estimating $\mathbf{C}$ by $\mathbf{C}'$ by sampling c columns, such as [125, 74], but not between $\mathbf{K} = \mathbf{C}\mathbf{C}^\top$ and $\mathbf{K}' = \mathbf{C}'\mathbf{C}'^\top$, which I aim to analyze in this section. The bound I start with is [74]:

$$||\mathbf{C} - \mathbf{C}'||_F \leq ||\mathbf{C} - \mathbf{C}_k||_F + \epsilon \max(n\mathbf{C}_{ii}), \tag{5.3}$$

valid if $c \geq 64k/\epsilon^4$ (c is the number of columns that we sample from $\mathbf{C}$ to form $\mathbf{E}$, i.e. the codebook size), where k is the sufficient rank to estimate the structure of $\mathbf{C}$, and $\mathbf{C}_k$ is

the optimal rank k approximation (given by Singular Value Decomposition (SVD), which cannot be computed in practice).

Fixing k to the value that retains enough energy from $\mathbf{C}$, I get a bound that gives a minimum ϵ to plug in Eqn. 5.3 for every c (sample dictionary size). This gives a useful bound of the form $\epsilon \geq M \left(\frac{1}{c}\right)^{\frac{1}{4}}$ for some constant M (that depends on k). Hence:

$$||\mathbf{C} - \mathbf{C}'||_F \leq O + M \left(\frac{1}{c}\right)^{\frac{1}{4}}, \tag{5.4}$$

where O and M constants that are dataset specific.

However, having bounded the error $\mathbf{C}$ is not yet sufficient to establish how the code size will affect the classifier performance. In particular, it is not clear how the error on $\mathbf{C}$ affect the error on the kernel matrix $\mathbf{K}$. Similarly, having a kernel matrix of different quality will affect classification performance. Recent work [30] proves a linear relationship between kernel matrix degradation and classification accuracy. Furthermore, in Section 5.1.3, I provide a proof that shows that the degradation of $\mathbf{K}$ is also proportional to the degradation of $\mathbf{C}$. Hence, the error bound on $\mathbf{K}'$ is of the same form as the one we obtained for $\mathbf{C}$:

$$||\mathbf{K} - \mathbf{K}'||_F \leq O' + M' \left(\frac{1}{c}\right)^{\frac{1}{4}}. \tag{5.5}$$

Note that the bound above also applies to the case when further steps, such as pooling, is carried out after coding, provided that such steps produce output feature dimensions that have a one-to-one correspondence with the dictionary entries. Pooling over multiple spatial regions does not change the analysis, as it could be deemed as concatenating multiple kernel matrices for the data.

Evaluating Bounds

I empirically evaluate the bound on the kernel matrix, used as a proxy to model classification accuracy (as justified by [30]), which is the measure of interest. To estimate the constants in the bounds, I do interpolation of the observed accuracy using the first three samples of accuracy versus codebook size, which is of practical interest: one may want to quickly run a new dataset through the pipeline with small dictionary sizes, and then quickly estimate what the accuracy would be when running a full experiment with a much larger dictionary (which would take much longer to run) with this formulation. I always performed Nyström sampling schemes by doing K-means instead of random selection (although the accuracy between both methods does not change too much when c is sufficiently large).

In Figure 5.2 I plot the accuracy (on both train and test sets) on four datasets: CIFAR-10 and STL from vision, and WSJ and TIMIT from speech. The implementation details of each dataset can be found in Section 5.1.5. The bound is designed to predict training accuracy [30], but I also do regression on testing accuracy for completeness. Note that testing accuracy will in general also be affected by the generalization gap, which is not captured by the bound analysis.

The results show that in all cases, the red dashed line is a lower bound of the training actual accuracy, and follows the shape of the empirical accuracy, predicting its saturation.

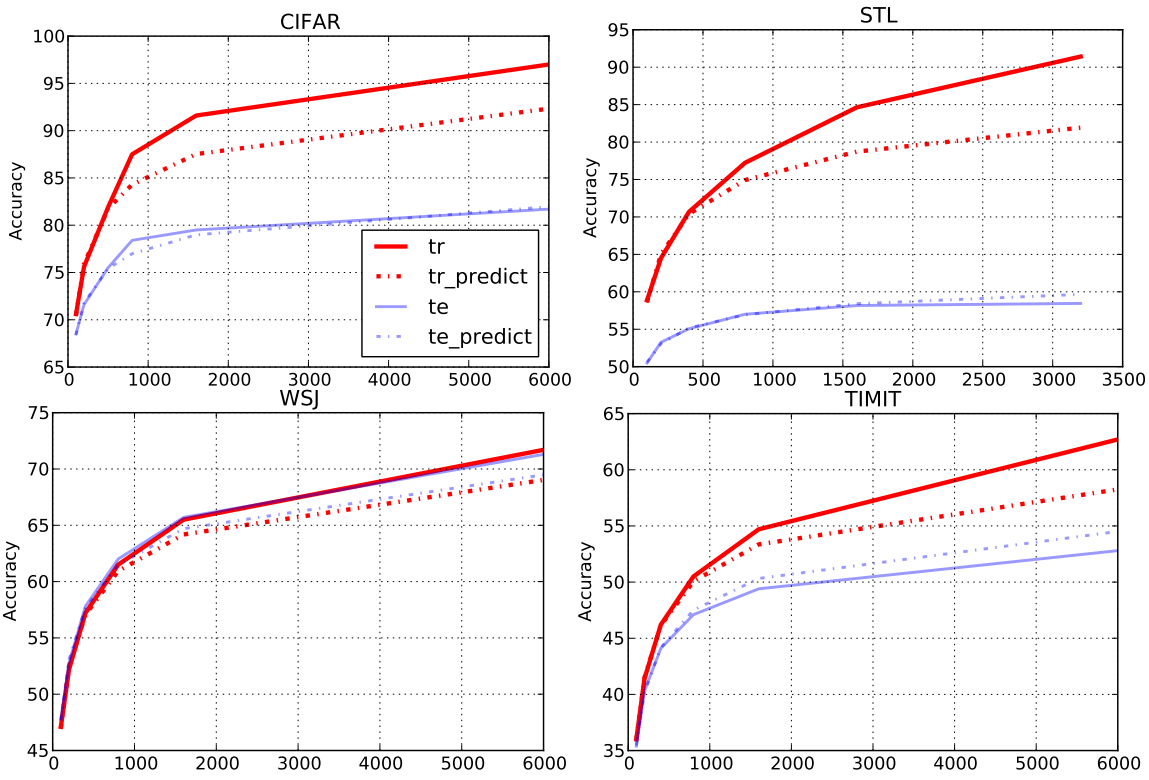

Figure 5.2. The actual training and testing accuracy (solid) and the predicted accuracy using our bound (dashed), on four datasets: CIFAR, STL, WSJ and TIMIT from left to right.

In the testing case, this model is slightly optimistic when overfitting exists (e.g., STL and TIMIT), but correctly predicts the trend with respect to the number of dictionary entries.

The implication of linking Nyström sampling theory to current learning pipelines has several immediate consequences: first, it clarifies why random sampling or K-means produce very reasonable dictionaries that are able to perform well in terms of classification accuracy [144, 26, 74]; more importantly, due to known bounds such as the one derived in this section, I can model how the codebook size will affect performance by running a few experiments with smaller codebook sizes, and extrapolating to larger (and more computationally expensive to compute) codebook sizes by means of Eq. 5.5, thus predicting accuracies before running potentially long jobs.

5.1.3 Relationship between $\mathbf{K}'$ and $\mathbf{C}'$

I briefly prove the bound here. Recall that $\mathbf{K} = \mathbf{C}\mathbf{C}^\top$ and $\mathbf{K}' = \mathbf{C}'\mathbf{C}'^\top$, and since $\mathbf{C}$ and $\mathbf{C}'$ are symmetric, $\mathbf{K} = \mathbf{C}^2$ and $\mathbf{K}' = \mathbf{C}'^2$. Note that the Frobenius norm satisfies subadditivity and submultiplicativity properties [83], i.e.,

$$||A + B||_F \leq ||A||_F + ||B||_F, \text{ and} \tag{5.6}$$
$$||AB||_F \leq ||A||_F||B||_F. \tag{5.7}$$

Thus,

$$\begin{aligned} ||\mathbf{K} - \mathbf{K}'|| &= ||\mathbf{C}^2 - \mathbf{C}'^2|| \\ &= ||(\mathbf{C} - \mathbf{C}')\mathbf{C} + \mathbf{C}'(\mathbf{C} - \mathbf{C}')|| \\ &\leq ||(\mathbf{C} - \mathbf{C}')\mathbf{C}|| + ||\mathbf{C}'(\mathbf{C} - \mathbf{C}')|| \\ &\leq ||(\mathbf{C} - \mathbf{C}')||||\mathbf{C}|| + ||\mathbf{C}'||||(\mathbf{C} - \mathbf{C}')|| \\ &\leq ||(\mathbf{C} - \mathbf{C}')||||\mathbf{C}|| + ||\mathbf{C}' - \mathbf{C}||^2 + \\ &\quad + ||\mathbf{C}||||(\mathbf{C} - \mathbf{C}')|| \\ &= ||(\mathbf{C} - \mathbf{C}')|| \left(||(\mathbf{C} - \mathbf{C}')|| + 2||\mathbf{C}||\right) \\ &= \mathcal{O}(||(\mathbf{C} - \mathbf{C}')||) \end{aligned} \tag{5.8}$$

where all the $||.||$ are the Frobenius norms, and where in the last line we assumed that $||(\mathbf{C} - \mathbf{C}')||$ is sufficiently small and $||\mathbf{C}||$ is constant w.r.t. c. Thus, one can expect that the approximation quality of $\mathbf{K}'$ will be similar than $\mathbf{C}'$, and [30] shows that the quality of the kernel approximation $\mathbf{K}'$ will determine the accuracy of the final classifier, which I will also empirically show in the experiments.

5.1.4 The metric in the coding space

In the derivation linking recent coding strategies [27] to Nyström sampling, I noted that the approach taken when considering doing subsampling of the coding matrix $\mathbf{C}$ to form a new code matrix to which I want to apply linear SVM is given by:

$$\mathbf{K}' = \mathbf{C}'\mathbf{C}'^\top = \mathbf{E}\mathbf{W}^{-1}\mathbf{E}^\top\mathbf{E}\mathbf{W}^{-1}\mathbf{E}^\top = \mathbf{E}\mathbf{\Lambda}\mathbf{E}^\top$$

where $\mathbf{E}$ is a matrix with the coded feature vector stacked as rows, and covers various encoding techniques (including threshold encoding or sparse coding), as can be seen in Figure 4.3. However, most of the work in the literature does not consider the square matrix $\mathbf{\Lambda}$ which arises when derivating the new kernel matrix from a Nyström sampling point of view. This is a square $c \times c$ matrix, where c is the dictionary size. Furthermore, the matrix is symmetric and PSD, which means that one can interpret it as a metric in the c dimensional coding space.

Further note that, if the selected columns when doing Nyström sampling are orthogonal, $\mathbf{\Lambda}$ is going to be diagonal, and as a consequence the effect of not considering it will be negligible, as it would act as a per dimension standard deviation normalization, which is typically done before the linear SVM regardless. Even though uniformly sampling columns of the original coding matrix $\mathbf{C}$ (that is, to randomly select samples from our training set as dictionary elements) yields good performance [27], methods such as Orthogonal Matching Pursuit perform better, specially for small values of c. This can now be partially explained by the fact that, since most of these methods did not consider $\mathbf{\Lambda}$, the gap between the correct implementation of Nyström sampling and what they were doing was artificially closed by selecting samples that were dissimilar, yielding a closer to diagonal $\mathbf{\Lambda}$ matrix.

However, since $\mathbf{\Lambda}$ is necessary to have a better estimate of $\mathbf{C}$ when, instead of doing SVD one approximates it via Nyström , I report in Section 5.1.2 an experiment in which I efficiently transform the features that are passed to the linear SVM so that the metric is also considered. Note that, if I took $\mathbf{E}' = \mathbf{E}\mathbf{W}^{-1}\mathbf{E}^\top$, then $\mathbf{K}' = \mathbf{E}'\mathbf{E}'^\top$. In this case, I would need to multiply each of the rows of $\mathbf{E}$ by a matrix to obtain "normalized" codes $\mathbf{E}'$ in which the metric is the identity, so standard linear SVM could be applied directly to $\mathbf{E}'$. Note that this is very wasteful, as $\mathbf{E}'$ is $N \times N$, so the gains of doing Nyström are lost (recall that $\mathbf{E}$ is $N \times k$). However, one can compute $\mathbf{\Lambda}$ once, and compute its Cholesky decomposition (i.e., write $\mathbf{\Lambda} = \mathbf{L}\mathbf{L}'$), with $\mathbf{L}$ a lower triangular $k \times k$ matrix. Thus, I can define $\mathbf{E}'' = \mathbf{E}\mathbf{L}$ so that $\mathbf{K}' = \mathbf{E}''\mathbf{E}''^\top$, but now $\mathbf{E}''$ is $N \times k$, which means that essentially the cost of this is the same as without accounting for the metric matrix by just using $\mathbf{E}$.

5.1.5 Dataset description

Here I describe the experimental results on four well known classification benchmarks: CIFAR-10, MNIST, TIMIT and WSJ. The CIFAR-10 dataset and the MNIST dataset both contain large amount of training/testing data, with the former focusing on object classification and the latter focusing on conventional OCR task. TIMIT is a speech database consisting of read digits that contains two orders of magnitude more training samples than the other datasets, and has the largest output label space as it has phone states as the output, and WSJ is a corpus with roughly five times more data than TIMIT, and consists of read sentences of the Wall Street Journal corpus.

CIFAR-10 The CIFAR-10 dataset [72] contains 10 object classes with a fair amount of training examples per class (5000), with images of small size (32x32 pixels). For this dataset, I followed the standard pipeline defined in [27]: dense 6x6 local patches with ZCA whitening are extracted with stride 1, and thresholding coding with $\alpha = 0.25$ is adopted for encoding. The codebook is trained with OMP-1. The features are then average-pooled on a 2×2 grid to form the global image representation.

TIMIT I report our experiments using the popular speech database TIMIT. The speech data is analyzed using a 25-ms Hamming window with a 10-ms fixed frame rate. The speech is represented using first- to 12th-order Mel frequency cepstral coefficients (MFCCs) and energy, along with their first and second temporal derivatives. The training set consists of 462 speakers, with a total number of frames in the training data of size 1.1 million. The development set contains 50 speakers, with a total of 120K frames, and is used for cross validation. Results are reported using the standard 24-speaker core test set consisting of 192 sentences with 7333 phone tokens and 57920 frames.

The data is normalized to have zero mean and unit variance. All experiments used a context window of 11 frames. This gives a total of $39 \times 11 = 429$ elements in each feature vector. I used 183 target class labels (i.e., three states for each of the 61 phones), which are typically called "phone states", with a one-hot encoding.

The pipeline adopted is otherwise unchanged from the previous dataset. However, I did not apply pooling, and instead coded the whole 429 dimensional vector with a dictionary found with OMP-1, with the same parameter α as in the vision tasks. The competitive results with a framework known in vision adapted to speech was reported in Chapter 4 and in [129].

WSJ All experiments were conducted on the 5000-word speaker independent WSJ0 (5k-WSJ0) task [101]. The training material from the SI84 set (7077 utterances, or 15.3 hours of speech from 84 speakers) is separated into a 6877-utterance training set and a 200-sentence cross-validation (CV) set. Evaluation was carried out on the Nov92 evaluation data with 330 utterances from 8 speakers. The features and pipeline are exactly the same as we used for TIMIT. However, the phone labels were derived from the forced alignments generated using a 2818 8-mixture tied-state cross-word tri-phone GMM-HMM speech recognition system trained with maximum likelihood criterion.

5.1.6 Pooling Aware Dictionary Learning

The Nyström sampling view suggests that one could find a better subset of a large (potentially infinite) dictionary to obtain more informative features. In addition, existing work suggests that this could be often done in an efficient way with methods such as clustering. However, current clustering algorithms for dictionary learning [26, 27] only apply to the local coding step, and do not consider the pooling effect. In this section, I show that by explicitly learning the dictionary taking into account the whole pipeline shown in Figure 5.1 to include both local coding and pooling, one gets a much more compact feature representation.

Figure 5.3 shows two examples why pooling-aware dictionary learning may be necessary, as local patch-based dictionary learning algorithms often yield similar filters with small translations. Such filters, even when uncorrelated on the patch level, produce highly correlated responses when pooled over a certain spatial region, leading to redundancy in the feature representation.

Observing the effectiveness of clustering methods in patch-based dictionary learning, I propose to learn a final dictionary of size K in two stages: first, I adopt the K-means algorithm to learn a more over-complete starting dictionary of size M ($M >> c$) on patches, effectively "overshooting" the dictionary I aim to obtain. I then perform encoding and

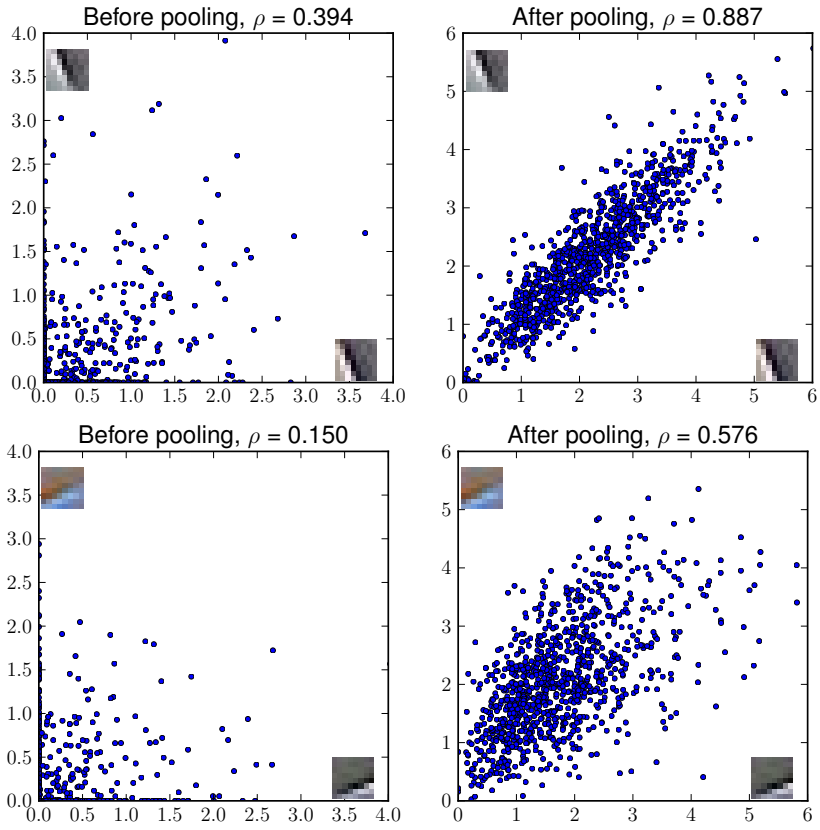

Figure 5.3. Two codes learned from a patch-based K-means algorithm that produce low correlation patch-based responses (left), but highly correlated responses after pooling (right). Such phenomena may root from various causes, such as codes with translational difference (above) and color difference (below).

pooling using the dictionary, and learn the final smaller dictionary of size c from the statistics of the M-dimensional pooled features.

Post-Pooling Feature Selection

The first step of the algorithm is identical to the patch-based K-means algorithm with a dictionary size M. After this, one can sample a set of image super-patches of the same size as the pooling regions, and obtain the M dimensional pooled features from them. Randomly sampling a large number of pooled features in this way allows us to analyze the pairwise similarities between the codes in the starting dictionary in a post-pooling fashion. One would then like to find a c-dimensional, lower dimensional subspace that best represents the M pooled features.

If I simply would like to find a low-dimensional representation from the M-dimensional pooled features, one would naturally choose SVD to find the K most significant projections of the covariance matrix. With a little abuse of terminology and denote the matrix of randomly selected pooled feature as $\mathbf{X}$ where each column is a feature vector, the SVD is carried out as

$$\mathbf{X} \approx \mathbf{U}_c \mathbf{\Lambda}_c \mathbf{V}_c^\top, \tag{5.9}$$

where $\mathbf{R}$ is the covariance matrix computed using the random sample of pooled features, the $M \times c$ matrix U_c contains the left singular vectors, and the $c \times c$ diagonal matrix $\mathbf{\Lambda}_c$ contains the corresponding singular values. The low-dimensional features are then computed as $\mathbf{x}_c = \mathbf{U}_c^\top \mathbf{x}$.

While the "oracle" low-dimensional representation by SVD guarantees the best c-dimensional approximation, it does not meet the goal since the dictionary size is not reduced, as SVD almost always yields non-zero coefficients for all the dimensions. Linearly combining the dictionary entries does not work either due to the nonlinear nature of the encoding algorithm. In this case, I would need the coefficients of only a subset of the features to be non-zero, so that a minimum number of filters need to be applied during testing time. Various machine learning algorithms aim to solve this, most notably structured sparse PCA [64]. However, these methods often requires a structured sparsity term to be applied during learning, making the training time-consuming and difficult to scale up.

Based on the analysis of the last section, the problem above could again be viewed as a Nyström sampling problem by subsampling the rows of the matrix $\mathbf{X}$ (corresponding to selecting codes from the large dictionary). Empirical results from the Nyström sampling then suggests the use of clustering algorithms to solve this. Thus, I resort to a simpler K-centroids method.

Specifically, I use affinity propagation [46], which is a version of the K-centroids algorithm, to select exemplars from the existing dictionary. Intuitively, codes that produce redundant pooled output (such as translated versions of the same code) would have high similarity between them, and only one exemplar would be chosen by the algorithm. I briefly explain the affinity propagation procedure here: it finds exemplars from a set of candidates where pairwise similarity $s(i, j)$ $(1 \leq i, j \leq M)$ can be computed. It iteratively updates two terms, the "responsibility" $r(i, j)$ and the "availability" $a(i, j)$ via a message passing

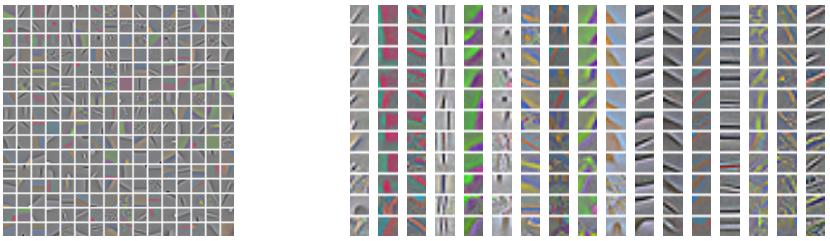

Figure 5.4. Visualization of the learned codes. Left: the selected subset of 256 centroids from an original set of 3200 codes. Right: The similarity between each centroid and the other codes in its cluster. For each column, the first code is the selected centroid, and the remaining codes are in the same cluster represented by it. Notice that while translational invariance is the most dominant factor, the algorithm does find invariances beyond that (e.g., notice the different colors on the last column). Best viewed in color.

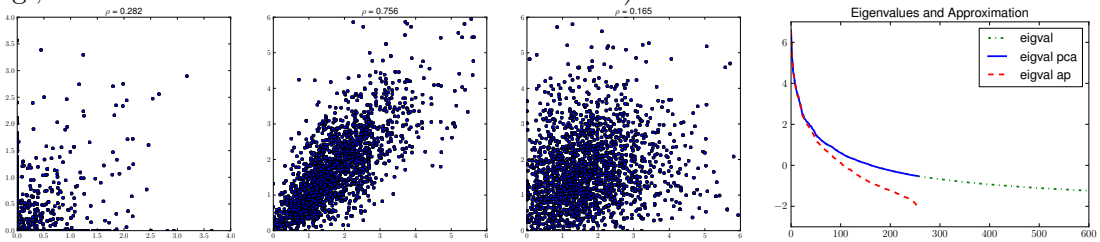

(a) (b) (c) (d)

Figure 5.5. (a)-(c): The filter responses before and after pooling: (a) before pooling, between codes in the same cluster (correlation $\rho = 0.282$), (b) after pooling, between codes in the same cluster ($\rho = 0.756$), and (c) after pooling, between the selected centroids ($\rho = 0.165$), (d): the approximation of the eigenvalues using the Nyström method (in log scale).

method following such rules [46]:

$$r(i,k) \leftarrow s(i,k) - \max_{k' \neq k}\{a(i,k') + s(i,k')\} \tag{5.10}$$

$$a(i,k) \leftarrow \min\{0, r(k,k) + \sum\nolimits_{i' \notin \{i,k\}} \max\{0, r(i',k)\}\}$$

$$(\text{if } i \neq k) \tag{5.11}$$

$$a(k,k) \leftarrow \sum\nolimits_{i' \neq k} \max\{0, r(i',k)\} \tag{5.12}$$

Upon convergence, the centroid that represents any candidate i is given by $\arg\max_k(a(i,k)+r(i,k))$, and the set of centroids $\mathcal{S}$ is obtained by

$$\mathcal{S} = \{k | \exists i, k \text{ s.t. } k = \arg\max_{k'}(a(i,k') + r(i,k'))\} \tag{5.13}$$

And I refer to [46] for details about the nature of such message passing algorithms. The similarity between two pooled dimensions (which correspond to two codes in the starting dictionary) i and code j, as in Eqn. (5.10)-(5.12), is to be computed as

$$s(i,j) = \frac{2R_{ij}}{\sqrt{R_{ii}R_{jj}}} - 2. \tag{5.14}$$

Note that this is equivalent to the negative Euclidean distance between the coded output i and the coded output j when the outputs are normalized to have zero mean and standard deviation 1. Note that related works such as [25] adopt a similar approach by max-pooling the outputs of similar codes to generate next-layer features in a deep fashion. This method shares the same merit while focusing on model compression by bounding the computation time in a single layer.

The motivation of such an idea is that clustering algorithms have been shown to be very effective in the context of Nyström sampling [74], and are often highly parallelizable, easily being scaled up by simply distributing the data over multiple machines. This allows us to maintain the efficiency of dictionary learning. Using a large, over-complete starting dictionary allows us to preserve most information from the patch-level, and the second step prunes away the redundancy due to pooling. Note that the large dictionary is only used during the feature learning time - after this, for each input image, I only need to encode local patches with the selected, relatively smaller dictionary of size c, not any more expensive than existing feature extraction methods.

5.1.7 Experiments

In this section I empirically evaluate two sets of experiments: using the bound to approximate the classification accuracy, and using the two-staged clustering algorithm, as suggested by Nyström sampling, to find better pooling invariant dictionaries.

Analysis of Selected Filters

To visually show what codes are selected by affinity propagation, I applied this approach to the CIFAR-10 dataset by first training an over-complete dictionary of 3200 codes following

[27], and then performing affinity propagation on the 3200-dimensional pooled features to obtain 256 centroids, which I visualize in Figure 5.4. Translational invariance appears to be the most dominant factor, as many clusters contain translated versions of the same Gabor-like code, especially for gray scale codes. On the other hand, clusters capture more than translation: clusters such as column 5 focus on finding the contrasting colors more than finding edges of exactly the same angle, and clusters such as the last column finds invariant edges of varied color. Note that the selected codes are not necessarily centered, as the centroids are selected solely from the pooled response covariance statistics, which does not explicitly favor centered patches.

One could also verify whether the second clustering stage captures the pooling invariance by checking the statistics of three types of filter responses: (a) pairwise filter responses *before pooling* between codes in the same cluster, (b) pairwise filter responses *after pooling* between codes in the same cluster, and (c) pairwise filter responses after pooling between the selected centroids. The distribution of such responses shown in Figure 5.5 verifies this argument: first, codes that produce uncorrelated responses before pooling may become correlated after the pooling stage (Figure 5.5(a,b)); second, by explicitly considering the pooled feature statistics, I was able to select a subset of the dictionary whose responses are lowly correlated (Figure 5.5(b,c)), preserving more information with a fixed number of codes. In addition, Figure 5.5(d) shows the eigenvalues of the original covariance matrix and those of the approximated matrix, showing that the approximation captures the largest eigenvalues of the original covariance matrix well.

Pooling Invariant Dictionary Learning

To evaluate the improvement introduced by learning a pooling invariant dictionary as in Section 5.1.6, I show in Figure 5.6 the relative improvement obtained on CIFAR-10 when I use a fixed dictionary size 200, but perform feature selection from a larger over-complete dictionary as indicated by the X axis. The SVD performance is also included in the figure as an "ideal case" for the feature selection performance. Learning the dictionary with this feature selection method consistently increases the performance as the size of the original dictionary increases, and is able to get about two thirds of the performance gain obtained by SVD (note again that SVD still requires the large dictionary to be used and does not save any testing time).

The detailed performance gain of the algorithm on the two datasets, using different over-complete and final dictionary sizes, is visualized in Figure 5.7. Table 5.1 summarizes the accuracy values of two particular cases - final dictionary sizes of 200 and 1600 respectively, on CIFAR. Note that my goal is not to get the best overall performance - as performance always goes up when more codes are used. Rather, I focus on two evaluations: (1) how much gain I get given a fixed dictionary size as the budget, and (2) how much computation time I save to achieve the same accuracy.

Overall, considering the pooled feature statistics always helps us to find better dictionaries, especially when relatively small dictionaries are used. During testing time, it costs only about 60% computation time with Pooling invariant Dictionary Learning (PDL) to achieve the same accuracy as K-means dictionary does. For the STL dataset, a large starting dictionary may lessen the performance gain (Figure 5.7(b)). I infer the reason to be that feature selection is more prone to local optimum, and the small training data of STL

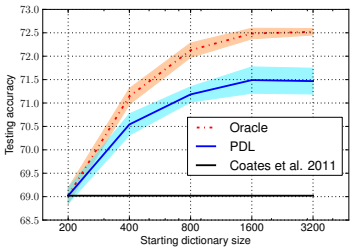

Figure 5.6. Performance improvement on CIFAR when using different starting dictionary sizes and a final dictionary of size 200. Shaded areas denote the standard deviation over different runs. Note that the x-axis is in log scale.

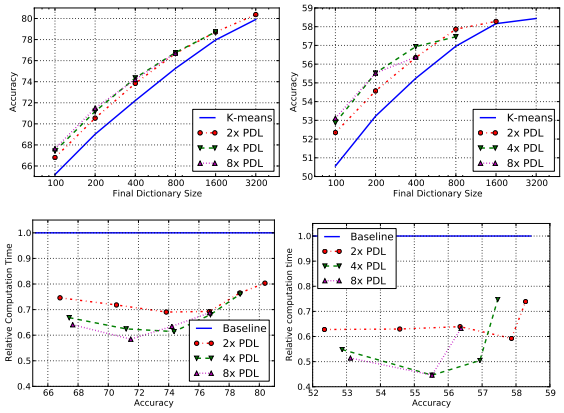

Figure 5.7. Above: accuracy values on the CIFAR-10 and STL datasets under different dictionary size budgets. "nx PDL" means learning the dictionary from a starting dictionary that is n times larger. Below: Relative computation time to achieve the same accuracy using dictionary obtained from PDL.

may cause the performance to be sensitive to suboptimal codebook choices. However, in general the codebook learned by PDL is consistently better than its patch-based counterpart, suggesting the applicability of the Nyström sampling view in feature learning with a multi-layer structure.

5.2 Analysis – Regarding Depth

5.2.1 Depth in Depth

It has been established that incorporating neural networks can be useful for speech recognition, and that machine learning methods can make it practical to incorporate a larger number of hidden layers in a "deep" structure. Here I incorporate the constraint of freezing the number of parameters for a given task, which in many applications corresponds to practical limitations on storage or computation. Given this constraint, I vary the size of each hidden layer as I change the number of layers so as to keep the total number of parameters constant. In this way I have determined, for a common task of noisy speech recognition (Aurora2), that a large number of layers is not always optimum; for each noise level there is

Table 5.1. Classification Accuracy on the CIFAR-10 and STL datasets under different budgets.

Task	Learning Method	Accuracy
CIFAR-10 200 codes	K-means	69.02
	2x PDL	70.54 (+1.52)
	4x PDL	71.18 (+2.16)
	8x PDL	71.49 (+2.47)
CIFAR-10 1600 codes	K-means	77.97
	2x PDL	78.71 (+0.74)

an optimum number of layers. I also use state-of-the-art optimization algorithms presented in this thesis to further understand the effect of initialization and convergence properties of such networks, and to have an efficient implementation that allows us to run more experiments with a standard desktop machine with a single GPU.

In the past decade, the term "deep learning" has been popularized thanks to its various successes in many applications in machine learning such as speech or vision. In the speech community, deep learning has achieved enough maturity so that a number of commercial applications use it as part of their acoustic or language models (some completely replacing mixture models).

Much of this progress has built on technology that was developed years ago. In particular, the hybrid HMM/MLP system, in which the output posteriors have been used (after division by class priors) as scaled likelihoods for HMMs, was developed over twenty years ago [16, 92, 61]. Alternatively, the tandem approach, in which the MLP outputs are used (typically after a few transformations) as features for an HMM/GMM system, has been used for many tasks. Still, the newer systems have advanced beyond these earlier ones, primarily in 3 ways: (1) while most (but not all [47, 45, 17]) of the earlier systems used monophone classes, the newer ones tend to use finer categories; (2) the most obvious difference is that the newer approaches use many hidden layers instead of one or two, which is partly made possible by (3) machine learning approaches to initialize the networks so that the layers closer to the input still perform some useful task despite being so "far" from the correction signals at the output.

Here I focus on the 2nd and 3rd aspects, since it has been taken as "common wisdom" that adding a significant number of layers is necessary for good performance. A number of papers have compared a "deep" network implementation to a standard MLP with a single large hidden layer, essentially always showing significant improvements from adding depth. However, I have not observed any careful study of the error rates for ASR when the number of parameters is kept constant over the different sized nets; in other words, determining the tradeoff between the depth and width of the network.

For the purpose of this section, I am using the Aurora2 task [102], which uses spoken digit strings with natural noises artificially added to achieve different SNRs. There are many limitations to this data set: it is small, it does not incorporate properties of natural conversational speech, adding noise artificially does not provide natural human signal modifications in the presence of noise (e.g., Lombard effect), and additionally the test set has been significantly plumbed, having been used by researchers for a decade, so the raw error

	MFCC	1-hid	2-hid	3-hid	4-hid	5-hid	6-hid	7-hid	8-hid
clean	0.97%	0.61%	0.51%	0.53%	0.55%	0.55%	**0.46%**	0.52%	0.51%
20dB	4.84%	2.27%	**1.80%**	1.89%	2.16%	1.98%	2.24%	2.00%	2.09%
15dB	14.65%	4.67%	**4.25%**	4.34%	4.83%	4.60%	5.11%	4.64%	5.00%
10dB	35.80%	12.05%	**10.53%**	11.08%	11.75%	10.92%	11.81%	10.87%	11.81%
5dB	65.78%	29.20%	26.23%	26.57%	27.47%	25.94%	27.02%	**24.61%**	26.45%
0dB	86.33%	58.35%	54.42%	53.02%	53.85%	52.67%	53.09%	**49.67%**	52.01%
neg5dB	92.75%	83.94%	80.32%	80.12%	81.26%	79.72%	79.09%	**76.06%**	78.61%
AVG	43.02%	27.30%	25.44%	25.37%	25.98%	25.20%	25.55%	**24.06%**	25.21%
UsableAVG	14.06%	4.90%	**4.27%**	4.46%	4.83%	4.51%	4.91%	4.51%	4.85%

Table 5.2. Table of Word Error Rates (WER) for Aurora2 experiments. The MFCC column corresponds to the use of MFCCs plus first and second derivatives as the features for the HMM. The others correspond to network features with each column corresponding to the indicated number of hidden layers. In each case the resulting features are appended to the MFCC-based features. The AVG row gives the average of the WERs for all the SNRs, while the UsableAVG row is the average of WERs for all the SNRs of 10 dB and higher.

rates are not particularly relevant. All this being said, it is a commonly used data set, and once the reader sees that the performance is in a reasonable range, he or she can focus on the comparative results – how performance varies for the corresponding depths and widths.

5.2.2 Factors in Deep Learning

Since many researchers have been studying deep learning, I want to further discuss key points that, although widely discussed in the community, are important to both the speech community, and other applied machine learning fields.

Depth

The main point of this work is to analyze how the depth of the model affects the performance in Aurora2 recognition. To this effect, I consider a standard neural network with sigmoid hidden units and an output layer consisting of a softmax function that maps real numbers to numbers with probabilistic properties. As discussed in Section 2, most of the recent success of neural networks has been attributed to having deep architectures (i.e. having many hidden layers, e.g., 5 or more). In [88, 119, 31] the effect of adding more layers is shown to improve performance by up to a few percent (absolute), but often adding more layers adds more parameters to the network, thus allowing for a more powerful model. In this section, I do a fair comparison varying the number of hidden layers while preserving a reasonable measure of complexity of the model (in terms of the number of parameters). A limitation on the number of parameters can often be a proxy for realistic constraints on storage or computation, or in some cases for cost.

Initialization

Although pretraining was originally proposed as a better starting point to the optimization to find the "optimal" parameters to the network, later work suggested that other simpler initialization schemes were quite successful by incorporating the effect of vanishing gradients [10]. However, since pretraining in a small dataset such as Aurora2 still may have its benefits, all the results reported here use standard RBM initialization. I do not report results without pretraining, but even given the size of the dataset it did not seem to have a large effect – overall, the results for deeper models were the same except for models deeper than 4 layers, where on average they were 2% absolute worse).

Optimization

Instead of using standard gradient descent methods, I used an improved algorithm based on the idea behind Hessian Free optimization that I presented in Chapter 3. These methods have already proven successful within the speech community (e.g. [69, 132]), and differ from other common methods in two ways:

- The second order information deals (in part) with the vanishing gradients problem. One of the effects of this, besides achieving faster convergence rates, is to greatly reduce the importance of pretraining.
- The fact that I use a step size tuned on a separate random batch of data than the one used to compute the gradient has good implications for reducing generalization error. As a result, I do not require early stopping as I do not observe overfitting, even with more parameters than samples. This is confirmed by observing errors on an independent cross-validation set.

Training was performed on a single GPU (NVIDIA GTX 580), and was run for 50 epochs (i.e. 50 passes through all the data), taking about 2 hours to complete. No overfitting was observed (i.e., cross validation likelihood kept improving every epoch), even for a network of 2.4M parameters trained on 1.4M samples.

5.2.3 Experiments and Results

For this section, I use the Aurora 2 data set described earlier in this thesis (Chapter 3). To remind the reader, Aurora2 is a connected digit corpus which contains 8,440 sentences of clean training data and 56,056 sentences of clean and noisy test data. The test set comprises 8 different noises (subway, babble, car, exhibition, restaurant, street, airport, and train-station) at 7 different noise levels (clean, 20dB, 15dB, 10dB, 5dB, 0dB, -5dB), totaling 56 different test scenarios, each containing 1,001 sentences. Since I am interested in the performance of various deep learning architectures in mismatched conditions, all systems were trained only on the clean training set but tested on the entire test set. The inputs to each network consist of a context window of 9 frames of PLP-12 (13 parameters including C0) and its first and second derivatives; that is, 9 x 39 input variables. The hidden layers are all the same size, and are adjusted in length to make the number of parameters the same for each experiment. The outputs of each network consist of 55 units corresponding

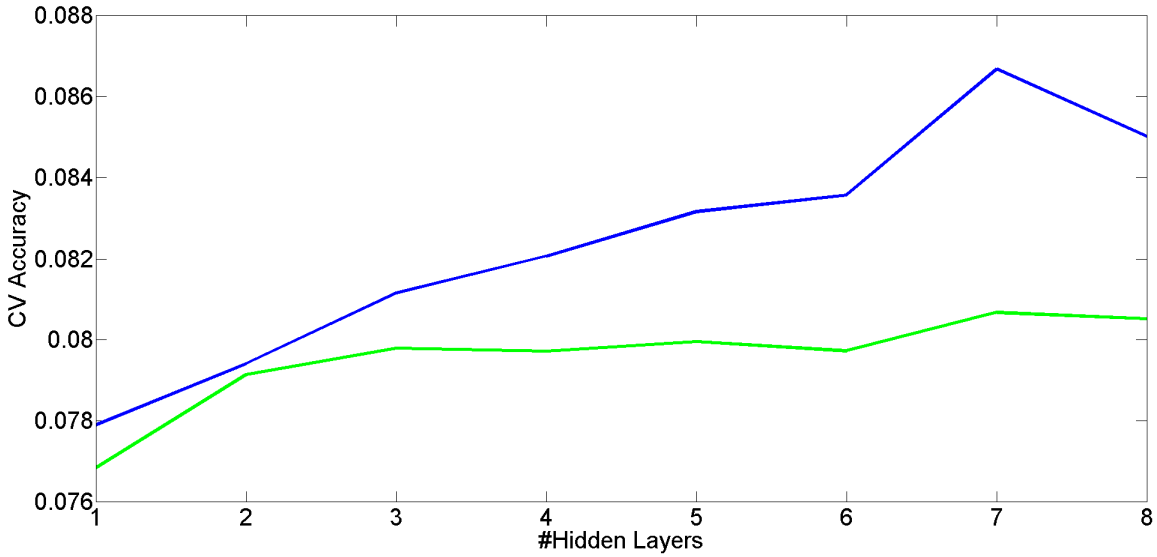

Figure 5.8. Cross validation frame error (y-axis) for varying number of hidden layers (x-axis), with the same number of units in each hidden layer for each choice of the number of layers, with this size chosen to keep the number of parameters constant. The blue curve corresponds to frame classification errors for nets that are initialized with random weights before the optimization, while the green curve shows results from the same architecture as the blue but gives frame classification error when pretraining is used. All the networks are trained using a second order batch method on a single GPU.

to phonetic categories for training. During HMM training and recognition, these outputs are used in Tandem mode, and in particular, used as features after taking the logarithm, transforming with PCA, and appending to an additional 39 features comprising MFCC-12 (including C0) and its first and second derivatives.

The parameters for the HTK decoder used for this experiment are the same as that for the standard Aurora2 setup described in [102]. The setup uses whole word HMMs with 16 states with a 3-Gaussian mixture with diagonal covariances per state; skips over states are not permitted in this model. This is the setup that was used in the ETSI standards competition.

The basic architecture considered for the DNN was inspired by the MNIST hand written digit recognition task [59] and the baseline is the same that I used in recent work (further details on the training procedure can be found in [133].

Figure 5.8 shows the frame accuracy (without an HMM) on a held out set of 800 utterances for cross validation. To my surprise, the shallow network seems to perform better than any of the deep variants (even when pretraining is used) when fixing the number of parameters to 2.4M (the same as in [133]). However, it is important to note that the cross validation data comprises clean speech only, and that the only source of variation is speaker variability. Furthermore, pretraining has a bigger impact with networks of depth 3 and more, as observed by the fact that without it, networks tend to perform worse as the model gets deeper. Although not plotted, the training curves show that training error actually improves with depth (reaching a minimum at 4 hidden layers). I can partially conclude

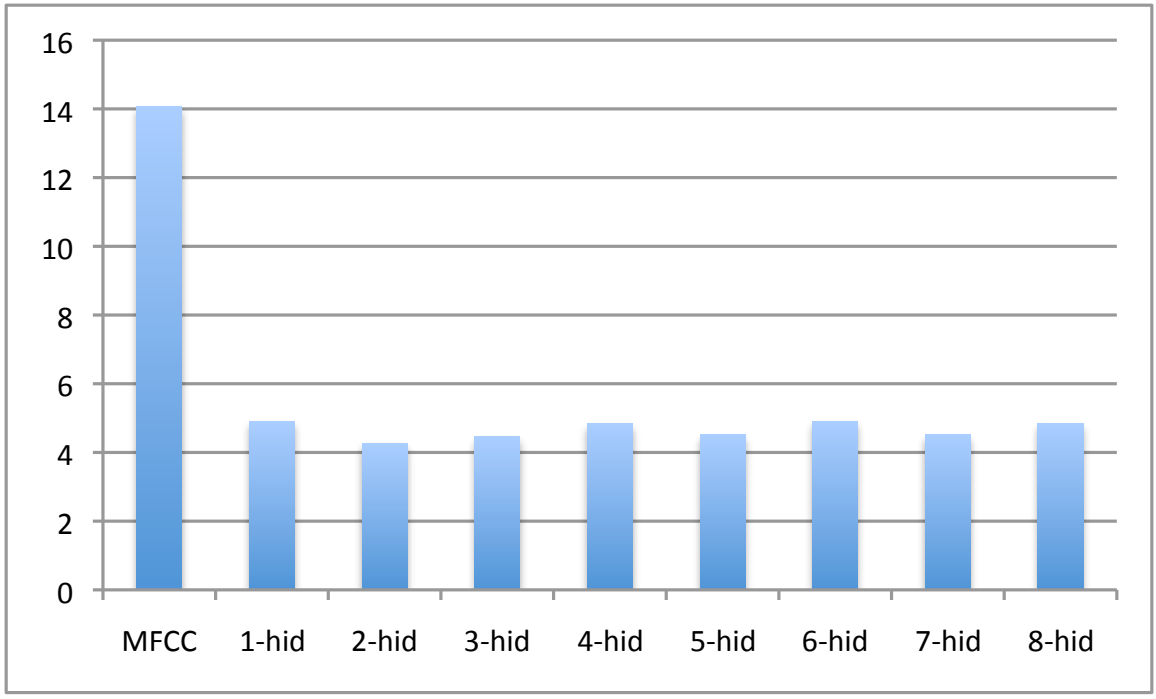

Figure 5.9. The bar graphs correspond to the WERs from the bottom row of the previous table, and illustrate the average error rates over a reasonable range of SNRs for the different feature extraction modules (10 dB or higher). All of the Tandem methods add significant value to the MFCCs, but there is essentially no benefit to use more than 2 hidden layers.

that, given the same number of parameters, the deeper models are able to fit more complex data (as seen by the improvement on training error), but do not gain any generalization capabilities for the noiseless case.

As interesting as this result is, for speech word error rate is more important than frame accuracy (especially since the curves above only show the MLP results, and are not affected by the HMM which certainly has significant effects on the recognized sequence). The results from the experiments are given in table 5.2, with the best result for each noise level highlighted with bold font. There are many results here, so it is useful to further indicate performance over a practical range, namely for those SNRs of at least 10 dB. This is indicated in the figure pictorially in figure 5.9, showing essentially no improvement after 2 hidden layers are used. This figure is for an average of error rates over each example. The full table is of course more complicated, in particular showing utility for more layers in some of the noisier cases; however, none of the results in the $<$ 10 dB SNR cases are good enough to be usable.

I only report results with pretraining, as it does indeed help when the model gets deeper. This is compatible with previous work: pretraining generally helps, especially when the amount of data is small compared to the size of the model (as in this case). As a consequence, when no pretraining is used, the results for deeper models are slightly worse – but, thanks to the way I optimize the model, not severely so [82].

There are many follow-up experiments that should be run in order to better understand

the results. In keeping with modern practice in "deep" network usage, I have used many more parameters than the more standard rules of thumb would suggest – more than one parameter per data pattern. My view was that this gave the "deep" approaches their best chance to do well. However, the design space should be further explored, for instance by using many more parameters, as well as by using many fewer (I did also experiment with half and double the amount of parameters, but the conclusions with those models would have been the same). In the results reported here, I always used RBM retraining, which has been shown to be effective for such tasks; however, I have also been running experiments without the pretraining, and discriminant methods can provide alternative initialization of the layers. For simplicity's sake, I used the network outputs in Tandem mode, and it would be good to try the same test using the hybrid HMM/MLP approach. The network architecture that I focus on here uses the same number of units per hidden layer, although I have other experiments running with different shapes. Finally, the task is relatively small, and I do not know if there might be different results for speech that is more variable (e.g., conversational), as well as with a much larger amount of training data.

Despite these intriguing possibilities for future work, what has already been done certainly does suggest that, given a particular parameter budget, it is not at all obvious that resources need to be allocated to a very large number of layers. It is reasonable to conclude that researchers and developers who are working on a new task should compare results for different depths using the maximum number of parameters that they deem practical for their application (assuming that they are using some reasonable method to check for overfitting) and, keeping that fixed, do comparisons such as those reported here. They may be quite surprised to find that a "middling" depth is quite sufficient.

5.2.4 Depth in Vision

In this section, I describe work in progress that is under submission for the upcoming ICML 2014. A preprint can be found in [40]. I did most of the analysis regarding feature depth and generalization, which fits this thesis chapter perfectly, but for completeness I include work mostly conducted by Jeff Donahue who reproduced the state-of-the-art object recognition system on one of the larger and most challenging object recognition datasets as presented in [73].

Architecture Description

In this approach, a deep convolutional model (i.e., a deep convolutional neural network (CNN)) is first trained in a fully supervised setting using a state-of-the-art method [73]. Various features are extracted from this network (i.e., the activations of the hidden layers are taken as the features). Even though the forward pass computed by the architecture in this section does achieve state-of-the-art performance on ILSVRC-2012, two questions remain:

- Do features extracted from the CNN generalize to other datasets?
- How do these features perform versus depth?

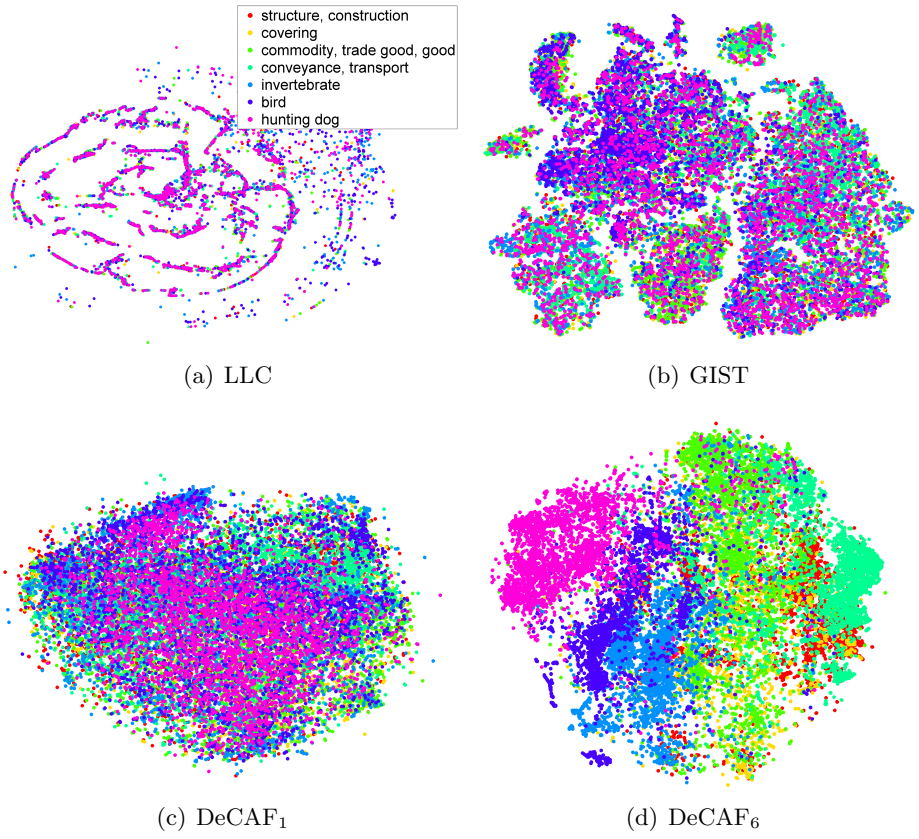

(a) LLC (b) GIST

(c) DeCAF_1 (d) DeCAF_6

Figure 5.10. This figure shows several t-SNE feature visualizations on the ILSVRC-2012 validation set. (a) LLC , (b) GIST, and features derived from the CNN: (c) DeCAF_1, the first pooling layer, and (d) DeCAF_6, the second to last hidden layer (best viewed in color).

I address these questions both qualitatively and quantitatively, via visualizations of semantic clusters below.

The publicly available implementation made by our vision group at ICSI, DeCAF, can be found at `http://decaf.berkeleyvision.org/`, in addition to the network parameters to allow for out-of-the-box feature extraction without the need to re-train the large network. This also aligns with the philosophy of supervised transfer: one may view the trained model as an analog to the prior knowledge a human obtains from previous visual experiences, which helps in learning new tasks more efficiently.

As the underlying architecture for the features, the deep convolutional neural network architecture proposed by [73] is used, which won the ImageNet Large Scale Visual Recognition Challenge 2012 [11] with a top-1 validation error rate of 40.7%. [1] I chose this model due to its performance on a difficult 1000-way classification task, hypothesizing that the activations of the neurons in its late hidden layers might serve as very strong features for a variety of object recognition tasks. A similar approach has recently been used to output

[1]The model entered into the competition actually achieved a top-1 validation error rate of 36.7% by averaging the predictions of 7 structurally identical models that were initialized and trained independently. Jeff trained only a single instance of the model; hence I refer to the single model error rate of 40.7%.

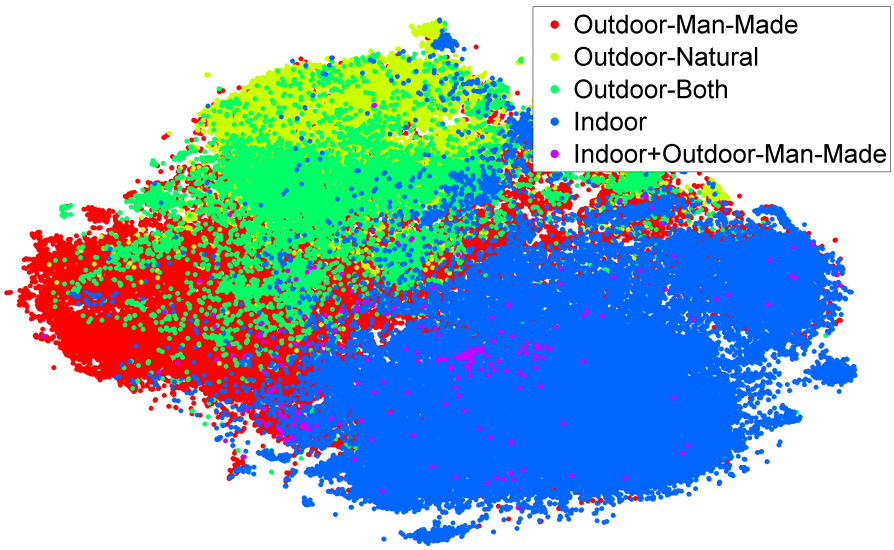

Figure 5.11. In this figure I show how our features trained on ILSVRC-2012 generalized to SUN-397 when considering semantic groupings of labels (best viewed in color).

word embeddings from the same architecture (see [48]). Its inputs are the mean-centered raw RGB pixel intensity values of a 224×224 image. These values are forward propagated through 5 convolutional layers (with pooling and ReLU non-linearities applied along the way) and 3 fully-connected layers to determine its final neuron activities: a distribution over the task's 1000 object categories. This instance of the model attains an error rate of **42.9%** on the ILSVRC-2012 validation set – 2.2% shy of the 40.7% achieved by [73].

I refer to [73] for a detailed discussion of the architecture and training protocol, which Jeff closely followed with the exception of two small differences in the input data. First, he ignores the image's original aspect ratio and warp it to 256×256, rather than resizing and cropping to preserve the proportions. Secondly, he did not perform the data augmentation trick of adding random multiples of the principle components of the RGB pixel values throughout the dataset, proposed as a way of capturing invariance to changes in illumination and color[2].

Feature Generalization and Visualization

I visualized the model features to gain insight into the semantic capacity of DeCAF and other features that have been typically employed in computer vision. In particular, I compare the features described in the previous subsection with GIST features [99] and LLC features [135].

I visualize features in the following way: I run the t-SNE algorithm [128] to find a 2-dimensional embedding of the high-dimensional feature space, and plot them as points colored depending on their semantic category in a particular hierarchy. For the reader

[2]According to personal communication with the authors, this scheme reduced their models' test set error by over 1%, likely explaining much of the network's performance discrepancy.

that may not be interested in reading the t-SNE paper, this algorithm can be thought as a non-linear (and non-parametric) way to do dimensionality reduction. I did this on the validation set of ILSVRC-2012 to avoid overfitting effects (as the deep CNN used in this experiments was trained only on the training set), and also used an independent dataset, SUN-397 [138], to evaluate how dataset bias affects the results (see e.g. [126] for a deeper discussion of this topic).

One would expect features closer to the output (softmax) layer to be linearly separable, so it is not very interesting (and also visually quite hard) to represent the 1000 classes on the t-SNE derived embedding.

I first visualize the semantic segregation of the model by plotting the embedding of labels for higher levels of the WordNet hierarchy; for example, a strong feature for visual recognition should cluster indoor and outdoor instances separately, even though there is no explicit modeling through the supervised training of the CNN, as each class is treated independently regardless of the common characteristics that two visual classes may share. Figure 5.10 shows the features extracted on the validation set using the first pooling layer (DeCAF_1), and the second to last fully connected layer (DeCAF_6), showing a clear semantic clustering in the latter but not in the former. This is compatible with common deep learning knowledge that the first layers learn "low-level" features, whereas the latter layers learn semantic or "high-level" features. Furthermore, other features such as GIST or LLC fail to capture the semantic difference in the image (although they show interesting clustering structure).[3]

More interestingly, in Figure 5.11 I show the top performing features (DeCAF_6) on the SUN-397 dataset. Even there, the features show very good clustering of semantic classes (e.g., indoor vs. outdoor). This suggests DeCAF is a good feature for general object recognition tasks. Consider the case where the object class that we are trying to detect is not in the original object pool of ILSVRC-2012. The fact that these features cluster several intermediate nodes of WordNet implies that these features are an excellent starting point for generalizing to unseen classes. More experiments and evidence on how powerful these features are can be found in the preprint [40].

[3]Some of the features were very high dimensional (e.g., LLC had 16K dimension), in which case I preprocess them by randomly projecting them down to 512 dimensions – random projections are cheap to apply and tend to preserve distances well, which is all the t-SNE algorithm cares about.

Chapter 6

Keyword Spotting: A Speech Application

In this chapter I present a speech application that looks at keyword detection – an important speech task that poses many research challenges as well as having tremendous commercial impact. In particular, Section 6.1 shows how optimization techniques (Chapter 3) become key and can be applied to very limited resource languages. Furthermore, in Section 6.2, a direct application of the techniques proposed in Chapter 4 is shown to provide computationally efficient keyword detection, crucial for deploying such technology to mobile devices. I recently filed a patent with Google and the system presented in this chapter is now being deployed to millions of phones in the world as part of Google Voice in the Android Operating System.

6.1 Keyword Spotting for Limited Resources

6.1.1 Limited Data and the BABEL Project

Keyword detection is the task of deciding whether a certain word appears in an audio segment. It can be seen as a subproblem of speech recognition, and this is mostly what motivated the approach that ICSI took on the IARPA Babel program [1][1]. The goal of the program "is to rapidly develop speech recognition capability for keyword search in a previously unstudied language, working with speech recorded in a variety of conditions with limited amounts of transcription." This paradigm contrasts with the one presented in the next section, where a single word (known a priori, and from a language with large amounts of data) is the main object of the keyword detection system.

Although in a detection task one typically cares about the precision and recall of the detector, since in Babel we are given a long list of keywords with very different characteristics

[1]Supported by the Intelligence Advanced Research Projects Activity (IARPA) via Department of Defense US Army Research Laboratory contract number W911NF-12-C-0014. The U.S. Government is authorized to reproduce and distribute reprints for Governmental purposes notwithstanding any copyright annotation thereon. Disclaimer: The views and conclusions contained herein are those of the authors and should not be interpreted as necessarily representing the official policies or endorsements, either expressed or implied, of IARPA, DoD/ARL, or the U.S. Government.

(e.g., common words and extremely rare words), averaging across each keyword does not seem to be the optimal metric. Instead, they define the Actual Term Weighted Value (ATWV), which is a weighted average (with keyword specific weights based on how frequent the keyword is in the test bed) of a metric related to probability of misses and false alarms. In particular, for a posting entry i with keyword k, TWV(k,i) is:

$$\mathrm{TWV}(k,i) = \mathbf{I}(s(i) > th(k)) \left(\frac{1}{N_k} \mathbf{I}(i = hit) - \frac{\beta}{T - N_k} \mathbf{I}(i = FA) \right)$$

where $s(i)$ is the score for the i-th entry, $\beta = 999.9$, T is the total evaluation time in seconds, and N_k counts how many times keyword k occurs in the current dataset. This metric basically counts the posting entry only if the score is above a certain (keyword specific) threshold. If the posting entry i was a hit, it gives a reward (which is larger for rare keywords), and if it was a false alarm it has a cost (that is approximately constant since T is typically much larger than N_k). ATWV is then simply:

$$\mathrm{ATWV} = \frac{1}{|K|} \sum_k \sum_{i_k} \mathrm{TWV}(k, i_k) \tag{6.1}$$

where i_k goes through every index in the posting list that contains keyword k as a candidate, and $|K|$ is the total number of keywords. Note that ATWV is upper bounded by 1.

In this chapter, I propose to smooth ATWV based on recent work [95] which suggests that direct optimization of a smoothed discrete figure of merit (such as ATWV) is a cost effective method to achieve close to optimal solutions.

6.1.2 The ICSI System and Babel

The ICSI system can be split into two major subsystems: standard speech recognition, and the keyword search system. I describe them in the following two sections:

6.1.3 The recognition system

The Kaldi speech recognition toolkit [105], along with the TNet[2] toolkit, were used for recognition and lattice generation.

The full system description can be found in [109], and an updated version in [136], but here I summarize it for completeness.

The ICSI system uses 13 MFCCs as primary features after cepstral mean subtraction. It extracts pitch and probability-of-voicing (PoV) features using a sub-band autocorrelation classification, SAcC [77]. These two features are smoothed, interpolated, and then pasted with the cepstral features to form a 15-dimensional feature vector. While ICSI uses Δ and $\Delta\Delta$s for early systems in the initialization, it uses a variant of HLDA features for the final systems. The LDA transformation takes as input a context of 7 spliced static MFCC vectors and is trained using the context dependent states as targets; the features are projected down to 30 dimensions. During training, this LDA matrix is composed with global MLLT matrices as well as speaker dependent fMLLR matrices [49].

[2] http://speech.fit.vutbr.cz/software/neural-network-trainer-tnet

It also uses 30-dimensional tandem bottleneck (BN) features [52] that are obtained using a hierarchical NN [127]. See [109] for more details. For the tandem features, the system pastes combinations of cepstral, pitch and bottleneck features together to form the tandem feature vector. Note that HLDA is applied to the cepstral part of the features only, while MLLT and fMLLR are applied to the combined feature stream.

Following this is an HMM system with a standard continuous acoustic model where the emission probabilities of the context dependent states are derived from subspace Gaussian mixture models (SGMM) [104]. It uses a 3-gram language model on the training transcripts, and apply Kneser-Ney smoothing and interpolated counts [122, 70].

The KWS system

The KWS system consists of three steps: i) converting recognition lattices to indexes, ii) searching the indexes for a given KW and constructing a posting list, iii) and setting the KW-specific detection threshold in order to optimize ATWV. These are further described below. Note that the KWS systems described here are entirely word-based, i.e., ICSI system does not combine the word-based search with a separate subword-based search in order to handle out-of-vocabulary (OOV) KWs, e.g., as in [85, 68].

i. ICSI uses "lattice-tool" from SRILM [122] to convert lattices to word-level indexes. They set the lattice-tool parameter that controls how far apart in time two occurrences of a word have to be in the lattice before considering to be separate entries in the index to be 0.1 sec.

ii. For single word KWs the posting list is simply all of the occurrences of the KW sorted by their posterior probabilities. To construct the posting list for a multi-word KW ICSI follows [85]: the individual words are first retrieved from the index in the correct order with respect to their start and end times, but occurrences are discarded when the time gap between adjacent words is more than 0.5 seconds. The surviving occurrences are assigned a detection probability equal to the minimum of the individual word probabilities.

iii. To determine the detection threshold for a given KW they used an empirical threshold to approximately maximize TWV for each keyword. However, much of my system and improvements produce a threshold-less system, so this step is omitted in the experiments reported in Section 6.1.4. However, for the baselines in the Standard Metrics section, this step is still performed as it produces much better thresholds than setting them to a fixed number for all keywords.

The data

The audio data in each language is conversational telephone speech recorded in a variety of environments and handset types. There were several languages that program participants worked with, and in this chapter I used Pashto (release babel104b-v0.4bY), Vietnamese (release babel107b-v0.7), and Bengali (release babel103b-v0.3). Each language comes with about 80 hours of transcribed training data (Full Language Pack), a pronunciation lexicon that covers the words in the training data, and a 10 hour development test set. All of the results in this chapter report KWS results using the keywords (KW) provided for the evaluation. Also, when I report results on the evaluation data I will be restricting the results

to the subsets, called "eval-part1", where the ground truth was released to participants: a 15 hour subset in the case of Vietnamese and 5 hour subsets for the rest of the languages. I have also tested the system on a new language released after the first year of Babel, Bengali, to show that the approach generalizes.

6.1.4 Discriminative Posting Refinements

My contributions to the ICSI Babel system have been mostly about modifying the posting lists by changing the score from each keyword candidate, trying to achieve better overall performance. I have considered several features (besides the posting entry) to enhance the posterior estimate of the detected posting entry (i.e., keyword and time segment pair). Here is an example of a very short posting list:

```
CONV#14 house 1.3s-1.9s 0.56
CONV#15 house 6.3s-6.8s 0.12
CONV#15 castle 0.3s-1.2s 0.94
```

Note that each keyword candidate has a time, score (from lattice-tool) and conversation id associated with it.

The features that I considered are:

- Acoustic Features: features inspired by the sparse coding features presented in Chapter 4, by taking a window (centered around the keyword candidate)
- Acoustic Quality Features: features such as signal to noise ratio (SNR) extracted with SNREval[3] and speaking rate [93]
- Keyword Specific Features: features such as the frequency or length of a keyword
- Lattice Specific Features: since posting lists are derived from lattices, I used arching measurements around the keyword as an additional hint for confidence (the score output in step ii. is already a good estimate)
- Neural Network Posterior Features: neural networks are used to predict phone states per frame. I took the entropy around the keyword of these posterior estimates as another proxy to confidence

All the features above were computed, whenever possible, at the posting list level (i.e., only on the span of the keyword candidate), at the utterance level (i.e., on the span of the speech utterance given by the speech/non-speech detector on the whole conversation side), and at the global level (i.e., considering the whole conversation).

Initially, I attempted to learn standard classifiers using these features. In particular, I considered both linear classifiers (logistic regression and SVM), as well as non-linear classifiers (NN). I built a simple dataset where, for each entry in the posting list, I assign a corresponding label whether the entry was a hit (i.e., the keyword was indeed in the ground truth), or not. This binary classification task was very unbalanced since the posting lists were typically very biased to produce a large number of false alarms. In the following subsection I define some baselines and how vanilla classifiers performed in this task.

[3] `http://labrosa.ee.columbia.edu/projects/snreval/`

System	Accuracy	Negated Log Likelihood	ATWV
Majority Voting	97.25%	N/A	N/A
ICSI	N/A	N/A	0.4010
Baseline	97.79%	0.08	0.3989
SVM	98.21%	0.11	0.3976
Logistic Regression	98.09%	0.07	0.4005
Neural Network	97.98%	0.06	0.4012
Upper Bound	100.0%	0.0	0.71

Table 6.1. Several models and metrics measured on the training set.

Optimizing Standard Metrics

In Table 6.1 I show accuracy, likelihood, and ATWV for the training data, which consists of about 400K posting entries for Pashto. The baseline system uses as features the scores that are already present in the posting lists (and that are used by the ICSI system) without any additional features, and trains a simple logistic regression (with one parameter and a bias). The rest used all the features available, but SVM used hinge loss (optimizing accuracy), and Logistic Regression and Neural Network used cross entropy (optimizing likelihood).

Note that, in general, accuracy and likelihood are not great measures of ATWV (which I further discuss in the following section), and ICSI and Baseline systems, even though they use the same features, do not exhibit the same performance. This can be explained because the features get scaled by the logistic regression model (Baseline) which has a negative effect on the following module that sets the threshold for each keyword.

As another example of how unrelated is ATWV to standard binary decision tasks, Figure 6.1 shows the Receiver Operating Characteristic (ROC) curve for the ICSI system (blue), the Logistic Regression (red) and the Neural Network (green). It is clear that the green curve is better at any point of the precision / recall curve, but in terms of ATWV both systems perform similarly. The reason, which is also described in detail in a recent thesis from one of the members of the ICSI team [106], is due to the fact that rare keywords should be regarded higher than common keywords (as they have higher TWV). Instead of trying an ad-hoc method (such as biasing the dataset) to achieve this, I chose to directly optimize ATWV, which is described in the following section.

Optimizing ATWV

As previously discussed, instead of optimizing accuracy or likelihood, I will optimize ATWV, which is the object of interest for Babel. Even though I could use discrete optimization techniques such as the Powell method [107] as used recently in [66], I prefer smooth objective functions as these are faster to optimize, and can use more sophisticated regression models such as neural networks. Recall from equation 6.1 that ATWV is a discrete objective as it is a function of thresholding the decision function for sample i, $s(i)$. Thus, I take the simple approach of smoothing the unit step with the sigmoid function, so that:

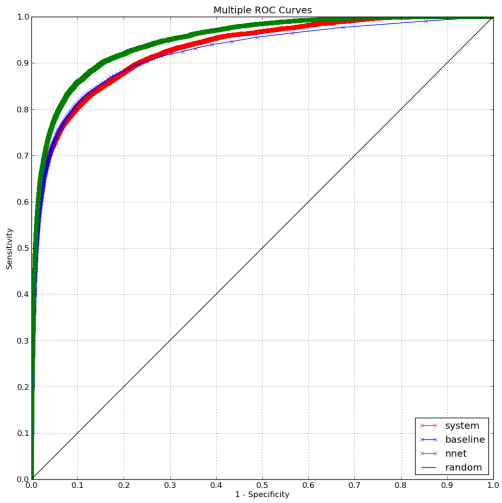

Figure 6.1. Receiver operating characteristic.

$$\mathbf{I}(x > 0) \approx \sigma(\mathcal{S}x) = \frac{1}{1 + \exp(-\mathcal{S}x)}$$

which converges to the left hand side as $\mathcal{S} \to \infty$. Recent work [95] suggests that optimizing a non-convex approximation of the discrete function is almost always better than to find a convex relaxation (such as replacing $I(x > 0)$ with the hinge loss). In fact, the SVM approach in the previous section (with some modifications) would be close to doing such convex relaxation. But, since the dataset is quite small (less than a million samples), I found the direct optimization of a smooth version of ATWV more compelling. As a result, I define from equation 6.1:

$$\text{smoothATWV} = \frac{1}{|K|} \sum_k \sum_{i_k} \sigma(\mathcal{S}(s(i_k) - th(k))) \left(\frac{1}{N_k} \mathbf{I}(i_k = hit) - \frac{\beta}{T - N_k} \mathbf{I}(i_k = FA) \right)$$

which now can be differentiated with respect to $s(i_k)$, and further to the parameters with chain rule (assuming I parameterize $s(i_k; \boldsymbol{\theta})$, which will be referred to as the model). As a result, I define a new objective function in which I can find the optimal parameters $\boldsymbol{\theta}$ that optimize ATWV (or, rather, an approximation to it). Lastly, since the model typically has a bias which can partially absorb $th(k)$, and having a model that has a common threshold that is keyword independent has certain advantages (e.g., for system combination), I set $th(k) = 0.5 \; \forall k$. This also has the advantage of eliminating step iii in Section 6.1.3.

With this approach, and setting $\mathcal{S} = 10$, I ran L-BFGS on two kinds of model: the first, a log linear model, and the second, a neural network. In both cases, the input for the posting entry i are the features $\mathbf{x}_i$, and the parameters of the model are $\boldsymbol{\theta}$, resulting in $s(i; \boldsymbol{\theta}) = f(\mathbf{x}_i, \boldsymbol{\theta})$ with $f(.)$ being either $\sigma(.)$ (for the log linear model) or a neural network with one binary output. Figure 6.2 shows how good of an approximation the smooth ATWV

System	Features	ATWV (train)	ATWV (validation)
ICSI	Score	0.4010	0.3685
Log Linear Model	Score	0.4065	0.3752
Log Linear Model	+KW features	0.4118	0.3799
Log Linear Model	+KW features +Acoustic features	0.4138	**0.3835**
Neural Network	+KW features +Acoustic features	0.4297	0.3764

Table 6.2. Several models and features when optimizing directly for ATWV in the Pashto BABEL dataset.

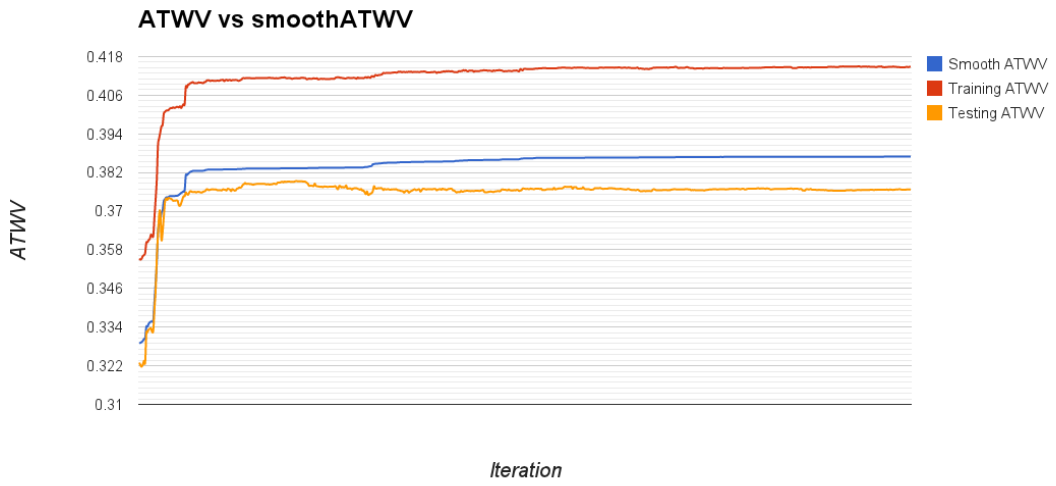

Figure 6.2. Smooth ATWV as the training progresses, as well as ATWV on both training and testing for Pashto for the system with only the score feature.

is (blue vs. red curve), as well as showing that the whole framework can indeed learn a better ATWV than the baseline of 0.4010.

In Table 6.2 I show the results of my experiments. First, note that the neural network, even though it fits the training data better than the simpler log linear model, it overfits and the testing ATWV is not competitive (even though it is better than the original ICSI system). Secondly, even when considering only the features used in the ICSI system (i.e. step ii of Section 6.1.3), the resulting system is superior (0.3752 vs. 0.3685). This means that, even though a lot of effort has been put trying to find the optimal threshold for the score coming from the lattices, the automated system can do a better job figuring out how to optimize ATWV directly.

As a last note, even when applying the Log Linear Model with Score features trained on Pashto on a different language (Bengali), the ATWV of the resulting system is also better. The Bengali ICSI system has an ATWV of 0.3123, whereas transferring the model from Pashto to Bengali yielded a slight improvement with an ATWV of 0.3133. Also, when optimizing the model using Bengali, I was expecting similar gains than with Pashto. Indeed, the ATWV with all the features was of 0.3287, a significant improvement with very

System	ATWV (validation)
ICSI A	0.3870
ICSI B	0.3697
A+B Heuristic	0.4446
A+B My System	**0.4534**

Table 6.3. System combination on the Vietnamese development data comparing human heuristics and my method to optimize directly for ATWV.

little computational overhead. Lastly, I also performed an experiment using the limited language pack (i.e., less training data), and on Bengali I obtained an improvement from 0.1287 ATWV to 0.1476.

6.1.5 Further Improvements of ATWV

In this last section, I describe current and future efforts that would further improve ATWV. Since I found an efficient method to directly optimize this metric, I wanted to see how one could incorporate this in other parts of the system. In fact, part of what the ICSI system already was doing was to optimize ATWV on single scalar values such as language or acoustic modeling scales using a simplex method which did not require to smooth the ATWV, and were already improving it by as much as 10% relative.

System Combination using Optimized ATWV

Another idea I tried that seems to help in terms of ATWV is system combination. Although it is out of the scope of this thesis to review system combination in the Babel project, the main idea is to replace the human designed heuristic to combine systems by one that would be learned with the procedure described in this chapter. The way I generate systems is by randomly selecting subsets of front-end features, and by merging posting lists of such systems. If an entry of system A overlaps with an entry of system B, the heuristic I found to work best added the two scores. My method found the optimal way of linearly combining scores of two (or more) systems with little computational overhead (certainly none when comparing to training the full system).

Results using Vietnamese can be found in Table 6.3. I use a different language than in previous sections to show generalization of the technique across languages. Indeed, even though I tested several heuristics and converged to keeping the sum of two scores when segments from different systems overlap, learning how to linearly combine the systems (or, potentially, adding other features such as the max of the scores, etc.) yielded an improvement of almost 1% (the weights found by my system favored ICSI A, as that system had initially a better ATWV).

6.2 Keyword Spotting for Unlimited Resources

6.2.1 Computational Budget and Unlimited Data

In this section I describe two systems that I developed towards robust and efficient keyword detection. The work that I present here has been patented by me and other people at Google and is being deployed as part of the standard Android Operating System to detect when a user intends to give a voiced command to a portable device, even when such device is on standby. The first system, which I call SparseHotword, does not use any additional information besides the training data for a specific word. The second system is based on an acoustic model trained on a large corpus, and I call it DeepHotword. The motivation of this work is to build a decoder free system, where I only use acoustic models to achieve detection – this contrasts with the limited data scenario discussed previously in this chapter, and can be done here thanks to the abundant amount of examples of the keyword to be detected. I considered two different scenarios, one in which I do offline detection (that is, for a given utterance, has the target word occurred?), and one in which I do online detection, where a decision is made at each time step. Initial experiments show that the performance achieved by both systems is either equal or better than a system based on fully decoding the utterance (similar to the one presented earlier, but inspired by [51]), while being more computationally efficient, necessary if we want to run such systems on a device all the time as it listens for its user to issue a command.

In particular in this case, I am interested in detecting a single word (e.g. "Google") that will activate an Android based smart phone on standby to perform a task. This device, thus, should be listening all the time for such word. A common problem in portable devices is battery life, and limited computation capabilities. Because of this, I aim for a hotword detection system that is both accurate and computationally efficient. None of the approaches require decoding, which is often regarded as the most computationally expensive part in typical hotword systems.

The first approach does not use any additional data, and consists of an unsupervised phase – one in which I learn models with no need of labels – followed by a supervised model for classification based on features extracted with the unsupervised model. The second approach uses an acoustic model trained with a separate set of data to explore transfer learning from a domain that is related. However, instead of decoding using the acoustic model, I just extract features from it and, as in the first model, run a simple classifier.

6.2.2 Proposed Methods

In the following subsections I fully describe the two approaches that I took towards robust and efficient hotword recognition.

SparseHotword

Background Sparse coding is a popular method based on unsupervised learning of feature representation that has become very popular in the computer vision and machine learning

community. It can be formulated as an optimization method, where, given an input signal $\mathbf{x}$, I want to find a code $\mathbf{c}$ that depends on a (learned) dictionary $\mathbf{D}$ as follows:

$$\{\mathbf{c}, \mathbf{D}\} = \arg\min_{\{\mathbf{c},\mathbf{D}\}} ||\mathbf{x} - \mathbf{D}\mathbf{c}||_2^2 + ||\mathbf{c}||_1 \tag{6.2}$$

Intuitively, sparse coding tries to find a dictionary and code so that the reconstruction (in L2 sense) will be as close to the original as possible (first term), while keeping the code as sparse as possible (second term).

The machine learning community has studied how to solve this minimization problem that is convex in both $\mathbf{c}$ and $\mathbf{D}$, but not jointly. Recently, an approach that was much simpler was empirically shown to perform well on a computer vision object detection task [27], as well as on phone classification [129]. This approach consisted on constructing $\mathbf{D}$ by either running k-means, or by randomly sampling $\mathbf{x}$ and use samples as dictionary atoms.

After finding $\mathbf{D}$, I form $\mathbf{c}$ by a simple matrix-vector product followed by a non-linearity that induces sparsity:

$$\mathbf{c} = \max(0, \mathbf{D}\mathbf{x} - \alpha) \tag{6.3}$$

where α is a hyperparamter that I find via cross-validation.

A recent paper [39] theoretically shows why such an approach performs as well as the original sparse coding approach, suggesting that coding as in eq. 6.3 is equivalent to taking one step into the gradient direction of eq. 6.2.

One of the main advantages of sparse coding is that it does not require lots of data to perform well, and that it can form the dictionary from data in a completely unsupervised way (i.e. it does not require more labeled training data). After finding the code $\mathbf{c}$ for each training example $\mathbf{x}$, I proceed in the usual way, which is to pool codes together for each instance (e.g. image or utterance), and to learn a linear classifier in the pooled code space from training data, typically using a linear SVM.

Hotword Detection In this problem, $\mathbf{x}$ is a spectro-temporal signal that comes from 40 mel filter banks, looking at 25 ms. of analysis, and shifting the analysis window by 10 ms. at a time. In particular, I obtain a 2D signal of $40N$ where N is the number of frames that I stack together. I stack this 2D signal in the vector $\mathbf{x}$ of $40\mathbf{N}$ dimensions and code it using eq. 6.3 to obtain a C dimensional vector (I tried C from 500 to 2000 in these experiments).

Following the coding of $\mathbf{x}_t$ at each time step t in an utterance, I operate in either offline or online mode. In offline mode, I take each code $\mathbf{c}_t$ and pool all the codes together at the end of the detected utterance. Thus, for each utterance u I obtain a single pooled vector:

$$\mathbf{c}_{pooled} = pool\_offline(\mathbf{c}_1, \ldots, \mathbf{c}_T)$$

where pool can be average, max (component-wise), or root mean square (L2 pooling), and T is the total utterance duration. Note that the resulting vector $\mathbf{c}_{pooled}$ is of the same dimension as the original code space, i.e. C, and that, regardless of utterance duration T, the pooling vector does not change. These vectors are then fed to a linear SVM for classification.

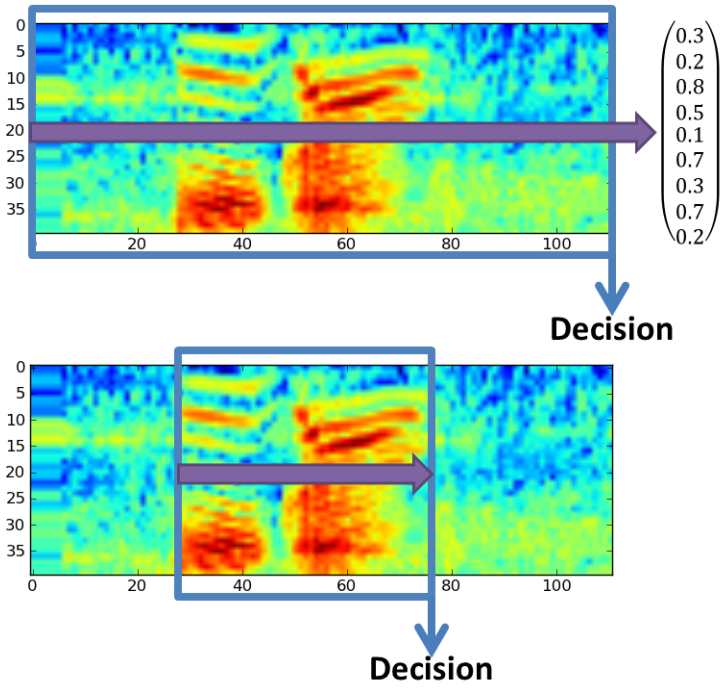

Figure 6.3. An utterance in offline mode detection (top) and online detection (bottom). The arrow represents pooling. In offline mode, a feature is extracted per utterance, while in online mode, a feature is extracted per time step.

In online mode, which I consider more interesting in a real time scenario such as hotword detection using a mobile device, I take a pooling window of size N_p, and perform the pooling operation just on that window. Thus,

$$\mathbf{c}_{pooled,t} = pool\_online(\mathbf{c}_{t-N_p}, \ldots, \mathbf{c}_t)$$

In this case, I obtain a pooled code for each time step t, and at test time I feed that to the classifier so I can decide if a keyword is present or not in an online fashion. During training, only a single pooled window is considered in the following way: for negative utterances, a window is randomly chosen, and for positive utterances, I take the temporal position at the end of the target word, and the previous N_p codes and pool them together.

Figure 6.3 shows the offline (top) and online (bottom) operations of pooling on the same utterance.

DeepHotword

One of the chief advantages of SparseHotword is that it requires no additional training data as it learns how to code an utterance with no supervision. However, it would be good to use more resources in an efficient way, as they may be available for languages with substantial amounts of transcribed data. Most keyword detection systems start with decoding the utterance, which implicitly is using these extra resources: both acoustic and

language models are typically trained with lots of data. Once decoded, the lattice generated can be used to extract useful features in a discriminative way.

One disadvantage of such a method is that decoding generally involves many components which are usually tuned for word error rate, not necessarily to detect a particular word. Furthermore, there is some computational overhead to decode, which in some applications such as activation through voice may be critical. Thus, I propose to use the acoustic models trained with a large corpus (which does not necessarily need to overlap with the corpus used to train the hotword detector), while not performing a full decoding pass.

To this effect, I have a large deep neural network trained on billions of frames of English data. The input consists of 26 frames (i.e. $N = 26$), and the network has 3 hidden layers of 2000 units each. The output layer has 8000 HMM clustered states. Let $\mathbf{h}\{i\}$ be the activations (after the non-linearity) at the i-th layer. I will use this as the code, and I will pool them in the same way that I did with sparse codes:

$$\mathbf{c}_{pooled} = pool\_offline(\mathbf{h}\{i\}_1, \ldots, \mathbf{h}\{i\}_T)$$
$$\mathbf{c}_{pooled,t} = pool\_online(\mathbf{h}\{i\}_{t-N_p}, \ldots, \mathbf{h}\{i\}_t)$$

I do not use the output as features as they lie in a high dimensional space (more prone to overfitting), and because HMM clustered states are not what I care about. However, both tasks are related, and using the representations learned to achieve phone classification is an obvious way to do transfer learning to hotword detection. To this effect, I observed that deeper layers yield better performance, which will be more extensively discussed in the next section. A possible explanation would be the fact that the hidden units closer to the output make phone states more linearly separable, and my approach uses a linear SVM (which is very fast to train and test) on the code space. Note that the idea of using activations of a huge network trained on large amounts of data for an independent (but related) task has been explored in this thesis in the vision domain (Chapter 5, section 5.2.4).

6.2.3 Experiments

In this section I describe the experiments that I ran using both SparseHotword and DeepHotword systems. Although there are several differences between the two in terms of how each of them trains the representation that is input to a linear classifier, both of them used exactly the same data to train such classifier. The training set consists of 10000 utterances that contain the target word – "Google" – in isolation, and 20000 utterances that do not contain it. Each utterance is obtained from the voice search feature available from Android phones, so there is a large variety of channel, noise and speaker conditions. The typical length of "Google" was roughly 600 ms., and the typical negative examples were longer (a few seconds, although they typically contained several words and some silence).

I preprocess each utterance by removing silence surrounding the speech. I extract 40 dimensional acoustic features by taking the logarithm of 40 mel frequency filter banks response on the amplitude of the short term Fourier transform of the acoustic signal, with a step size of 10 ms and a window analysis of 30 ms. These features are commonly used as the input of acoustic models for ASR (frequently with a truncated DCT transform to extract MFCC coefficients).

Both systems use the same acoustic features, but SparseHotword uses sparse coding to find a suitable dictionary and coding function to represent the features in a (soft and sparse) vector quantized space, while DeepHotword uses the activations of a pretrained deep neural network on a much larger corpus of billions of frames, trained to perform HMM state recognition [62].

Hyperparameter tuning

There are a number of parameters to be tuned, such as the context window (i.e. the stacking of several 40 dimensional acoustic features over time), the coding technique and dictionary type and size (in SparseHotword), the layer used to extract the features that will be input to the pooling step (in DeepHotword), the pooling window size and method, and the regularization parameter of the linear SVM. All these parameters were optimized using a grid search and a large computer cluster.

For the DeepHotword system, the context size is predetermined by the architecture of the pretrained neural network. In this case, I tried a small network with 11 frames as input, and a bigger network with 26 frames. Both these networks had weights pretrained on a large corpus, but these weights were not further tuned to avoid overfitting. I extract features from the hidden activations of the network. The best hidden layer to extract these activations turned out to be the one right before the output layer, presumably due to the fact that it is the layer which clusters phonetic units in a linearly separable way (as it is the input to the softmax layer).

The SparseHotword system had more parameters to tune. I found that a context of 30 or 40 frames as the input to the encoder was better than smaller contexts of 10 or 20 frames, and, in accordance with [27], the learning of the dictionary did not seem very critical, as randomly sampling from the training data yielded similar results than Orthogonal Matching Pursuit (OMP), a variant of k-means. The dictionary size is another important characteristic: if set too big, it may overfit, but if set too low, the local representation may not capture all the non-linearities needed to perform hotword detection. In general, as observed in computer vision, increasing the size does seem to always help due to the very well regularized classifier that I trained after extracting the codes – a linear SVM. However, gains diminish when increasing the codebook size at the expense of computation, and I found 2000 to be a good tradeoff between the two. I also experimented with data normalization before coding, and observed that zero component analysis (ZCA – a form of whitening) did not help, but contrast normalization (removing mean and dividing by the standard deviation for each frame) consistently helped.

Lastly, the pooling, common to both systems, had two important parameters: the pooling window size, and the pooling method. For offline mode, I found out that pooling together the whole utterance was best. However, when using a fixed window to operate in online mode, the best results were obtained with window sizes from 60 to 90 frames (slightly longer than the word that I are detecting). Consistent with findings in the literature, the best pooling method for sparse coding was max pooling (i.e., taking the max component wise), while RMS or L2 pooling was found to be the best to pool together neural network activations.

System	Offline Miss	Online Miss	Ops./frame
Random	99%	99%	0
Baseline	N/A	10%	¿0.2M
SparseHotword	2.3%	9.8%	1.7M
DeepHotword (small)	3.3%	6.1%	0.2M
DeepHotword (big)	0.5%	0.9%	22.3M

Table 6.4. Table with the main results. I report miss rate at a fixed false alarm level (1%) for various systems and operating modes (offline and online).

Results

The main results are shown in Table 6.4. The miss rates are reported on a held out set of 200 positive utterances and 1000 negative utterances, and the miss rate is computed at 1% false alarm level per utterance (not per frame), so the offline and online figures mean the same, even though in online mode a (potentially wrong) decision can be made at each time step, which makes the whole utterance wrong. The baseline system that I used was based on decoding of the utterance, followed by feature extraction (mostly from the decoded lattices, but also including other information such as posteriograms), and a logistic regression classifier.

On the fourth column of the results in Table 6.4 I also show the amount of operations required per frame. Since we care about computational efficient models, it is important to note that a trade-off exists between less computation at the cost of higher miss rates. In particular, the small neural network used in DeepHotword (small) was 100 times smaller than the DeepHotword (big), with about an order of magnitude more misses. However, in comparison with the SparseHotword system, which did not use any additional training data, the smaller network performs substantially better at a fraction of computation – again, there is a trade off between training data and miss rate in this case. One may also argue that a deeper model is more robust than the sparse, shallow model. However, I did not investigate this issue further, although the fact that taking layers closer to the input in the neural networks exhibited worse miss rates probably implies that depth matters for this task.

Further discussion

An example of a positive utterance is shown in Figure 6.4, where I show an utterance where "Google" is present, with the corresponding score. I manually inspected some of the missclassified utterances and found that some of them may be human transcription errors (e.g. "eagle" instead of "Google" as a false negative, or "Google maps ..." as a false positive).

Furthermore, I started exploring learning pooling by feeding the input codes to a recurrent neural network (very similar to the system presented in Chapter 3), and targeting the presence or not of the hotword as the output. Preliminary results show that this approach is not as competitive as pooling with a fixed function, but more needs to be explored.

In summary, having lots of data and a small set of hotwords (or keywords) to detect implies that a direct approach in which we do not decode is very competitive. I used this

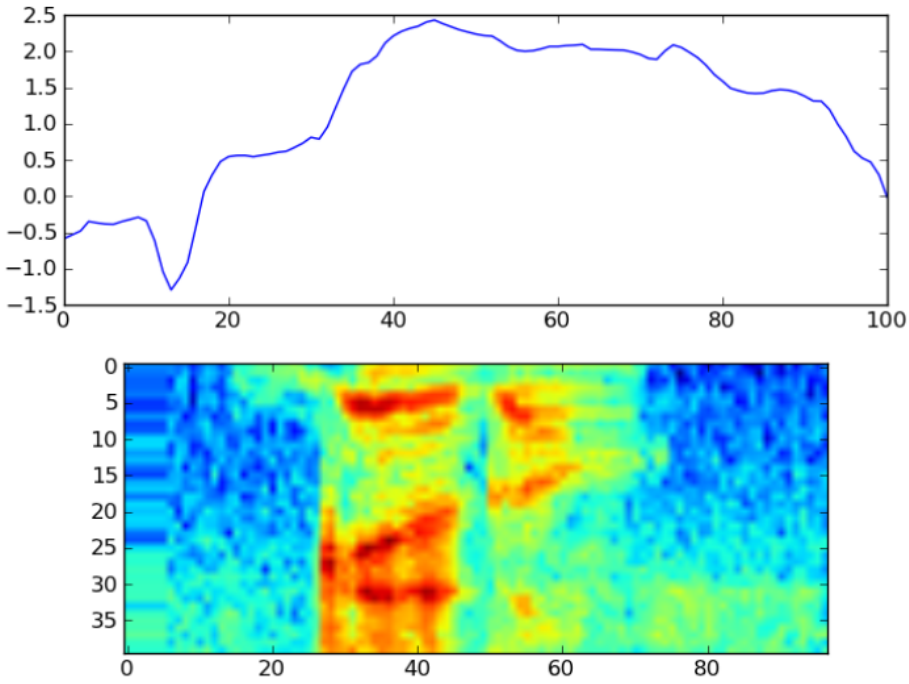

Figure 6.4. A positive utterance in the test set, and the online score produced by one of the proposed systems in this section.

in the context of a commercial application that wakes up a device when a spoken term is detected, and is currently being used in millions of phones worldwide as the Google Android Operating System.

Chapter 7

Conclusions

I now summarize and conclude the main points that I presented in my thesis. Most of the work here has also been published in conference papers, and a reader only interested in a particular topic may want to read those publications instead.

7.1 Optimization

In this chapter I discussed some of the many optimization challenges involving deep learning and machine learning. In particular, one has to deal with high dimensional complex, large-scale data, and non-linear models yielding non-convex objective functions. As a result, my efforts focused on building a method able to run on platforms able to process large-scale datasets whilst dealing with non-convex objective functions.

I proposed Krylov Subspace Descent, which is an improvement over other existing Hesian free methods. As such, it uses curvature to deal with ill-conditioned problems by effectively pre-multiplying gradients by the inverse Hessian to speed up learning. These approaches are also appealing since they use large batches that, thanks to instruction level parallelism, exploit very well specialized hardware such as current GPUs.

The method never stores the Hessian matrix (which would be prohibitive), and generalizes to non-convex optimization problems thanks to using the idea of building a low dimensional, easy to optimize Krylov subspace (which arise naturally in conjugate gradient descent).

I show how my method compares favorably with traditional techniques such as stochastic gradient descent, LBFGS or other Hessian Free methods in a large variety of datasets and models. Current state-of-the-art, however, still mostly uses stochastic gradient descent as it is a very powerful method, specially when paired with momentum and carefully chosen initializations. I definitely recommend using those techniques unless your models are extremely deep or recurrent – even then, stochastic gradient descent can provide reliable estimates at a reasonable cost.

7.2 Models

Diverging from deep learning mainstream, I attempted to approach deep architectures that had easier to optimize objectives. In this chapter, I introduce sparse coding and linear models for speech recognition (these models had been extensively used in computer vision and other fields). Furthermore, I present an extension of these in a deep architecture that involves several convex problems, random projections, and non-linearities, retaining most of classic neural networks and derived models representational power, whilst exploiting convexity in several ways (e.g. parallel batch learning with convergence guarantees).

Experimental results show excellent performance and ease of training for many model architectures and scales. In particular, we show clear advantages when using our techniques for small (thousands of parameters) sparse models on small image classifications tasks such as CIFAR-10, moderate gains on larger speech models (with millions of parameters and samples), and moderate gains on large scale object classification for Imagenet.

7.3 Analysis

In this chapter, I studied two important properties in deep learning that are yet to be fully understood by the research community: depth and size in deep models.

Regarding size, I proposed a new interpretation of sparse coding viewed as Nyström sampling, and how it can help explaining performance vs. size. Furthermore, together with Yangqing Jia we developed a new idea based on this analysis that allowed us to find an algorithm to "simplify" an overcomplete representation, achieving better performance for a given layer size (or, equivalently, achieving smaller sizes for a desired performance).

In terms of understanding why depth matters in deep architectures, I did two empirical tests in this Chapter. I studied how, in the context of acoustic modeling for speech recognition, layer depth affected recognition performance and generalization whilst maintaining model parameters under a budget. The observation, which has also been observed in other studies formulated in the same way, concludes that more depth does not always imply better, although it seems to provide better generalization under mismatched (noisy) conditions.

The other study that I performed involved a well known architecture consisting of a deep convolutional neural network trained to classify objects in an image. In my study, I show how features derived from each layer extract higher (semantic) level of information that other classic features used in object recognition cannot extract, specially when looking at "deeper" layers (i.e., closer to the output).

7.4 Applications

In the last part of my thesis, I presented work that I did in keyword recognition. The main results are split by two different domains: one with limited resources (e.g., for a new language), and for which we want to detect keywords that are given to us (e.g., by an agency). The other approach involved a commercial system to detect a specific keyword to

trigger a more complex recognition system used in current smart phones, and for which I had large amounts of data.

The solutions involved deep learning, although the most successful application was with the larger datasets in the commercial systems, in which a hidden representation from an acoustic model trained with billions of samples was used, and for which we did not need to perform automatic speech recognition. The more constrained scenario were some keywords were out of vocabulary and the data was limited involved speech recognition and lattice scores to decide whether a word was present or not. In this second scenario, my efforts involved optimizing non-smooth functions related to a particular metric that scored the system, aiming to refine the predictions coming out of the lattices.

7.5 Concluding Remarks

During my years as a graduate student at UC Berkeley, I have learned a lot as a researcher, and also about the topics that I covered in this thesis. I became very interested in the "magic" of machine learning; initially I was a believer that all you need is machine learning to solve hard problems (such as the ones presented in this thesis). However, over years of experience, based not only on my own experiences but also by interacting with an excellent group of people and community, I have realized that the data and the learning algorithm are small pieces of the solution of problems.

Nonetheless, the first few chapters of this thesis aim to develop algorithms that are smarter (i.e., one does not need to tune too many parameters or know a lot about the underlaying data), and models that are powerful and also sufficient for the kinds of data that one may want to process. Chief examples of such models are the recurrent neural network to model speech signals, or convolutional neural networks to model image formation are. I also devoted a lot of effort to develop algorithms that could run on many machines and/or cores, as this has been a common trend in modern computation, with lots of resources available in a distributed fashion, and I have no doubt this tend will continue as more resources (i.e., computational and data) are made available to researchers.

I also wanted to shed some light on what I consider one of the outstanding questions in deep learning: why do depth and size matter? Having more complex models (in terms of the functions that they can represent) is a major factor on why the deeper and larger models work better. However, the generalization properties of such models are a vastly unexplored area of theoretic research that may have important implications for both machine learning and neuroscience if it turns out that our brain does, in fact, do deep learning as a robust model that generalizes well.

Lastly, working on hard problems such as the ones described in the last chapter is fun, and more often than not requires a scientist to go out of the mainstream and innovate to achieve a desirable outcome. In this regard, I would recommend anyone facing a hard machine learning problem to look at the data and analyze the errors produced by "vanilla" models.

I am eager to see what is next, while looking back after these amazing years at Berkeley. I am looking forward to see what machine learning is heading to (is there going to be another comeback like the one with neural networks?). In the future, I will try to bring

further understanding of human intelligence by making our models closer to how we believe our brain works (e.g., by adding top-down connections known to be in the brain that are not present in current neural networks). While doing so, I hope to push the envelope of fascinating fields such as language, speech, or vision, by contributing to the research community as well as producing technology that will be made available to the general population for the greater good.

Bibliography

[1] IARPA Babel Program - Broad Agency Announcement (BAA). `http://www.iarpa.gov/Programs/ia/Babel/solicitation_babel.html`, 2011.

[2] A Abdullah, R C Veltkamp, and M A Wiering. An ensemble of deep support vector machines for image categorization. In *SOCPAR*, 2009.

[3] S Amari. Natural gradient works efficiently in learning. *Neural Computation*, 10:251–276, 1998.

[4] L Bahl and F Jelinek. Decoding for channels with insertions, deletions, and substitutions with applications to speech recognition. *IEEE Transactions on Information Theory*, 21(4):404–411, 1975.

[5] J Baker. The DRAGON system – An overview. *IEEE Transactions on Acoustics, Speech, and Signal Processing*, ASSP-23(1):24–29, 1975.

[6] P L Bartlett and S Mendelson. Rademacher and gaussian complexities: Risk bounds and structural results. *The Journal of Machine Learning Research*, 3:463–482, 2003.

[7] L Baum and T Petrie. Statistical Inference for Probabilistic Functions of Finite State Markov Chains. *The Annals of Mathematical Statistics*, 37(6):1554–1563, 1966.

[8] Y Bengio. Learning deep architectures for AI. *Foundations and Trends in Machine Learning*, 2(1):1–127, 2009.

[9] Y Bengio and X Glorot. Understanding the difficulty of training deep feedforward neural networks. In *AISTATS 2010*, volume 9, pages 249–256, May 2010.

[10] Y Bengio, P Simard, and P Frasconi. Learning long-term dependencies with gradient descent is difficult. *IEEE Transactions on Neural Networks*, 5(2):157–166, 1994.

[11] A Berg, J Deng, and L Fei-Fei. ImageNet large scale visual recognition challenge 2012. 2012.

[12] O Boiman, E Shechtman, and M Irani. In defense of nearest-neighbor based image classification. In *CVPR*, 2008.

[13] L Bottou. Online Learning and Stochastic Approximations, 1998.

[14] L Bourdev, S Maji, T Brox, and J Malik. Detecting people using mutually consistent poselet activations. In *ECCV*, 2010.

[15] Y Boureau, F Bach, Y LeCun, and J Ponce. Learning mid-level features for recognition. In *CVPR*, 2010.

[16] H Bourlard and N Morgan. Connectionist Speech Recognition. A Hybrid Approach. *Kluwer Press*, 1994.

[17] H Bourlard, N Morgan, C Wooters, and S Renals. CDNN: A Context Dependent Neural Network for Continuous Speech Recognition. In *Proc. ICASSP*, 1992.

[18] L Breiman. Random forests. *Machine learning*, 45(1):5–32, 2001.

[19] J Bridle. An efficient elastic-template method for detecting given words in running speech. In *Brit. Acoust. Soc. Meeting*, pages 1–4, 1973.

[20] R Byrd, G Chiny, W Neveitt, and J Nocedal. On the use of stochastic hessian information in optimization methods for machine learning. *(submitted for publication)*, 2010.

[21] J Carreira, R Caseiro, J Batista, and C Sminchisescu. Semantic segmentation with second-order pooling. In *ECCV*, 2012.

[22] A Castrodad and G Sapiro. Sparse modeling of human actions from motion imagery. Preprint, 2011.

[23] O Chapelle and D Erhan. Improved Preconditioner for Hessian Free Optimization. In *NIPS Workshop on Deep Learning and Unsupervised Feature Learning*, 2011.

[24] B Chen. Learning Discriminant Narrow-band Temporal Patterns for Automatic Recognition of Conversational Telephone Speech. *Ph.D. Thesis, University of California at Berkeley*, 2005.

[25] A Coates, A Karpathy, and A Ng. Emergence of object-selective features in unsupervised feature learning. In *NIPS*, 2012.

[26] A Coates, H Lee, and A Ng. An analysis of single-layer networks in unsupervised feature learning. In *AISTATS*, 2011.

[27] A Coates and A Ng. The importance of encoding versus training with sparse coding and vector quantization. In *ICML*, 2011.

[28] W Cohen and V R de Carvalho. Stacked sequential learning. In *IJCAI*, 2005.

[29] R Collobert, F Sinz, J Weston, and L Bottou. Trading convexity for scalability. In *ICML*, 2006.

[30] C Cortes, M Mohri, and A Talwalkar. On the impact of kernel approximation on learning accuracy. In *AISTATS*, 2010.

[31] G Dahl, D Yu, L Deng, and A Acero. Context-Dependent Pre-trained Deep Neural Networks for Large Vocabulary Speech Recognition. *IEEE Transactions on Audio, Speech, and Language Processing*, 2012.

[32] N Dalal. Histograms of oriented gradients for human detection. In *CVPR*, 2005.

[33] S Davis and P Mermelstein. Comparison of parametric representations for monosyllabic word recognition in continuously spoken sentences. *Acoustics, Speech and Signal Processing, IEEE Transactions on*, 28(4):357–366, 1980.

[34] J Dean, G Corrado, R Monga, K Chen, M Devin, Q Le, M Mao, M Ranzato, A Senior, P Tucker, K Yang, and A Ng. Large Scale Distributed Deep Networks. In *NIPS*, 2012.

[35] L Deng, J Li, J Huang, K Yao, D Yu, F Seide, M Seltzer, G Zweig, X He, J Williams, Y Gong, and A Acero. Recent Advances Of Deep Learning For Speech Research At Microsoft. In *Proc. ICASSP*, 2013.

[36] L Deng and D O'Shaughnessy. *Speech processing: a dynamic and optimization-oriented approach*, volume 17. CRC, 2003.

[37] L Deng, M Seltzer, D Yu, A Acero, A Mohamed, and G Hinton. Binary Coding of Speech Spectrograms Using a Deep Auto-encoder. In *Interspeech*, 2010.

[38] L Deng and D Yu. Deep convex network: A scalable architecture for deep learning. In *Interspeech*, 2011.

[39] M Denil and N de Freitas. Recklessly approximate sparse coding. *arXiv preprint arXiv:1208.0959*, 2012.

[40] J Donahue, Y Jia, O Vinyals, J Hoffman, N Zhang, E Tzeng, and T Darrell. DeCAF: A Deep Convolutional Activation Feature for Generic Visual Recognition. *arXiv preprint arXiv:1310.1531*, 2013.

[41] D Donoho. Compressed sensing. *Information Theory, IEEE Transactions on*, 52(4):1289–1306, 2006.

[42] J Duchi, E Hazan, and Y Singer. Adaptive Subgradient Methods for Online Learning and Stochastic Optimization. *J. Mach. Learn. Res.*, pages 2121–2159, 2011.

[43] D Erhan, Y Bengio, A Courville, P Manzagol, P Vincent, and S Bengio. Why does unsupervised pre-training help deep learning? *The Journal of Machine Learning Research*, 11:625–660, 2010.

[44] L Fei-Fei and P Perona. A bayesian hierarchical model for learning natural scene categories. In *CVPR*, 2005.

[45] H Franco, M Cohen, N Morgan, D Rumelhart, and V Abrash. Context-dependent connectionist probability estimation in a hybrid hidden Markov model-neural net speech recognition system. In *Proc. IJCNN*, 1992.

[46] B Frey and D Dueck. Clustering by passing messages between data points. *Science*, 315(5814):972–976, 2007.

[47] J Fritsch. ACID/HNN: A Framework for Hierarchical Connectionist Acoustic Modeling. In *Proc. ASRU*, 1997.

[48] A Frome, G Corrado, J Shlens, S Bengio, J Dean, M Ranzato, and T Mikolov. Devise: A deep visual-semantic embedding model. In *NIPS*, 2013.

[49] M Gales. Maximum likelihood linear transformations for hmm-based speech recognition. 12:75–98, 1998.

[50] B Gold, N Morgan, and D Ellis. *Speech and Audio Signal Processing*. Wiley, 2nd edition, 2011.

[51] D Grangier, J Keshet, and S Bengio. Discriminative Keyword Spotting. In *Automatic Speech and Speaker Recognition: Large Margin and Kernel Methods*. John Wiley and Sons, 2009.

[52] F. Grezl, M. Karafiat, S. Kontar, and J. Cernocky. Probabilistic and bottleneck features for lvcsr of meetings. In *Proc. ICASSP*, pages 757–760, 2007.

[53] A Griewank and G Corliss, editors. *Automatic Differentiation of Algorithms: Theory, Implementation, and Application*. SIAM, 1991.

[54] H Hermansky, D Ellis, and S Sharma. Tandem connectionist feature extraction for conventional HMM systems. In *Proc. ICASSP*, 2000.

[55] H Hermansky and F Valente. Hierarchical and parallel processing of modulation spectrum for ASR applications. In *Proc. ICASSP*, 2008.

[56] A Higgins and R Wohlford. Keyword recognition using template concatenation. In *Acoustics, Speech, and Signal Processing, IEEE International Conference on ICASSP'85.*, volume 10, pages 1233–1236. IEEE, 1985.

[57] G Hinton, L Deng, D Yu, G Dahl, A Mohamed, N Jaitly, A Senior, V Vanhoucke, P Nguyen, T Sainath, and B Kingsbury. Deep Neural Networks for Acoustic Modeling in Speech Recognition. *IEEE Signal Processing Magazine*, 28:82–97, 2012.

[58] G Hinton, S Osindero, and Y Teh. A fast learning algorithm for deep belief nets. *Neural Comput.*, 18:1527–1554, 2006.

[59] G Hinton and R Salakhutdinov. Reducing the dimensionality of data with neural networks. *Science*, 313(5786):504, 2006.

[60] HG Hirsch and D Pearce. The Aurora experimental framework for the performance evaluation of speech recognition systems under noisy conditions. In *ISCA ITRW ASR: Challenges for the Next Millennium*, 2000.

[61] M Hochberg, S Renals, A Robinson, and D Kershaw. Large vocabulary continuous speech recognition using a hybrid connectionist-HMM system. In *Third International Conference on Spoken Language Processing*, 1995.

[62] N Jaitly, P Nguyen, A Senior, and V Vanhoucke. Application Of Pretrained Deep Neural Networks To Large Vocabulary Speech Recognition. In *Proceedings of Interspeech*, 2012.

[63] K Jarrett, K Kavukcuoglu, M A Ranzato, and Y LeCun. What is the best multi-stage architecture for object recognition? In *ICCV*, 2009.

[64] R Jenatton, G Obozinski, and F Bach. Structured sparse principal component analysis. In *AISTATS*, 2010.

[65] Y Jia, O Vinyals, and T Darrell. On Compact Codes for Spatially Pooled Features. In *ICML*, 2013.

[66] D Karakos, R Schwartz, S Tsakalidis, L Zhang, S Ranjan, T Ng, R Hsiao, G Saikumar, I Bulyko, L Nguyen, J Makhoul, F Grezl, M Hannemann, M Karafiat, I Szoke, K Vesely, L Lamel, and V Le. Score normalization and system combination for improved keyword spotting. In *ASRU*, 2013.

[67] T Kawabata, T Hanazawa, and K Shikano. Word spotting method based on hmm phoneme recognition. *The Journal of the Acoustical Society of America*, 84:S62, 1988.

[68] B Kingsbury, J Cui, X Cui, M Gales, K Knill, J Mamou, L Mangu, D Nolan, M Picheny, B Ramabhadran, R Schluter, A Sethy, and P Woodland. A high-performance Cantonese keyword search system. In *Proc. ICASSP*, pages 8277–8281, 2013.

[69] B Kingsbury, T Sainath, and H Soltau. Scalable minimum Bayes risk training of deep neural network acoustic models using distributed hessian-free optimization. In *Proc. Interspeech*, 2012.

[70] R Kneser and H Ney. Improved Backing-Off for n-gram Language Modeling. In *Proc. ICASSP*, pages 181–184, 1995.

[71] T Kohonen. *Self-Organizing Maps*. Springer-Verlag, 2001.

[72] A Krizhevsky. Learning multiple layers of features from tiny images. Technical report, 2009.

[73] A Krizhevsky, I Sutskever, and G Hinton. ImageNet classification with deep convolutional neural networks. In *NIPS*, 2012.

[74] S Kumar, M Mohri, and A Talwalkar. Sampling methods for the nyström method. *JMLR*, 13(Apr):981–1006, 2012.

[75] Q Le, J Ngiam, A Coates, A Lahiri, B Prochnow, and A Ng. On optimization methods for deep learning. In *ICML*, 2011.

[76] Y LeCun, L Bottou, Y Bengio, and P Haffner. Gradient-based learning applied to document recognition. *Proc. of the IEEE*, 86(11):2278–2324, 1998.

[77] B Lee and D Ellis. Noise Robust Pitch Tracking using Subband Autocorrelation Classification (SAcC). In *Proc. Interspeech*, 2012.

[78] Y Lin, T Zhang, S Zhu, and K Yu. Deep coding network. In *NIPS*, 2010.

[79] D Lowe. Distinctive image features from scale-invariant keypoints. *IJCV*, 2004.

[80] J Mairal, F Bach, J Ponce, and G Sapiro. Online learning for matrix factorization and sparse coding. *JMLR*, 11:19–60, 2010.

[81] S Maji, A Berg, and J Malik. Classification using intersection kernel support vector machines is efficient. In *Computer Vision and Pattern Recognition, 2008. CVPR 2008. IEEE Conference on*, pages 1–8. Ieee, 2008.

[82] J Martens. Deep learning via Hessian-free optimization. In *ICML*, 2010.

[83] C Meyer. *Matrix Analysis and Applied Linear Algebra*. SIAM, 2001.

[84] T Mikolov, M Karafiat, L Burget, J Cernocky, and S Khudanpur. Recurrent Neural Network based Language Model. In *Interspeech*, 2010.

[85] D Miller, M Kleber, C Kao, O Kimball, T Colthurst, S Lowe, R Schwartz, and H Gish. Rapid and accurate spoken term detection. In *Proc. Interspeech*, pages 314–317, 2007.

[86] A Mohamed, G Dahl, and G Hinton. Deep belief networks for phone recognition. In *NIPS Workshop*, 2009.

[87] A Mohamed, G Hinton, and G Penn. Understanding how Deep Belief Networks perform acoustic modelling. In *Proc. ICASSP*, 2012.

[88] A Mohamed, D Yu, and L Deng. Investigation of Full-Sequence Training of Deep Belief Networks for Speech Recognition. In *Interspeech*, 2010.

[89] J Morales and J Nocedal. Enriched Methods for Large-Scale Unconstrained Optimization. *Computational Optimization and Applications*, 21:143–154, 2000.

[90] N Morgan and H Bourlard. Factoring networks by a statistical method. *Neural Computation*, 4(6):835–838, 1992.

[91] N Morgan and H Bourlard. An Introduction to Hybrid HMM/Connectionist Continuous Speech Recognition. *IEEE Signal Processing Magazine*, pages 25–42, 1995.

[92] N Morgan and H Bourlard. Continuous Speech Recognition. *Signal Processing Magazine*, 3(12):24–42, 2006.

[93] N Morgan and E Fosler-Lussier. Combining multiple estimators of speaking rate. In *Proc. ICASSP*, 1998.

[94] J Mutch and D Lowe. Multiclass object recognition with sparse, localized features. In *CVPR*, volume 1, pages 11–18. IEEE, 2006.

[95] T Nguyen and S Sanner. Algorithms for direct 0–1 loss optimization in binary classification. In *International Conference on Machine Learning (ICML)*, pages 1–9, 2013.

[96] J Nocedal and S Wright. *Numerical Optimization*. Springer, 2000.

[97] J Nocedal and S Wright. *Numerical Optimization*. Springer, New York, 2nd edition, 2006.

[98] E Nyström. Über Die Praktische Auflösung von Integralgleichungen mit Anwendungen auf Randwertaufgaben. *Acta Mathematica*, 54(1):185–204, 1930.

[99] A Oliva and A Torralba. Modeling the shape of the scene: A holistic representation of the spatial envelope. *IJCV*, 2001.

[100] B Olshausen and D Field. Sparse coding with an overcomplete basis set: A strategy employed by v1? *Vision research*, 37(23):3311–3325, 1997.

[101] D Paul and J Baker. The design for the Wall Street Journal-based CSR corpus. In *ICSLP*, 1992.

[102] D Pearce and H Hirsch. The Aurora Experimental Framework for the Performance Evaluation of Speech Recognition Systems under Noisy Conditions. In *ISCA ITRW ASR2000*, 2000.

[103] B Pearlmutter. Fast exact multiplication by the Hessian. *Neural Computation*, 6:147–160, 1994.

[104] D Povey, L Burget, M Agarwal, P Akyazi, F Kai, A Ghoshal, O Glembek, N Goel, M Karafiát, A Rastrow, R Rose, P Schwarz, and S Thomas. The subspace Gaussian mixture model - A structured model for speech recognition. 25:404–439, 2011.

[105] D Povey, A Ghoshal, et al. The Kaldi Speech Recognition Toolkit. In *Proc. ASRU*, 2011.

[106] R Prabhavalkar. *Discriminative Articulatory Feature-based Pronunciation Models with Application to Spoken Term Detection*. PhD thesis, 2013.

[107] W Press, S Teukolsky, W Vetterling, and B Flannery. *Numerical Recipes: The Art of Scientific Computing*. Cambridge University Press, New York, NY, USA, 2007.

[108] L Rabiner and B Juang. Fundamentals of speech recognition. 1993.

[109] K Riedhammer, V Hai Do, and J Hieronymus. A Study on LVCSR and Keyword Search for Tagalog. In *Proc. Interspeech*, 2013.

[110] R Rigamonti, M Brown, and V Lepetit. Are sparse representations really relevant for image classification? In *CVPR*, 2011.

[111] E Roberts. Neural Networks – History. `http://www-cs-faculty.stanford.edu/~eroberts/courses/soco/projects/neural-networks/History/`. Accessed: 01/09/2013.

[112] T Robinson, M Hochberg, and S Renals. IPA: Improved phone modelling with recurrent neural networks. In *ICASSP*. IEEE, 1994.

[113] F Rosenblatt. The Perceptron–a perceiving and recognizing automaton. Technical Report 85-460-1, Cornell Aeronautical Laboratory, 1957.

[114] N Roux, Y Bengio, and P Manzagol. Topmoumoute online natural gradient algorithm. In *NIPS*, 2007.

[115] T Sainath, B Ramabhadran, M Picheny, D Nahamoo, and D Kanevsky. Exemplar-based sparse representation features: from timit to lvcsr. *Audio, Speech, and Language Processing, IEEE Transactions on*, (99):1–1, 2011.

[116] R Salakhutdinov and G Hinton. Learning a nonlinear embedding by preserving class neighbourhood structure. In *AISTATS*, 2007.

[117] A Saxe, P Koh, Z Chen, M Bhand, B Suresh, and A Ng. On random weights and unsupervised feature learning. In *ICML*, 2011.

[118] N Schraudolph. Fast curvature matrix-vector products for second-order gradient descent. In *Neural Computation*, 2002.

[119] F Seide, G Li, and D Yu. Conversational Speech Transcription Using Context-Dependent Deep Neural Networks. In *Interspeech*, 2011.

[120] G Sivaram and H Hermansky. Multilayer perceptron with sparse hidden outputs for phoneme recognition. In *ICASSP*, pages 5336–5339. IEEE, 2011.

[121] G Sivaram, S Nemala, M Elhilali, T Tran, and H Hermansky. Sparse coding for speech recognition. In *ICASSP*, pages 4346–4349. IEEE, 2010.

[122] A Stolcke. SRILM – an extensible language modeling toolkit. In *Intl. Conf. Spoken Language Processing*, 2002.

[123] I Sutskever, J Martens, and G Hinton. Generating text with recurrent neural networks. In *ICML*, 2011.

[124] L Talbert, G Groner, J Koford, R Brown, P Low, and C Mays. A Real-Time Adaptive Speech-Recognition System. In *Technical Documentary Report ASD-TDR-63-660, Stanford Electronic Laboratories*, 1963.

[125] A Talwalkar and A Rostamizadeh. Matrix coherence and the nystrom method. *arXiv preprint arXiv:1004.2008*, 2010.

[126] A Torralba and A Efros. Unbiased look at dataset bias. In *CVPR*, 2011.

[127] F Valente, J Vepa, C Plahl, C Gollan, H Hermansky, and R Schlüter. Hierarchical neural networks feature extraction for LVCSR system. In *Proc. Interspeech*, pages 42–45, 2007.

[128] L van der Maaten and G Hinton. Visualizing data using t-sne. *JMLR*, 9, 2008.

[129] O Vinyals and L Deng. Are Sparse Representations Rich Enough for Acoustic Modeling? In *Interspeech*, 2012.

[130] O Vinyals, Y Jia, L Deng, and T Darrell. Learning with Recursive Perceptual Representations. In *NIPS*, 2012.

[131] O Vinyals and N Morgan. Deep vs. Wide: Depth on a Budget for Robust Speech Recognition. In *Proceedings of INTERSPEECH*, 2013.

[132] O Vinyals and D Povey. Krylov Subspace Descent for Deep Learning. In *AISTATS*, 2012.

[133] O Vinyals and S Ravuri. Comparing Multilayer Perceptron to Deep Belief Network Tandem Features for Robust ASR. In *ICASSP*, 2011.

[134] O Vinyals, S Ravuri, and D Povey. Revisiting Recurrent Neural Networks for Robust ASR. In *ICASSP*, 2012.

[135] J Wang, J Yang, K Yu, F Lv, T Huang, and Y Gong. Locality-constrained linear coding for image classification. In *CVPR*, 2010.

[136] S Wegmann, A Faria, A Janin, K Riedhammer, and N Morgan. The tao of atwv: Probing the mysteries of keyword search performance. In *ASRU*, 2013.

[137] D H Wolpert. Stacked generalization. *Neural networks*, 5(2):241–259, 1992.

[138] J Xiao, J Hays, K Ehinger, A Oliva, and A Torralba. Sun database: Large-scale scene recognition from abbey to zoo. In *CVPR*, 2010.

[139] J Yang, K Yu, and Y Gong. Linear spatial pyramid matching using sparse coding for image classification. In *CVPR*, 2009.

[140] J Yang, K Yu, and T Huang. Efficient highly over-complete sparse coding using a mixture model. In *ECCV*, 2010.

[141] D Yu, F Seide, G Li, and L Deng. Exploiting sparseness in deep neural networks for large vocabulary speech recognition. In *ICASSP*, pages 5336–5339. IEEE, 2012.

[142] K Yu and T Zhang. Improved Local Coordinate Coding using Local Tangents. In *ICML*, 2010.

[143] K Yu, T Zhang, and Y Gong. Nonlinear learning using local coordinate coding. *NIPS*, 22:2223–2231, 2009.

[144] K Zhang, I Tsang, and J Kwok. Improved nyström low-rank approximation and error analysis. In *ICML*, 2008.